

ANALYSIS AND DESIGN OF A MAGNETIC BEARING

Vladimir Soukup

B. Sc. (Electrical Engineering) Czech Technical University

**A THESIS SUBMITTED IN PARTIAL FULFILLMENT OF
THE REQUIREMENTS FOR THE DEGREE OF
MASTER OF APPLIED SCIENCE**

in

**THE FACULTY OF GRADUATE STUDIES
DEPARTMENT OF ELECTRICAL ENGINEERING**

**We accept this thesis as conforming
to the required standard**

THE UNIVERSITY OF BRITISH COLUMBIA

June 1988

© Vladimir Soukup , 1988

In presenting this thesis in partial fulfilment of the requirements for an advanced degree at the University of British Columbia, I agree that the Library shall make it freely available for reference and study. I further agree that permission for extensive copying of this thesis for scholarly purposes may be granted by the head of my department or by his or her representatives. It is understood that copying or publication of this thesis for financial gain shall not be allowed without my written permission.

Department of Electrical Engineering

The University of British Columbia
Vancouver, Canada

Date Sept. 23, 1988

Abstract

Magnetic bearings have recently begun to be employed in rotating machinery for vibration reduction, elimination of oil lubrication problems and prevention of failures. This thesis presents an analysis and design of an experimental model of a magnetic suspension system. The magnetic bearing, its control circuit and the supported object are modeled. Formulas are developed for the position and current stiffness of the bearing and the analogy with a mechanical system is shown. The transfer function is obtained for the control and experimental results are presented for the double pole one axis magnetic support system.

Table of Contents

Abstract	ii
List of Figures	v
1 INTRODUCTION	1
2 DYNAMIC MODEL OF MAGNETIC BEARINGS	6
2.1 Introduction	6
2.2 Lifting Force of an Electromagnet	6
2.3 Stiffness of Magnetic Bearings	9
2.4 Mechanical Analogy of Magnetic Bearing	11
2.5 Mathematical Model of Magnetic Bearing	13
3 SOLUTION OF THE DIFFERENTIAL EQUATION	15
3.1 Introduction	15
3.1.1 Critical Points of a System	16
3.1.2 Transformation of the 2 nd Order to the 1 st Order Differential Equations	17
4 LINEARIZED MODEL OF MAGNETIC BEARINGS	21
4.1 Introduction	21
4.2 Linear Approximation of an Electromagnetic Force	22
4.3 Linearized Model and the Transfer Function	23

5	IMPLEMENTATION OF A MAGNETIC BEARING	26
5.1	Introduction	26
5.2	Velocity Transducer	27
5.3	Position Transducers	28
5.4	Power Drivers	31
5.4.1	Voltage Driver	31
5.4.2	Current Feedback	33
5.4.3	Current Driver	34
6	MEASUREMENTS	36
6.1	Introduction	36
6.2	Double Ended and Single Ended Models	36
6.3	Electric Time Constant of the Electromagnet	38
6.4	Position Constant of the Hall Effect Sensor	39
6.5	Velocity Constant	39
6.6	Measurement of The Position Stiffness	41
7	CONCLUSIONS	45
	Bibliography	47
	APPENDIX	49

List of Figures

1.1	Model for a Magnetic Suspension System	2
1.2	Radial Suspension of a Rotor	3
2.3	Coordinate System of the Double Ended Suspension System	7
2.4	The Electromagnet	7
2.5	Model of an Analogous Mechanical System	11
2.6	Characteristic Roots of a Second Order System in the Complex Plane .	13
4.7	Graphical Representation of Transfer Function Poles in the s plane . . .	24
5.8	Velocity Transducer	27
5.9	Resonant Circuit Measurement Method	29
5.10	Phase-Locked Loop	29
6.11	Voltage vs. Current in a Series RL Circuit	38
6.12	Measurement of the Velocity Constant	40

Chapter 1

INTRODUCTION

The idea of suspending a mechanical object in a magnetic field is not new. It spans nearly 150 years back to the year 1842 when S. Earnshaw [1] developed a theorem which states that a system using permanent magnets or electromagnets without control of current is inherently unstable. His work was later followed by W. Braunbeck [2] and others. Although Earnshaw was right, there are now magnetic suspension systems that use both permanent magnets and electromagnets with controlled currents together in that the permanent magnets are employed to carry all static loads whereas the electromagnets are used just for control purposes to stabilize the system. These systems are known as VZP (for " Virtually Zero Power "), because such an arrangement results in minimal power requirements since they approach zero power consumption as a limit, regardless of how much mass is suspended. This type of suspension system is especially convenient in applications where space, weight and power are limited.

Now a magnetically suspended 1100 kg shaft capable of spinning at 10,000 rpm or higher is becoming a commercial reality. Already such shafts turning at various speeds are being used in grinding and polishing machinery, vacuum pumps, compressors, turbines, generators and centrifuges. Electronically controlled magnetic bearings offer two major advantages: there is no mechanical wear and no frictional losses or lubrication requirements.

In order to fully position a rotating shaft, a magnetic force must be applied along five axes: two perpendicular axes at each shaft end and a fifth axis parallel to the

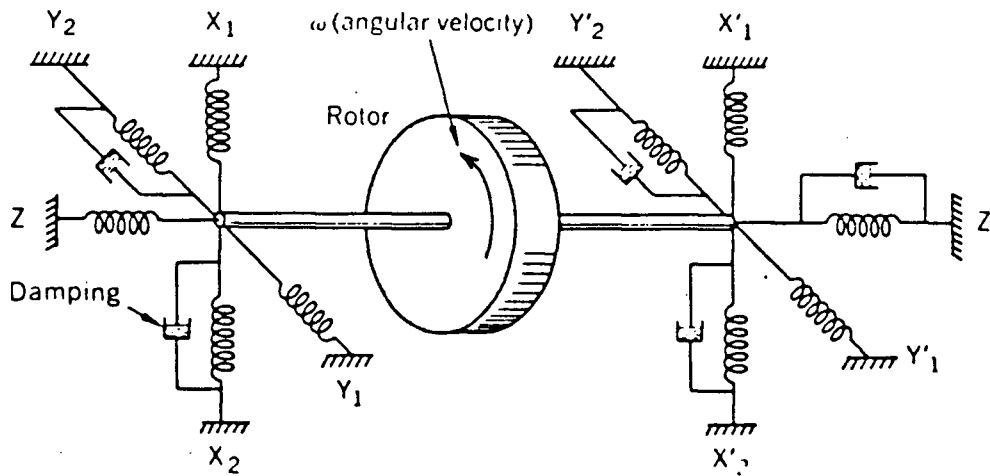


Figure 1.1: Model for a Magnetic Suspension System

shaft's rotational axis. A complete model [3] for such a suspension system resembles a set of springs and dampers where each spring represents one electromagnet and is shown in Fig.1.1. This thesis deals with analysis and design of just one axis control (axial suspension). Once the control circuitry is developed and its characteristics found satisfactory, it will be used in the remaining axes as well.

The electronic system is intended to control the position of the rotor by acting on the current in the electromagnets on the basis of the signal from the position and velocity sensors. The signal from the position sensor is compared with the difference signal, which defines the rotor's nominal position. If the reference signal is zero, the nominal position is in the centre of stator. By acting upon the reference signal, it is possible to shift the nominal position of the shaft by up to half the air gap. The error signal is proportional to the difference between the nominal position and actual position of the

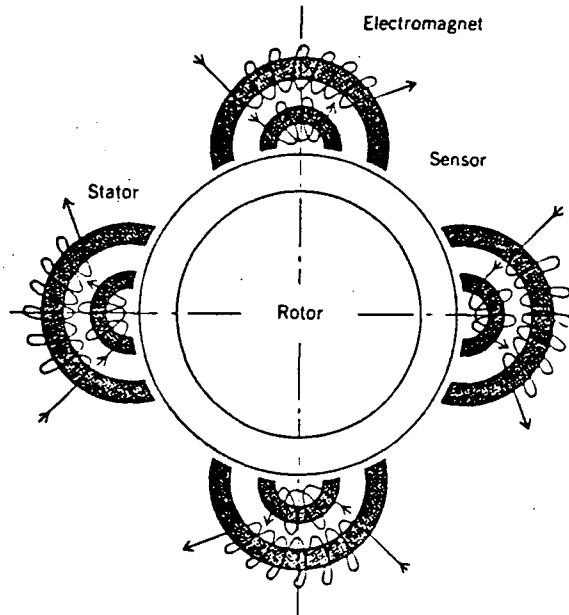


Figure 1.2: Radial Suspension of a Rotor

rotor in any given time. This signal is transmitted to the analog signal processing part which produces a control signal to the power amplifier. The ratio of the output signal to the error is chosen so as to maintain the rotor as precisely as possible at its nominal position and to return it rapidly to the nominal position, with a well damped movement, in the event of any disturbance. The servo system defines the stiffness and damping of the magnetic suspension.

Practical radial suspension [4], as shown in Fig.1.2., is used on each end of the shaft. In this arrangement there is no mechanical contact between rotor and stator. Rotor size has little effect on the signal processing of the control circuit. Only the power amplifier design depends on bearing capacity.

The time constants of typical electromagnets might be as large as several hundred milliseconds and yet the magnet-amplifier combination must act as a closed loop control system with a bandwidth of at least 10 kHz [5]. A fairly substantial reserve voltage

to force rapid current change in the electromagnet, in order to overcome the inductive voltage, is therefore an essential feature in the design of DC power amplifiers for controlled DC electromagnets. This requirement can lead to large power dissipation and low efficiencies in quiescent operating conditions.

Switching amplifiers are much more efficient than linear amplifiers and only converters of this type are considered in this thesis. The switching amplifiers can cover a wide range of power ratings from small applications, such as spindles for revolving mirrors where very high rotating speed and high speed stability is required, to large turbine generators where magnetic bearings do not require regular maintenance. High frequency switching amplifiers (choppers), using pulse-width modulation to control a duty-ratio of the switching element and thus electric current for the electromagnets, provide an effective and economical solution. This is described in more detail in Chapter 5.

In order to modify the force-distance characteristic so that the current in the electromagnet, and thus the force of attraction, decreases as the gap decreases (and vice versa), some form of feedback control must be used. From physical laws governing the equation of an electromagnet it becomes obvious that the system is highly nonlinear.

To analyze this system and to explore possible linearization techniques in the case of a vertical arrangement of the magnetic bearing is the purpose of this thesis.

The chapters in the thesis are arranged to form logical blocks. The general case of an electromagnet is discussed in Chapter 2, covering the derivation of equations for the lifting force and position and current stiffnesses. The analogy to a mechanical system is also briefly described. The differential equation governing the non-compensated, unstable magnetic system is also derived here. Chapter 3 is focused more on the nonlinear equation and finding the type of singularity, by using a linearized form of the equation.

Chapter 4 continues with the linearized equation and a transfer function of the uncompensated system is found. Chapter 5 describes the practical realization of the magnetic bearing and gives an evaluation of different types of control. Some experimental results are given which are supplemented by material in Appendix. Chapter 6 discusses the measurement techniques, used to calibrate the actual model for the calculations and computer simulation. Overall conclusions are presented in chapter 7.

Chapter 2

DYNAMIC MODEL OF MAGNETIC BEARINGS

2.1 Introduction

In this chapter equations for the lifting force of an electromagnet and stiffnesses of the double-ended axial magnetic suspension will be deduced. A simplified view of such an arrangement and its coordinate system is introduced in Fig.2.3. Several assumptions will be made and their correctness will be evaluated in the conclusions of this thesis.

2.2 Lifting Force of an Electromagnet

An equation for the lifting force of a single electromagnet [9] can be obtained from the work done in the magnetic system to change the field energy as

$$F = -\frac{1}{2}i^2 \frac{dL}{dx} \quad (2.1)$$

where L is an inductance and x is an air gap of the electromagnet. For further analysis a few assumptions are made:

- magnetic reluctance of the iron core of the electromagnet is negligible in comparison to the reluctance of the air gap
- flux levels are well below saturation limits
- fringing and leakage effects are neglected

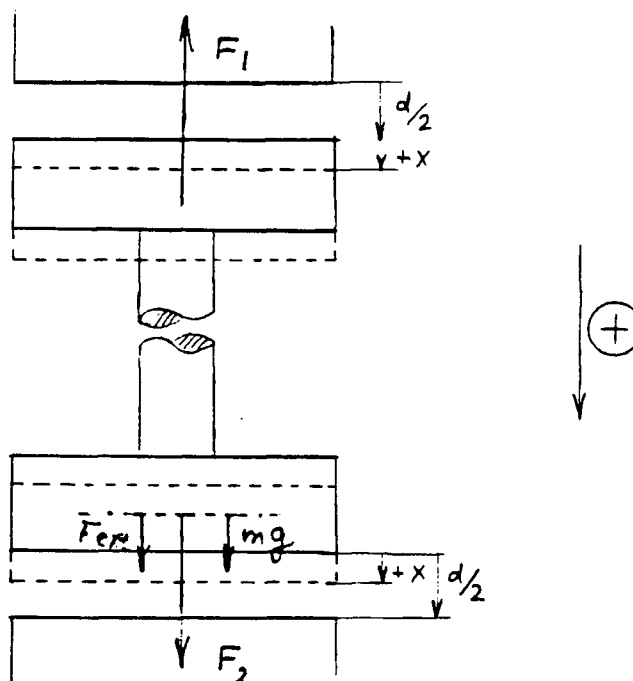


Figure 2.3: Coordinate System of the Double Ended Suspension System

For an electromagnet such as shown in Fig.2.4 the inductance is expressed as

$$L = \frac{N^2}{R_m} \quad (2.2)$$

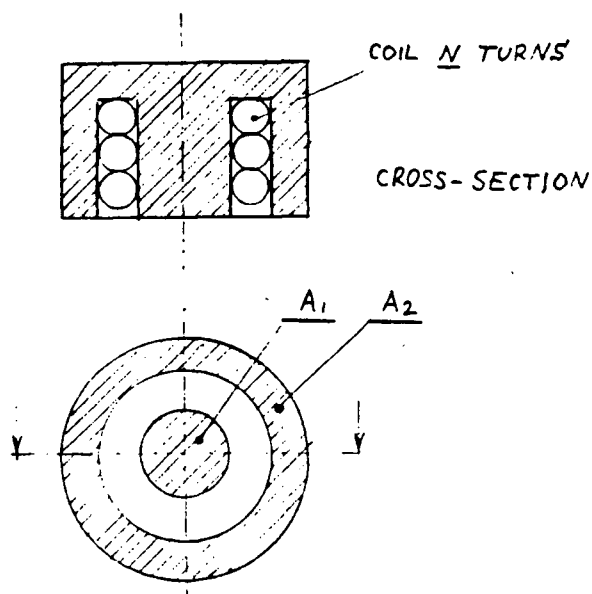


Figure 2.4: The Electromagnet

where the magnetic reluctance R_m

$$R_m = \frac{d/2 + x}{\mu_0 A_1} + \frac{d/2 + x}{\mu_0 A_2} = \frac{(d/2 + x)}{\mu_0} \left(\frac{1}{A_1} + \frac{1}{A_2} \right) \quad (2.3)$$

and using

$$\frac{1}{A_1} + \frac{1}{A_2} = \frac{A_1 + A_2}{A_1 A_2}$$

equation (2.3) can be written as

$$R_m = \frac{(d/2 + x)}{\mu_0} \left(\frac{A_1 + A_2}{A_1 A_2} \right) \quad (2.4)$$

Symbols used :

H [A/m]... magnetic field intensity

A_1, A_2 [m²]... cross-sectional area

B [T]... magnetic flux density

μ_0 [H/m]... permeability of free space

Φ [Wb]... magnetic flux

L [H]... inductance

R_m [1/H]... magnetic reluctance

N ... number of turns of the coil

x [m]... air gap

now the equation (2.4) can be substituted into (2.2), yielding

$$L = \frac{\mu_0 N^2}{(d/2 + x)} \left(\frac{A_1 A_2}{A_1 + A_2} \right) \quad (2.5)$$

and

$$\frac{dL}{dx} = - \frac{2\mu_0 N^2}{(d/2 + x)^2} \left(\frac{A_1 A_2}{A_1 + A_2} \right) \quad (2.6)$$

The magnetic flux can be derived from the magnetic equation

$$R_m \Phi = Ni \quad (2.7)$$

as

$$\Phi = \frac{Ni}{R_m} = \frac{Ni}{\frac{d/2+x}{\mu_0} \frac{A_1 A_2}{A_1 + A_2}} = \mu_0 N \left(\frac{A_1 + A_2}{A_1 A_2} \right) \frac{i}{(d/2 + x)} \quad (2.8)$$

and finally the force

$$F_1 = -\frac{1}{2} i^2 \left(\frac{-2\mu_0 N}{(d/2 + x)^2} \right) \frac{A_1 A_2}{A_1 + A_2} = \mu_0 N^2 \left(\frac{A_1 A_2}{A_1 + A_2} \right) \frac{i^2}{(d/2 + x)^2} \quad (2.9)$$

As μ_0, N, A_1, A_2 , are constants, equation (2.9) can be simplified to

$$F_1 = K \frac{i^2}{(d/2 + x)^2} \quad (2.10)$$

and similarly

$$F_2 = K \frac{i^2}{(d/2 - x)^2}$$

where

$$K = \mu_0 N^2 \left(\frac{A_1 A_2}{A_1 + A_2} \right) \quad (2.11)$$

From the analysis done so far, it is obvious that the lifting force of an electromagnet depends on two variables: the current i and the air gap x , and that the equation is not a linear function.

2.3 Stiffness of Magnetic Bearings

Since there are two independent parameters that can change, position x and current i , equation (2.10) can be used to define a position and current stiffness as

POSITION STIFFNESS:

$$K_x = \frac{\partial F_1}{\partial x} = -2K \frac{i^2}{(d/2 + x)^3}, \quad i = \text{const.} \quad (2.12)$$

CURRENT STIFFNESS:

$$K_i = \frac{\partial F_1}{\partial i} = 2K \frac{i}{(d/2 + x)^2}, \quad x = \text{const.} \quad (2.13)$$

Partial derivatives ∂x , ∂i are used rather than dx , di since the force F is a function of two independent variables x and i .

The stiffness terminology was used here since the situation is analogous to a spring. However, for the electromagnet the effective stiffness is negative; this reflects the physical behaviour in which a positive displacement of the shaft $+x$, from the top electromagnet, decreases the attractive force. Conversely, an actual spring would apply a force tending to restore the original position of the mass. The consequence of the negative spring stiffness causes the system to be essentially unstable.

In the compensated system a closed loop control is used to stabilize the position by changing the current and the effective stiffness.

2.4 Mechanical Analogy of Magnetic Bearing

There is an analogy between an electromagnet and the mass-spring-damper mechanical system [17]. The case of a mechanical system is shown in Fig.2.5.

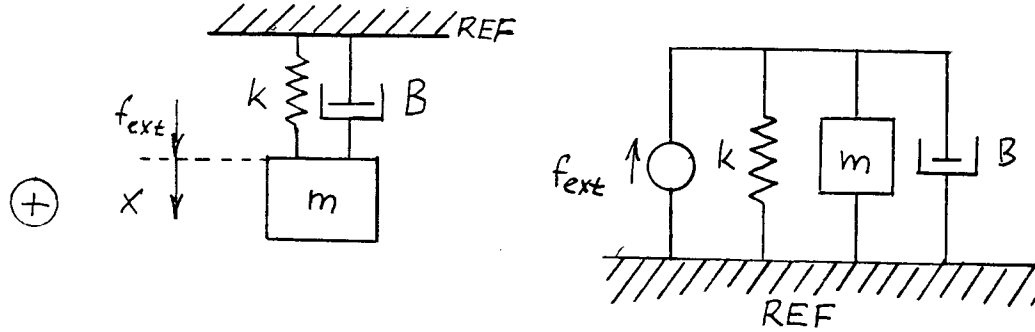


Fig.2.5: (a) simple mass-spring-damper mechanical system (b) corresponding network

The end of the spring and the damper have positions denoted as the reference position. If a force f_{ext} is applied to the mass m it will result in a displacement x . This displacement must be balanced by an extension of the spring forcing the mass to the original position. Fig.2.5(a) can be drawn into a network in Fig.2.5(b). According to Newton's law, sum of the forces at each node must add to zero. There is only one node here and the equation is

$$f_{ext}(t) = m\ddot{x} + B\dot{x} + kx$$

where x , \dot{x} and \ddot{x} are the displacement, velocity and acceleration of the mass m , B represents the damping and k is elastance or stiffness, which provides a restoring force represented by the spring. Assuming that m , B and k are constants and all initial conditions are zero, the Laplace transform can be used yielding

$$F_{ext}(s) = s^2 X(s)m + sX(s)B + X(s)k$$

and the transfer function between $F_{ext}(s)$ and the resulting displacement $X(s)$ is

$$\frac{X(s)}{F_{ext}(s)} = \frac{1}{m(s^2 + s\frac{B}{m} + \frac{k}{m})}$$

The expression

$$s^2 + s\frac{B}{m} + \frac{k}{m} = 0 \quad (2.14)$$

is called the *characteristic equation* of the system from Fig.2.5. Its roots reflect the behaviour of the system. Eq.2.14 can be compared to

$$s^2 + 2\xi\omega_n s + \omega_n^2 = 0 \quad (2.15)$$

yielding $\omega_n = \sqrt{\frac{k}{m}} \quad \xi = \frac{B}{2m\omega_n} \quad (2.16)$

Location of s roots in eq.2.14 corresponds to the stability and dynamic characteristics of the system.

In case of a single electromagnet with constant current any displacement of the mass from the balanced position will result in further move either towards or from the magnet. Thus the electromagnet with a constant current demonstrates a negative stiffness k . This instability is also apparent from the location of roots of eq.2.14. (Fig 2.6.), due to the positive real root, in the s -plane.

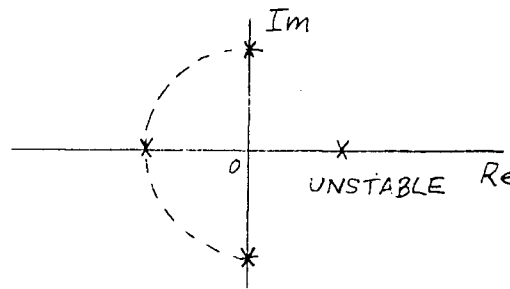


Figure 2.6: Characteristic Roots of a Second Order System in the s - Plane

To achieve a stable magnetic suspension the current in the electromagnet must be controlled, which will effectively change the negative stiffness k to a positive value and remove the positive root from the s -plane.

2.5 Mathematical Model of Magnetic Bearing

To obtain a mathematical model of the magnetic bearing an **equation of motion** is used which, for any mechanical model, is Newton's law

$$F = ma \quad (2.17)$$

where

$F[\text{N}]$... vector sum of all forces applied to the body in the system

$a[\text{ms}^{-2}]$... acceleration

$g[\text{ms}^{-2}]$... gravity constant

$m[\text{kg}]$... mass of the body

Application of this law involves defining convenient coordinates to account for the body's motion, i.e. **position, velocity and acceleration**. A simplified arrangement of the vertical magnetic bearing is shown in Fig. 2.3.

Here the total gap d is equal to the top plus bottom gap (in the state of equilibrium $d/2$ and $d/2$). F_1, F_2 are attractive forces of the top and bottom electromagnet.

The equation of motion can be written as

$$m \frac{d^2 x}{dt^2} = mg + F_2 - F_1 + F'_{ext} \quad (2.18)$$

or by using

$$\frac{d^2 x}{dt^2} = \ddot{x}$$

as

$$m\ddot{x} = mg + K \frac{i_2^2}{(d/2 - x)^2} - K \frac{i_1^2}{(d/2 + x)^2} + F'_{ext} \quad (2.19)$$

the term mg can be lumped together with F'_{ext} as F_{ext} and the equation can be written as

$$\ddot{x} = \frac{K}{m} \frac{i_2^2}{(d/2 - x)^2} - \frac{K}{m} \frac{i_1^2}{(d/2 + x)^2} + \frac{F_{ext}}{m} \quad (2.20)$$

The coordinate system is symmetrical around $d/2$ (as was shown in Fig.2.3), where $d/2$ is the origin of the new coordinate system. Thus x can vary in the range from $-d/2$ to $d/2$, where d is the total air gap of both electromagnets.

Chapter 3

SOLUTION OF THE DIFFERENTIAL EQUATION

1.1 Introduction

A function f is linear if:

$$f(x_1 + x_2) = f(x_1) + f(x_2) \quad (3.21)$$

and for any real number α

$$f(\alpha x) = \alpha f(x) \quad (3.22)$$

Any other function is nonlinear.

Equation (2.20), obtained from the equation of motion, evidently does not meet the above conditions. It is a nonlinear second order differential equation with time invariant coefficients.

Since frequency response techniques and root locus diagrams are not applicable to nonlinear systems, there is a need for a graphical tool to allow nonlinear behavior to be displayed. The **phase plane diagram**, which plots velocity $\dot{x}(t)$ vs. displacement $x(t)$, is a convenient technique. Although it is applicable only to second order processes, it can be used for higher order systems, which can be approximated by a second order equation. The variation of velocity $\dot{x}(t)$ vs. displacement $x(t)$ for a specific initial condition is called a **trajectory**. A set of trajectories for several initial conditions is called a **phase portrait**.

Let Σ represent a nonlinear second order dynamic system [13], which has two state variables x_1, x_2 . The vector $\mathbf{x} = (x_1, x_2)^T$ is an *element* of the real two-dimensional state space X or briefly $\mathbf{x} \in X$.

In the case where system Σ is time invariant and receives no input, $\mathbf{x}(t)$ is determined by $t, \mathbf{x}(0)$ and Σ . Thus:

$$\Sigma(t, \mathbf{x}_0) = \mathbf{x}(t)$$

and $\mathbf{x}(t)$ is called a *particular solution* for the system Σ .

The *trajectory* through any point $\mathbf{x} \in X$ is denoted $\pi(\mathbf{x})$ and is defined as

$$\pi(\mathbf{x}) = [\mathbf{x}(t) \mid \mathbf{x}(0)] = \mathbf{x}, \quad -\infty < t < \infty$$

The *positive semi-trajectory* π^+ through \mathbf{x} is defined

$$\pi^+(\mathbf{x}) = [\mathbf{x}(t) \mid \mathbf{x}(0)] = \mathbf{x}, \quad 0 < t < \infty$$

A point $\mathbf{x} \in X$ is called a *critical point* of the system Σ if

$$\Sigma(t, \mathbf{x}) = \mathbf{x}$$

for every $t \in \mathbb{R}^1$

3.1.1 Critical Points of a System

Critical (singular) points of a system are points of dynamic equilibrium. They correspond to positions of rest for the system and may be stable or unstable. The significant feature of a critical point is that all derivatives are zero. In other words, the derivatives of the state variables are zero.

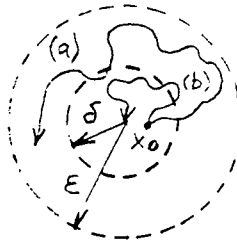
A critical point of the system Σ is:

(a) **stable** if, given a circular region of radius $\delta > 0$ around the critical point, there exists another circular region of radius ϵ concentric with the δ region, where $\epsilon > \delta$, such that every positive half trajectory starting in the δ region remains within the ϵ region.

A solution $\mathbf{x}(t)$, originating at $\mathbf{x}_0(t)$, t_0 is stable with respect to the critical point $\tilde{\mathbf{x}}$ if:

(1) $\mathbf{x}(t)$ is defined for all t satisfying $t_0 < t < \infty$

(2) if $|\mathbf{x}_0 - \tilde{\mathbf{x}}| < \delta$, for some positive constant δ , then there exists another positive constant ϵ such that $|\mathbf{x}(t) - \tilde{\mathbf{x}}| < \epsilon$, $\forall t \in (t_0, \infty)$



(b) **asymptotically stable** if, it is stable and if in addition, every half trajectory satisfying the conditions in (a), reaches the critical point in the limit as $t \rightarrow \infty$.

A solution is asymptotically stable to the critical point $\tilde{\mathbf{x}}$ if it is stable and in addition

$$\lim_{t \rightarrow \infty} |\mathbf{x}(t) - \tilde{\mathbf{x}}| = 0$$

Unlike linear systems, which have only one type of behaviour everywhere in the phase plane, nonlinear systems can have many different types of behaviour in different regions. If a linear approximation can be done in each region, then the knowledge of the whole system can be obtained.

3.1.2 Transformation of the 2nd Order to the 1st Order Differential Equations

If the nonlinear differential equation cannot be easily integrated, then a linearized form

of the equation can be obtained by means of Taylor or MacLaurin expansion. Once the linear form of the second order differential equation is available it can be rewritten into a form of two coupled differential equations of the first order.

Starting with the original nonlinear differential equation (2.20) and assuming $F_{ext}=0$

$$\ddot{x} = \frac{K}{m} \left[\frac{i_2^2}{(d/2 - x)^2} - \frac{i_1^2}{(d/2 + x)^2} \right] \quad (3.23)$$

The expansion with respect to x will be made about point $x = 0$ (i.e. MacLaurin expansion).

The current can be set to $i_1 = i_2 = i$ (const.) and the linearized differential equation will be derived:

$$\begin{aligned} \ddot{x}(x, i) &\approx \ddot{x}(0, i) + \frac{\partial \ddot{x}(0, i)}{\partial x} x \\ \ddot{x}(0, i) &= \frac{K}{m} \frac{i^2}{(d/2)^2} - \frac{K}{m} \frac{i^2}{(d/2)^2} = 0 \\ \frac{\partial \ddot{x}(0, i)}{\partial x} &= \frac{2K}{m} \frac{i^2}{(d/2)^3} + \frac{2K}{m} \frac{i^2}{(d/2)^3} = \frac{32Ki^2}{md^3} \end{aligned}$$

Thus the linearized equation will be:

$$\ddot{x}(x, i) \approx \frac{32Ki^2}{md^3} x$$

This equation can be written as a set of coupled differential equations and the character of the critical point determined according to the following theorem:

Let Σ be a second order linear system described by the equation:

$$\dot{\chi} = A\chi$$

A critical point occurs at

$$\dot{\chi} = \begin{pmatrix} 0 \\ 0 \end{pmatrix}$$

and the type of singularity depends on the eigenvalues of the matrix A accordingly:

- real and negative λ_1, λ_2 indicate *stable node*
- real and positive λ_1, λ_2 indicate *unstable node*
- real λ_1, λ_2 of opposite sign indicate *saddle point*
- complex λ_1, λ_2 with a negative real part indicate *stable focus*
- complex λ_1, λ_2 with a positive real part indicate *unstable focus*
- imaginary λ_1, λ_2 of opposite sign indicate *centre*

Using the linearized second order equation and making the following substitution :

$$x = x_1$$

$$\dot{x}_1 = x_2$$

yields

$$\dot{x}_1 = x_2 \tag{3.24}$$

$$\dot{x}_2 = \frac{32Kt^2}{md^3}x_1 \tag{3.25}$$

These two equations can be expressed in a matrix form:

$$\dot{\chi} = A\chi \tag{3.26}$$

where

$$\dot{\chi} = \begin{pmatrix} \dot{x}_1 \\ \dot{x}_2 \end{pmatrix} \tag{3.27}$$

$$A = \begin{pmatrix} a_{11} & a_{12} \\ a_{21} & a_{22} \end{pmatrix} \tag{3.28}$$

$$\chi = \begin{pmatrix} x_1 \\ x_2 \end{pmatrix} \quad (3.29)$$

Example

Equations (3.24), (3.25) can be evaluated for one practical situation:

$$K = 15.006 \times 10^{-6}$$

$$m = 0.683 \text{ kg}$$

$$d = 0.003 \text{ m (i.e. top and bottom air gap 1.5 mm)}$$

$$i_1 = i_2 = 2 \text{ A}$$

Then the A matrix will be

$$\mathcal{A} = \begin{pmatrix} 0 & 1 \\ 72670 & 0 \end{pmatrix} \quad (3.30)$$

with eigenvalues +269 and -269. Here, the eigenvalues are real and of opposite sign which indicates a **saddle point**.

Chapter 4

LINEARIZED MODEL OF MAGNETIC BEARINGS

4.1 Introduction

A great majority of physical systems are linear within some range of the variables. However, all systems ultimately become nonlinear as the variables are increased without limit.

A system is defined as linear in terms of the system excitation and response. In general, a *necessary condition of linearity* was given in the previous chapter by eq.(3.21) and (3.22). The physical meaning is as follows:

when the system at rest is subjected to an excitation $x_1(t)$, it provides a response $y_1(t)$. Furthermore, when the system is subjected to an excitation $x_2(t)$, it provides a corresponding response $y_2(t)$. For a linear system, it is necessary that the excitation $x_1(t) + x_2(t)$ results in a response $y_1(t) + y_2(t)$. This is called the principle of *superposition*.

Furthermore, it is necessary that the magnitude scale factor is preserved in the linear system. Again, consider a system with an input $x(t)$ which results in an output $y(t)$. Then it is necessary that the response of a linear system to a constant multiple α of an input $x(t)$ is equal to the response to the input multiplied by the same constant so that the output is equal to $\alpha y(t)$. This is called a property of *homogeneity*.

4.2 Linear Approximation of an Electromagnetic Force

In the case of the magnetic bearing, it was shown in Chapter 2, that the equations describing the system are highly nonlinear. Since, for a nonlinear system the *principle of superposition* does not hold, the Laplace transform cannot be used and a transfer function cannot be defined. It is very difficult to obtain some useful information about the system and to control it by using classical control methods.

The force-distance characteristic (Appen. p.54) shows that the measured characteristic resembles a straight line in the range of interest (i.e. $<0, 3>$ mm). Since the magnetic bearing is designed to operate at a fixed point ($d/2 = 1.5$ mm), the system is clearly a good candidate for linearization at that point. The **linear model** then represents behaviour of the system to a small signal or **perturbation** from the equilibrium point.

A nonlinear equation can be expressed in a Taylor expansion about a point x_0 or similarly in a McLaurin expansion about the point $x_0 = 0$. As the equation of the lifting force is a function of two variables (x, i) , the linearized equation will be:
will be:

$$F(x, i) \approx F(x_0, i_0) + \frac{\partial F(x_0, i_0)}{\partial x} x + \frac{\partial F(x_0, i_0)}{\partial i} i \quad (4.33)$$

the linearization can be illustrated by placing a *tangent plane* onto the nonlinear surface $f(x, i)$ in the point x_0, i_0 .

The lifting force of an electromagnet can be linearized about point (x_0, i_0) as above eq.(4.33). The forces F_1, F_2 were found in Chapter 1 to be

$$F_1 = K \frac{i_1^2}{(d/2 + x)^2} \quad (4.34)$$

$$F_2 = K \frac{i_2^2}{(d/2 - x)^2} \quad (4.35)$$

The linearized form of the forces F_1 , F_2 about an equilibrium point $x_0 = 0$ and i_{10} (resp. i_{20})

$$F_1(x, i) \approx K \frac{i_{10}^2}{(d/2)^2} - 2K \frac{i_{10}^2}{(d/2)^3} x + 2K \frac{i_{10}}{(d/2)^2} i \quad (4.36)$$

$$F_2(x, i) \approx K \frac{i_{20}^2}{(d/2)^2} + 2K \frac{i_{20}^2}{(d/2)^3} x + 2K \frac{i_{20}}{(d/2)^2} i \quad (4.37)$$

Note that $+x$ and $+i$ represent increments of the displacement and current..

4.3 Linearized Model and the Transfer Function

Now, the equation of motion

$$m\ddot{x} = F_2 - F_1 + F_{ext}$$

can be written, using linearized forces as

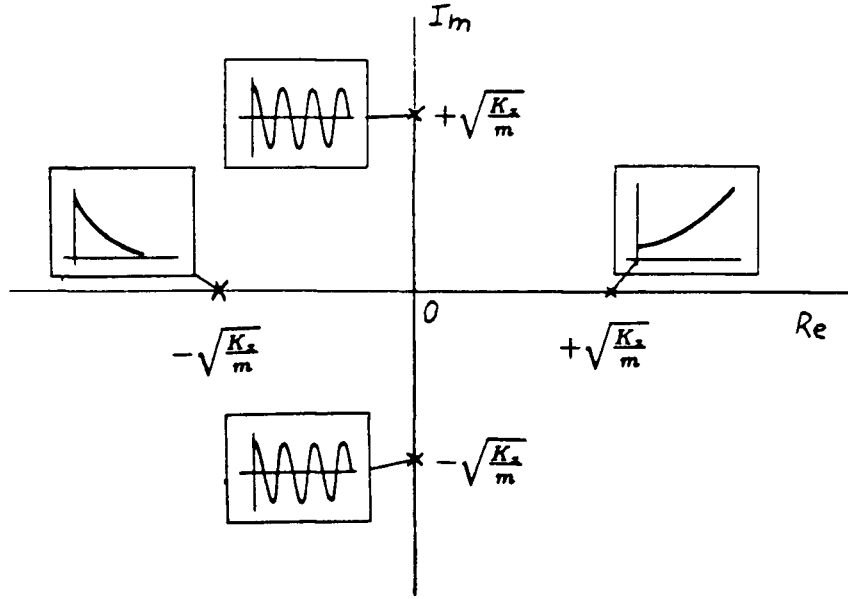
$$m\ddot{x} = K \frac{i_{20}^2}{(d/2)^2} + 2K \frac{i_{20}^2}{(d/2)^3} x + 2K \frac{i_{20}}{(d/2)^2} i - K \frac{i_{10}^2}{(d/2)^2} + 2K \frac{i_{10}^2}{(d/2)^3} x - 2K \frac{i_{10}}{(d/2)^2} (-i) + F_{ext} \quad (4.38)$$

A negative sign in $(-i)$ means a decrease of current in the top coil (F_1) as an opposite of the increase $(+i)$ of current in the bottom coil (F_2). It is assumed that $|+i| = |-i|$ in both coils. In a steady state the shaft will be in a stable position between the two electromagnets. The forces F_1 , F_2 will provide a resulting steady state force (due to bias currents i_{10} and i_{20}) which will compensate weight of the shaft (mg is part of F_{ext}):

$$K \frac{i_{20}^2}{(d/2)^2} - K \frac{i_{10}^2}{(d/2)^2} + F_{ext} = 0$$

The resulting equation using the stiffnesses (eq. 2.12, 2.13) will simplify to

$$m\ddot{x} = -K_x x - K_i i \quad (4.39)$$

Figure 4.7: Graphical Representation of Transfer Function Poles in the s plane

where

$$K_z(0, i_{10}, i_{20}) = 2K \frac{i_{10}^2}{(d/2)^3} + 2K \frac{i_{20}^2}{(d/2)^3}$$

$$K_i(0, i_{10}, i_{20}) = 2K \frac{i_{10}}{(d/2)^2} + 2K \frac{i_{20}}{(d/2)^2}$$

Now, the magnetic bearing can be approached as a linear system with small perturbations of current i , as an input and the air gap x , as an output. In order to express the transfer function (i.e. output x to input i), the equation of motion must be transformed from the *time domain* to the *s domain* by means of the **Laplace transformation**. Suppose that the initial conditions are all zero and there is no damping; then the equation (4.38) can be transformed into the s domain by means of Laplace transformation as

$$s^2 X(s)m = -K_z X(s) - K_i I(s) \quad (4.40)$$

Both K_z and K_i are negative so the mass simply accelerates to the surface of the

electromagnet. Thus no electromagnet by itself can operate as a bearing. Solving the equation of motion for the ratio $X(s)/I(s)$ gives

$$\frac{X(s)}{I(s)} = \frac{-K_i/m}{s^2 + K_z/m} \quad (4.41)$$

where K_z and K_i are negative values. Thus the roots of the system equation are $+\sqrt{\frac{K_z}{m}}$ and $-\sqrt{\frac{K_z}{m}}$. Due to the the positive root the system is unstable.

This is the case of a *negative spring* compared to a genuine spring (with no damping) where its roots would be both imaginary $+j\sqrt{\frac{K_z}{m}}$ and $-j\sqrt{\frac{K_z}{m}}$ located on the imaginary axis symmetrically to the origin. In that case there would be undamped oscillations with a *natural frequency* of

$$\omega_n = \sqrt{\frac{K_z}{m}}$$

And in a case with added damping the poles would be complex conjugates placed in the left half plane, so that the oscillations would cease in a finite time. The graphical representation is shown in Fig.4.7.

Chapter 5

IMPLEMENTATION OF A MAGNETIC BEARING

5.1 Introduction

Based on the theoretical analysis in Chapters 1, 2, 3 and the resulting linearized model in Chapter 4, several variants of the one axis magnetic suspension control circuits were built and tested for stability and reliability.

An evolution of the control circuitry followed practical experience and gained insight into the problems. After experimenting with different sensors and power drivers a simple, stable and reliable controller was constructed and is presented in this thesis. Three different ways of controlling the electromagnets were investigated and built. The comparison of their functions and the evaluation of results are discussed later in the conclusions.

The most critical part of any system is its interfacing with the physical environment i.e. the input sensors. The system developed here uses both position and velocity transducers and the quality of signals produced by them is very critical for the whole system. Experiments with substitution of the velocity signal by differentiating the position signal were also performed. The resulting lead forward compensator could not be practically used here, mainly because of the position signal quality. Any noise in the position signal is emphasized after differentiation. For this reason both velocity and position transducers are normally required in practice. A procedure for designing a lead compensator from a root-locus diagram is presented in the Appendix.

This compensator was tested experimentally, but the results confirmed the need for a separate velocity signal.

This chapter presents the evaluation of a practical design for the velocity and position sensors and discusses the design of a practical power circuit.

5.2 Velocity Transducer

The original velocity transducer consisted of an air coil with a permanent magnet connected with the shaft as shown in Fig.5.8(a). The resulting velocity signal was very

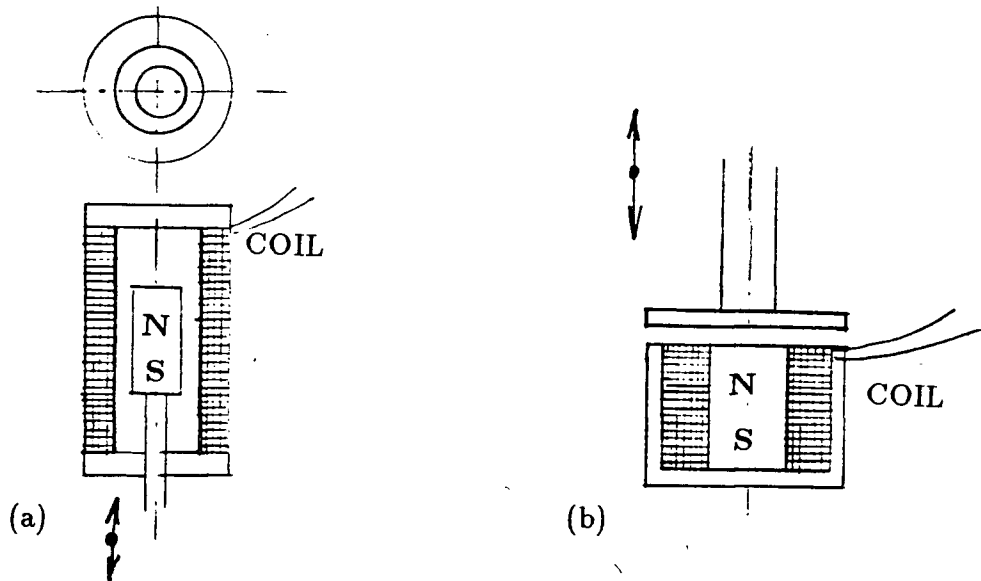


Figure 5.8: Velocity Transducer

small and sensitive to any external magnetic disturbance. A new transducer was built and it is shown in the same figure in (b). In that new design the coil is magnetically shielded by a ferromagnetic case which forms part of the magnetic circuit. The magnetic field is formed by a permanent magnet in the middle of the sensing coil. This way the resulting output voltage is proportional to axial velocity while practically insensitive to a radial movement. Since the gap between moving plate and the coil is very small, no noise is induced and the signal is of a very good quality.

The voltage induced in the coil is

$$v = N \frac{d\Phi}{dt}$$

where N represents number of turns of the coil and $\frac{d\Phi}{dt}$ is a change of magnetic flux, by change of the magnetic reluctance of the magnetic circuit.

The output voltage of the transducer can be easily increased either by increasing number of turns N or by adding a small amplifier close to the transducer: (as was done here).

5.3 Position Transducers

Several methods were used to sense the displacement of the shaft, with different results.

Resonant Circuit

A circuit consisting of a series arrangement of a coil L and a capacitor C was used in this method. A frequency generator was used to produce a sinusoidal signal with a frequency set on the side of the resonant curve. A change of inductance L then results in a change of the output voltage across the resonant circuit LC . The high frequency output signal is then processed by a peak detector to provide a DC voltage. This method did not provide a stable, reliable signal. One reason was that the frequency generator was not very stable and any change in the frequency or the amplitude added an unwanted offset which required manual correction. Also since the peak detector provides an "envelope" of the detected signal, any outside disturbance is automatically included in the resulting signal.

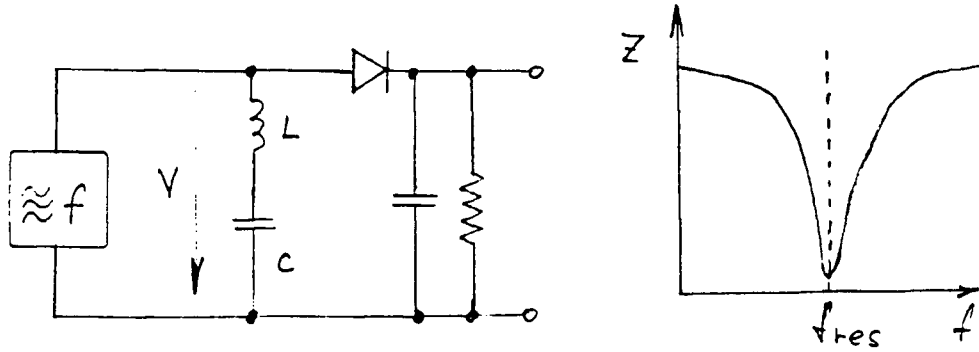


Figure 5.9: Resonant Circuit Measurement Method

Frequency Detector

In this circuit the sensing coil L forms a part of an oscillator [6] of frequency :

$$f = \frac{1}{2\pi\sqrt{LC}}$$

Thus as the inductance is changed by an axial displacement of the shaft the resulting change in frequency can be detected by a phase detector. A convenient solution [7], [8], provides a Phase-Locked Loop (PLL) circuit, which operates as following: a phase

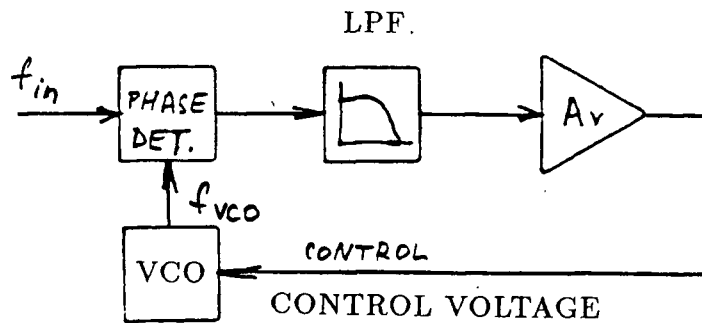


Figure 5.10: Phase-Locked Loop

detector compares two input frequencies and the output is a measure of their difference. If they differ in frequency, it gives a periodic output at the difference frequency. If f_{IN}

does not equal f_{VCO} , the phase-error signal, after being filtered and amplified, causes the VCO frequency to deviate in the direction of f_{IN} . The VCO will quickly "lock" to f_{IN} , maintaining a fixed phase relationship with the input signal. The filtered output of the phase detector is a DC signal, and the control input to the VCO is a measure of the input frequency. A phase-lock loop is shown simplified in Fig.5.10.

After initial difficulties with the low pass filter, the PLL worked well, but yet the long-time stability was not sufficient. The resulting DC output signal provided a voltage change of about 0.2V for the full gap range. This signal, compared to a reference voltage, results in an error signal which can be further amplified.

Hall Effect Sensor

This signal is of a good quality with long term stability and requires minimal additional processing. This technique was therefore used in all further experiments.

The disk, connected to the shaft and forming a part of the velocity transducer, was also used to produce position information. This was done by placing a Hall effect sensor on the top of the permanent magnet measuring the flux density B of the resulting magnetic field. The only drawback, which is the temperature sensitivity, can be solved by placing the sensor further from the heat source. It could be also improved by employing an electronic compensation technique, but in this case it was not necessary.

All the circuits listed in the Appendix use this type of sensor. Although the air gap - output voltage characteristic is nonlinear, as shown on p.54, it can be considered linear over the range of interest (air gap 0 - 3mm).

5.4 Power Drivers

Once the signals are detected and processed, they form a control signal for the power drivers. Two types of power drivers [9], can be used for the magnetic bearing.

A class A chopper (one quadrant) is shown on p. 66 . This circuit can decrease the output current, if desired, by effectively applying zero voltage across the electromagnet (i.e. using only the +V,+I quadrant). During that (off) time the current continues to flow through the freewheeling diode.

A class D chopper (two quadrant) is shown on p.67. Its advantage is that it can control the output current even further, by applying full negative supply voltage across the electromagnet, while the output current freewheels through the power supply. This could produce improved dynamic performance at increased cost. However, in the doubly excited system analyzed in this thesis, a fast rise in force in either direction is possible even if only one quadrant controllers are used. Therefore, for simplification, this was the only type of circuit considered here. The resulting system performed satisfactorily, but the investigation of two quadrant controllers can be carried in the future.

5.4.1 Voltage Driver

The first control circuit that was designed and built was simple, yet fully operational and gave us the "feel" of a magnetic suspension. The name voltage driver is used here to refer to a voltage output of the amplifier which is the result of input signals, position and velocity. The block diagram is shown in the Appendix on p.58. The relationship between the voltage applied across the electromagnet $V(s)$ and the resulting current $I(s)$ is expressed, using lumped parameters R and L as:

$$V(s) = sLI(s) + RI(s) = I(s)[sL + R]$$

and

$$I(s) = \frac{V(s)}{R} \frac{1}{s\frac{L}{R} + 1}$$

where $\tau = \frac{L}{R}$ is known as the *electric time constant*. The meaning of the above equation is that the current $I(s)$ is not linearly proportional to the voltage $V(s)$, but it is *lagging*. Furthermore τ depends on the air gap of the electromagnet. Since the linearized model is already being used, τ can be measured for the specific air gap and considered constant within a small range. The method of an air gap measurement is discussed in Chapter 6 and, for an air gap of 1.5mm, τ equals 15.6ms. The transfer function of the closed loop system is derived by consequent simplifications analogous to those, used on pp.62 - 65 for a current driver. Use of that procedure yields the transfer function

$$\frac{x}{x_{IN}} = \frac{K_p K_s}{s^2 m + s K_s K_v + K_p K_s H - K_z}$$

where

$$K_s = (K_{i1} + K_{i2}) \frac{1}{s\tau + 1}$$

and

$$K_z = K_{z1} + K_{z2}$$

From Chapters 2 and 3 K_i and K_z are known to be the current and position stiffnesses and are calculated in A43 for a fixed gap 1.5mm and several values of current. The electric time constant can be expressed from

$$\frac{1}{s\tau + 1} = \frac{1}{\tau(s + \frac{1}{\tau})}$$

as a pole $s = -\frac{1}{\tau}$ in s - plane of value -64.10. Its effect can be seen in the root locus where being close to the origin it constitutes a dominant pole pushing the root locus branch to the right half plane. Thus with no velocity feedback the system is unstable for any value of position gain K_p .

For an illustration several root locus plots are shown on pp.85 - 88. A region of stability is investigated for different values of the velocity gain K_v . Only a narrow range of K_p demonstrates a stable state. This is in full agreement with the practical experience, where the system had to be frequently adjusted. Since this arrangement could not be kept stable over a longer time, it was really of no practical use and it was abandoned.

5.4.2 Current Feedback

The situation with the unwanted dominant pole, due to the electric time constant, can be improved by introducing current feedback. As an example let

$$G = \frac{1}{s\tau + 1}$$

to be a transfer function of the electromagnet (i.e. I_{out}/V_{in}), resulting thus in a pole $s = -\frac{1}{\tau}$. Let K_{cur} be a gain of an amplifier connected in cascade with the electromagnet. Then by closing a negative unity feedback (see A6) the new transfer function will be

$$G = \frac{\frac{K_{cur}}{s\tau + 1}}{1 + \frac{K_{cur}}{s\tau + 1}} = \frac{K_{cur}}{s\tau + 1 + K_{cur}}$$

and the new pole will be at

$$s = -\frac{1 + K_{cur}}{\tau}$$

Thus by using current feedback the unwanted significant pole can be moved further from the origin into the left half plane and become less significant for the dynamics of the system. The model shown in the block diagram on p.59 is very similar to the voltage driver diagram. The current feedback can be implemented either only on one electromagnet (p.73) or on both ends (pp.74 - 75), where both currents are monitored independently.

The transfer function has again the same general form as with the voltage driver, only the K , is different, since it contains the local current feedback loop:

$$\frac{K_{cur} \frac{1}{s\tau + 1}}{1 + K_{cur} \frac{1}{s\tau + 1}}$$

5.4.3 Current Driver

It becomes obvious that by increasing the current loop gain without limit the original time constant $s = -\frac{1}{\tau}$ approaches $-\infty$. This practically means that the electric time constant becomes negligible and can be omitted. Thus the current driver is actually a transconductance amplifier with the transfer function

$$\frac{I_{out}}{V_{in}} = const.$$

By employing a current source the system will become much easier to stabilize and will remain stable both over a wider range of control parameters K_p , K_v and system parameters (which may drift over an extended period of time).

A block diagram of such a system and its simplification process is shown in detail on pp.60 - 65. The system used here will have, under normal operating conditions, a zero input (x_{in}) and is referred to as a "zero tracking regulator". For a measurement of dynamic characteristics it is convenient to observe the system response to a standard arbitrary input, such as an unit impulse, unit step, sinusoidal or square wave input which may represent both a driving function or a disturbance. As an example a sudden load being applied to the magnetically suspended rotor will result in a precendented reaction. This disturbance can correspond either to a position disturbance x_{in} or to a force disturbance F_{ext} . Thus by introducing the transfer function as $\frac{x}{x_{in}}$ or $\frac{x}{F_{ext}}$ is possible. The correspondence between those two functions becomes clear from the block diagram on pp.64 - 65. The only difference is a scaling factor.

The equations

$$\frac{x}{x_{in}} = \frac{K_p K_s}{s^2 m + s K_s K_v + K_p K_s H - K_z} \quad (5.42)$$

or

$$\frac{x}{x_{in}} = \frac{K_p K_s / m}{s^2 + s K_s K_v / m + (K_p K_s H - K_z) / m} \quad (5.43)$$

can be compared to the standard form of a second order differential function :

$$\frac{C}{s^2 + 2\xi\omega_n s + \omega_n^2} \quad (5.44)$$

$$\omega = \sqrt{\frac{K_p K_s H - K_z}{m}} \quad \xi = \frac{K_s K_v}{2m\omega_n}$$

where C is a constant and K_z is the position stiffness calculated from eq.2.12 and listed on pp.98 - 99.

An examination of the coefficients in the denominators provides an important insight into the change of an *unstable (negative) spring* situation to a real spring situation with a *positive (restoring) force* type. By increasing the position gain K_p , the *stiffness* of the bearing can be increased (theoretically to infinity). Practically this is not possible because of nonideal position and velocity signals. Also the *damping* of the system ξ depends on the velocity gain K_v .

The boundary of the theoretical stiffness and practical limitations due to a nonideal physical world will now be investigated.

Chapter 6

MEASUREMENTS

6.1 Introduction

In order to calibrate the model of one axis double ended vertical bearing, several measurements had to be done. A brief description of each measurement technique, together with the results obtained, are presented in this chapter.

The model used for the measurements was the current driver system with:

top and bottom gaps $d/2 = 1.5$ [mm]

mass of the shaft $m = 0.683$ [kg]

gravity constant $g = 9.81$ [m/s^2]

The other parameters were being changed for different measurements and they are specified in the appropriate place in the text.

6.2 Double Ended and Single Ended Models

All the analysis of the magnetic bearing so far was concerned with the "*double ended*" model, mainly for reasons of practical use and also because the equations obtained can be easily changed to describe the single ended model (i.e. using only the top electromagnet) by setting $i_2 = 0$ and thus ($\Rightarrow F_2 = 0$).

Although the single ended model is of little use for the practical bearing, it can be utilized for a convenient calibration of the model. As mentioned earlier, a number

of simplifications were used (those concerned with fringing, leakage, saturation and magnetic reluctance of iron). In order to obtain a practical model for further analysis, it must be checked that the model does not stray too far from reality.

A theoretical constant K was calculated in section 2.2. This can be checked experimentally as follows. The current in the bottom coil is set to zero and the current required by the top electromagnet to maintain a particular gap is then measured. The gap, which will be used in the constructed bearing is the most important. The equation of motion will simplify to

$$m\ddot{x} = mg - F_1 = 0 \quad (6.45)$$

so that

$$F_1 = mg$$

$$K \frac{i^2}{(d/2 + x)^2} = mg$$

(where $d/2$ is the gap) and since the values of mass m , gap and current can be easily obtained. A corrected value of the constant K can be thus determined from the equation:

$$K = \frac{mg(d/2)^2}{i^2} \quad (6.46)$$

In the case of the model used with $K_p = 150$ and $K_v = 0.6$, the current i_1 was found to be 1.19 [A], corresponding to a force of 6.73 [N]. For further values of the airgap see A51.

Thus a new constant of the electromagnet was found to be:

$$K = 10.646 * 10^{-6}$$

This corresponds to a 29% decrease from the originally calculated value 15.005×10^{-6} .

All the calculations in this thesis are based on this new, corrected value.

6.3 Electric Time Constant of the Electromagnet

A series combination of L and R is used here to represent the electromagnet. Thus by solving the equation for current as a function of applied unit step voltage we obtain

$$i = I_{max}(1 - e^{-\frac{t}{\tau}}) \quad (6.47)$$

where

$$I_{max} = \frac{V}{R}$$

represents a steady state value of a DC current. This equation can be evaluated for $t = \tau$, where τ is the electric time constant as defined earlier in section 5.4.1 to yield:

$$i = I_{max}(1 - e^{-\frac{\tau}{\tau}}) = I_{max}(1 - e^{-1}) = 0.632I_{max}$$

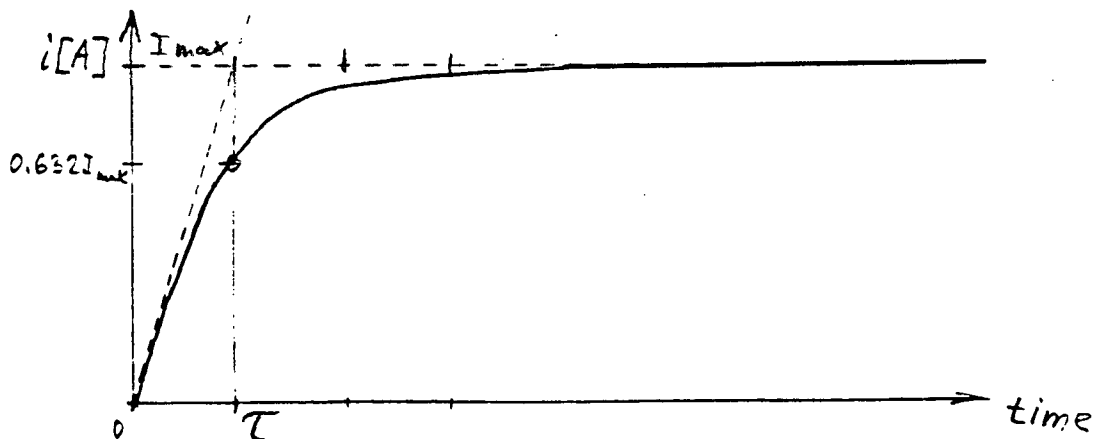


Figure 6.11: Voltage vs. Current in a Series RL Circuit

Now, using a low frequency square wave generator and a power amplifier, the output

voltage is applied across the electromagnet (fixed airgap) and the resulting current is displayed (by means of a current transducer) on an oscilloscope.

In the practical case $I_{max}=3.5$ [A] and 63.2% of which was 2.21 [A]. The time corresponding to this current level was found to be:

$$\tau = 15.6[ms]$$

6.4 Position Constant of the Hall Effect Sensor

The characteristic, i.e. the output voltage as a function of the air gap, of the Hall effect sensor was measured and is shown in A1. It can be seen that the function, in the range of $<0, 3>$ mm, can be substituted with a straight line of appropriate slope. The slope, and thus the transfer function, was found to be:

$$H = 110[V/m]$$

6.5 Velocity Constant

Similarly, the velocity sensor transducer had to be calibrated. The appropriate part of the block diagram, together with $x = x(t)$ and $\dot{x} = \dot{x}(t)$ is shown in Fig.6.12. Position and velocity response for a simulated impulse input and $K_p = 150$, $H = 110$ and $K_v = 0.6$ (underdamped case), were displayed on an oscilloscope simultaneously. The following can be written

$$x = X_{max} \sin \omega t$$

$$\omega = \frac{2\pi}{T} = 2\pi f$$

where ω [rad/s] is radian frequency, T [s] is the period and f [Hz] is cyclic frequency.

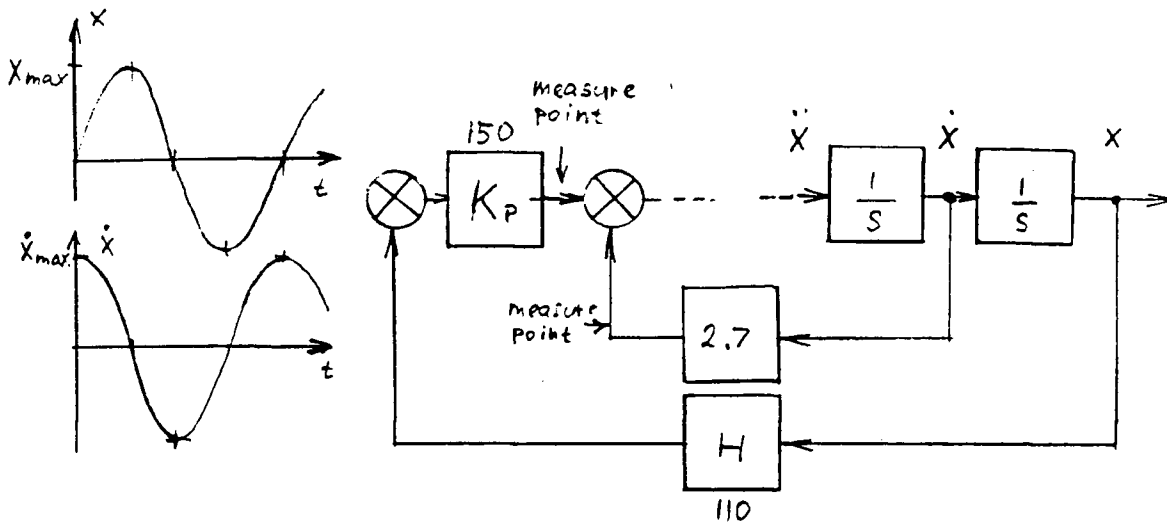


Figure 6.12: Measurement of the Velocity Constant

and for velocity

$$\dot{x} = \frac{dx}{dt} = \omega X_{max} \cos \omega t = \dot{X}_{max} \cos \omega t$$

The following data were obtained:

$T = 28$ [ms], so that:

$\omega = 224$ [rad/s]

$X_{max} = 8$ V ≈ 0.485 mm (i.e. $8/150/110$) yielding :

$$K_{Pabs} = 16495 \text{ [V/m]}$$

Similarly:

$X_{max} = 12$ V and

$X_{max} = \omega X_{max} = 224 * 0.485 * 10^{-3} = 0.1086$ [m/s]

$12/0.1086 = 110.5$ [V/m/s] and $110.5/2.7 = 40.93$ so that:

$$K_{Vabs} = 40.93 \text{ [V/m/s]}$$

6.6 Measurement of The Position Stiffness

As outlined briefly in 5.4.3 (page 34), a technique simulating an unit impulse response [10],[11],[12] was used here in order to obtain the stiffness values for the closed loop suspension system. An analogous system to the magnetic bearing is the mechanical mass-spring-damper system, as discussed earlier, where the input $R(s)$ and output $X(s)$ are related through the transfer function $T(s)$

$$T(s) = \frac{X(s)}{R(s)} = \frac{\omega_n^2}{s^2 + 2\xi\omega_n s + \omega_n^2} \quad (6.48)$$

The poles of the above equation are

$$s = -\xi\omega_n \pm j\omega_n\sqrt{1 - \xi^2}$$

If the unit impulse $\delta(t)$ is used as an input then the response of the system $X(s)$ will be equal to $T(s)$

$$X(s) = T(s)$$

since the Laplace transform $\mathcal{L}\delta(t) = 1$

The transient response in the time domain can be obtained by using inverse Laplace transform of $X(s)$ ($= T(s)$):

$$x(t) = \mathcal{L}^{-1}X(s) = \frac{1}{\omega_d} e^{-\xi\omega_n t} \sin\omega_d t = \frac{1}{\omega_n\sqrt{1-\xi^2}} e^{-\xi\omega_n t} \sin(\omega_n\sqrt{1-\xi^2})t$$

where

$\omega_n \dots$ natural radian frequency

$\omega_d \dots$ damped radian frequency

$\xi \dots$ damping ratio

$\alpha \dots$ damping coefficient

$\tau \dots$ time constant of the system

and the basic equations:

$$\omega_d = \omega_n \sqrt{\xi^2 - 1}$$

$$\alpha = \xi \omega_n$$

$$\tau = \frac{1}{\alpha}$$

$$\beta = \sqrt{1 - \xi^2}$$

$$\xi = \sin^{-1} \theta$$

$$\theta = \tan^{-1} \frac{\beta}{\xi}$$

As ξ decreases, the poles approach the imaginary axis and the system becomes increasingly oscillatory.

It is common to take several performance measures from the transient response to a step input. The swiftness of the response is measured by the *rise time* T_r and the *peak time* T_p . For underdamped systems with an overshoot, the 0-100 % *rise time* is a useful index. If the system is overdamped then the peak time is not defined and the 10-90 % *rise time* is normally used.

The similarity with which the actual response matches the step input is measured by the *percent overshoot*, P.O., and the *settling time*, T_s . The settling time, T_s , is defined as the time required for the system to settle within a certain percentage of the input amplitude. For a second order system with a closed-loop damping constant ξ , the response remains within 2 % after four time constants.

$$T_s = 4\tau = \frac{4}{\xi \omega_n}$$

In practice a demand for a fast response yet with an overshoot of less than 5 % can be matched by the minimum damping ratio of 0.707 with a resulting overshoot of 4.3 %.

The stiffness of the closed loop compensated system was obtained from the transient response to a simulated unit impulse (mechanical impulse).

The natural radian frequency of the undamped system ω_n was obtained from the oscilloscope, while position gain K_p and velocity gain K_v were set so that the system produced a sustained periodic oscillation. The damped radian frequency ω_d was obtained in a similar manner for different settings of K_p and K_v . Pictures were taken from the screen of a storage oscilloscope and they are shown together with computer simulated responses in Appendix pp.78 -83.

parameters		measured values		calculated values	
K_p	K_v	ω_d	ω_n	ξ	K_{comp}
100	0.6	222	227	0.209	12900
100	0.7	209	227	0.209	12900
100	2.7	122	227	0.844	12900
150	0.9	326	336	0.242	48600
150	1.5	290	336	0.505	48600
150	2.7	140	336	0.909	48600
150	5.0	97	336	0.957	48600

$$\xi = 1 - \left(\frac{\omega_d}{\omega_n}\right)^2 \quad K_{comp} = \frac{1}{m\omega_n^2}$$

where K_{comp} is the stiffness of the compensated system.

As can be seen from the table the natural radian frequency ω_n and the effective stiffness K depend on the position gain K_p , whereas the damping ratio ξ and thus the damped radian frequency ω_d depend on the velocity gain K_v .

An expression for a steady state error (i.e. in this case it would be the steady state displacement of the shaft if a constant force is applied) can be calculated, using the steady-state or the final-value theorem:

$$\lim_{t \rightarrow \infty} x(t) = \lim_{s \rightarrow 0} sX(s)$$

the situation corresponds to a unit step being applied

$$\lim_{s \rightarrow 0} sX(s) = \lim_{s \rightarrow 0} \frac{s}{s(s^2 + 2\xi\omega_n s + \omega_n^2)} = \lim_{s \rightarrow 0} \frac{1}{s^2 + 2\xi\omega_n s + \omega_n^2} = \frac{1}{\omega_n^2}$$

in case of the bearing it would be

$$\frac{1}{\frac{K_p K_s H - K_z}{m}} = \frac{m}{K_p K_s H}$$

Chapter 7

CONCLUSIONS

The goal of this thesis was to analyse and design a practical one-axis double-ended magnetic bearing. A complete analysis of the vertical arrangement was done, forming a good base for further investigation. This included: equation of motion, equation for the lifting force of an electromagnet, general expressions for stiffnesses, linearized form of the force and finally a model for small signals (perturbations).

From the analogy with a mechanical system, the equation for the position stiffness of the closed loop suspension system was derived and measured, using a simulation of the unit impulse response. The results were found to be in good agreement with the calculated values. The formula for a steady-state error, in the case of a unit step input (i.e. a case of a suddenly applied load) was derived from the final value theorem. A good insight into the system properties was obtained by using the root-locus plots and an example of a complete procedure for synthesizing any type of cascade compensator is presented in the Appendix.

A high importance was placed on the position transducer by analyzing its role in the ultimate bearing stiffnesses. This is still a vast area to be investigated. By comparing different types of transducers the Hall-effect transducer was found to be a very convenient type for its good quality output signal with no further processing necessary.

The key goal, which was to actually build a circuit that will perform the control function, was achieved. The identical circuitry can be now made for those remaining

four axes to completely suspend the rotor. Further investigation may still be necessary in the multi-axes suspension case, if a possible cross coupling would occur.

The future of magnetic bearings is still open which is obvious from a number of papers being published. Some other types of position transducer candidates would be capacitance sensors and optoelectric sensors. Further explorations of this topic promises to pose an interesting challenge.

Bibliography

- [1] Earnshaw, S., *On the nature of the Molecular Forces which regulate the Constitution of Luminiferous Ether*, Trans. Camb. Phil. Soc., 7, pp. 97-112 (1842)
- [2] Braunbeck, W., *Free Suspension of Bodies in Electric and Magnetic Fields*, Zeitschrift für Physik, 112, 11, pp. 753-63 (1939)
- [3] Habermann, W., Liard Guy L., *Practical Magnetic Bearings*, Société de Mécanique Magnétique, France; IEEE Spectrum, September (1979)
- [4] *ACTIDYNE - Application of Active Magnetic Bearings to Industrial Rotating Machinery*, Société de Mécanique Magnétique, France
- [5] Jayawant, B. V., *Electromagnetic Levitation and Suspension Techniques*, Edward Arnold Publishers (1981)
- [6] Fogiel, M., *The Electronic Problem Solver*, Research and Education Association, New York N.Y. (1982)
- [7] Horowitz, P., Hill, W., *The Art of Electronics*, Cambridge University Press (1983)
- [8] Geiger, Dana F., *Phaselock Loops for DC Motor Speed Control*, Wiley & Sons, Inc. (1981)
- [9] Dewan, S. B., Slemon, G.R., *Power Semiconductor Drives*, Wiley & Sons, Inc. (1984)
- [10] Dorf, R.C., *Modern Control Systems*, Addison-Wesley (1982)

- [11] Di Stefano J.J., *Feedback and Control Systems*, McGraw-Hill, 1976
- [12] Franklin Gene F., Powell David J., *Feedback Control of Dynamic Systems*, Addison-Wesley, 1986
- [13] Leigh J. R., *Essentials of Nonlinear Control Theory*, Peter Peregrinus Ltd., London, U.K., 1983
- [14] *SIGNETICS - Linear Circuits Catalog*, 1986
- [15] *UNITRODE - Linear Circuits Catalog*, 1986
- [16] Haberman H. et al., IEEE Spectrum, Sept. 1979, p.26
- [17] D'Azzo John J., Houpis Constantine H., *Linear Control System Analysis and Design*, McGraw-Hill, 3rd Edition, 1988

APPENDIX

List of Appendix

1	Output Voltage of the Hall Effect Sensor vs. Air Gap	54
2	Output Current vs. Input Voltage of the Current Driver using 3843 Integrated Circuit	55
3	Force of the Electromagnet acting on the Shaft vs. Displacement ($i_1 =$ $i_2 = 5 \text{ A const.}$)	56
4	Force vs. Displacement (calculated, 1st order approximation and 3rd order approximation)	57
5	Block Diagram for Small Signal with linearized Force (Voltage Driver) .	58
6	Block Diagram for Small Signal with Linearized Force (Current Feed- back)	59
7	Basic Block Diagram of a Magnetic Bearing (Current Driver)	60
8	Block Diagram with Linearized Force (Current Driver)	61
9	Block Diagram for Small Signal with Linearized Force (Current Driver)	62
10	Simplification 1 (Current Driver)	63
11	Simplification 2 (Current driver), Simplification 3 (Current Driver) . . .	64
12	Simplification 4 (Current Driver)	65
13	Class A Chopper (one quadrant switching amplifier)	66
14	Class D Chopper (two quadrant switching amplifier)	67
15	A Saw Wave Generator for the Comparator Circuit	68
16	Comparator Circuit as a Generator of Control Signals for the D Class Chopper	69
17	D Class Chopper (two quadrant switching amplifier)	70

18 Analog Part of the Control Circuit for the Magnetic Bearing (position and velocity signals)	71
19 Simple A Class Chopper (Voltage Driver)	72
20 Simple A Class Chopper (Current Feedback)	73
21 A Class Chopper (Current Feedback)	74
22 The Complete Control Circuit (Current Driver)	75
23 Block Diagrams of Integrated Circuits 5561 and 3842	76
24 Impulse Response of a Second Order Linear System (for different values of ξ)	77
25 Impulse Response of the Single Axis Magnetic Bearing	78
26 Impulse Response of the Single Axis Magnetic Bearing	79
27 Impulse Response of the Single Axis Magnetic Bearing	80
28 Impulse Response of the Single Axis Magnetic Bearing	81
29 Impulse Response of the Single Axis Magnetic Bearing	82
30 Impulse Response of the Single Axis Magnetic Bearing	83
31 Measured Stiffnesses of the Compensated Magnetic Bearing	84
32 Root Locus of the Stabilized System using a Voltage Driver	85
33 Root Locus of the Stabilized System using a Voltage Driver	86
34 Root Locus of the Stabilized System using a Voltage Driver	87
35 Root Locus of the Stabilized System using a Voltage Driver	88
36 Root Locus of the Stabilized System using a Current Feedback	89
37 Root Locus of the Stabilized System using a Current Feedback	90
38 Root Locus of the Unstable System (no velocity feedback)	91
39 Root Locus of the System (without the velocity feedback) using a Lead Cascade Compensator	92
40 RC Network Synthesis for a Feedback Amplifier	93

41	Root Locus of the Stabilized System using a Current Driver	96
42	Root Locus of the Stabilized System using a Current Driver	97
43	Calculated Values of Forces and Stiffnesses for the Uncompensated Sys- tem	98

Symbols used in the Appendix:

K_v ... velocity gain (adjustable)

K_p ... position gain (adjustable)

K_{cur} ... current loop gain (adjustable)

K_c ... system constant (-0.321 A/V)

K_c ... converter constant (+0.5, -0.5)

H ... Hall sensor constant (110 V/m)

K_x ... current stiffness of the uncompensated system (calculated)

K_i ... position stiffness of the uncompensated system (calculated)

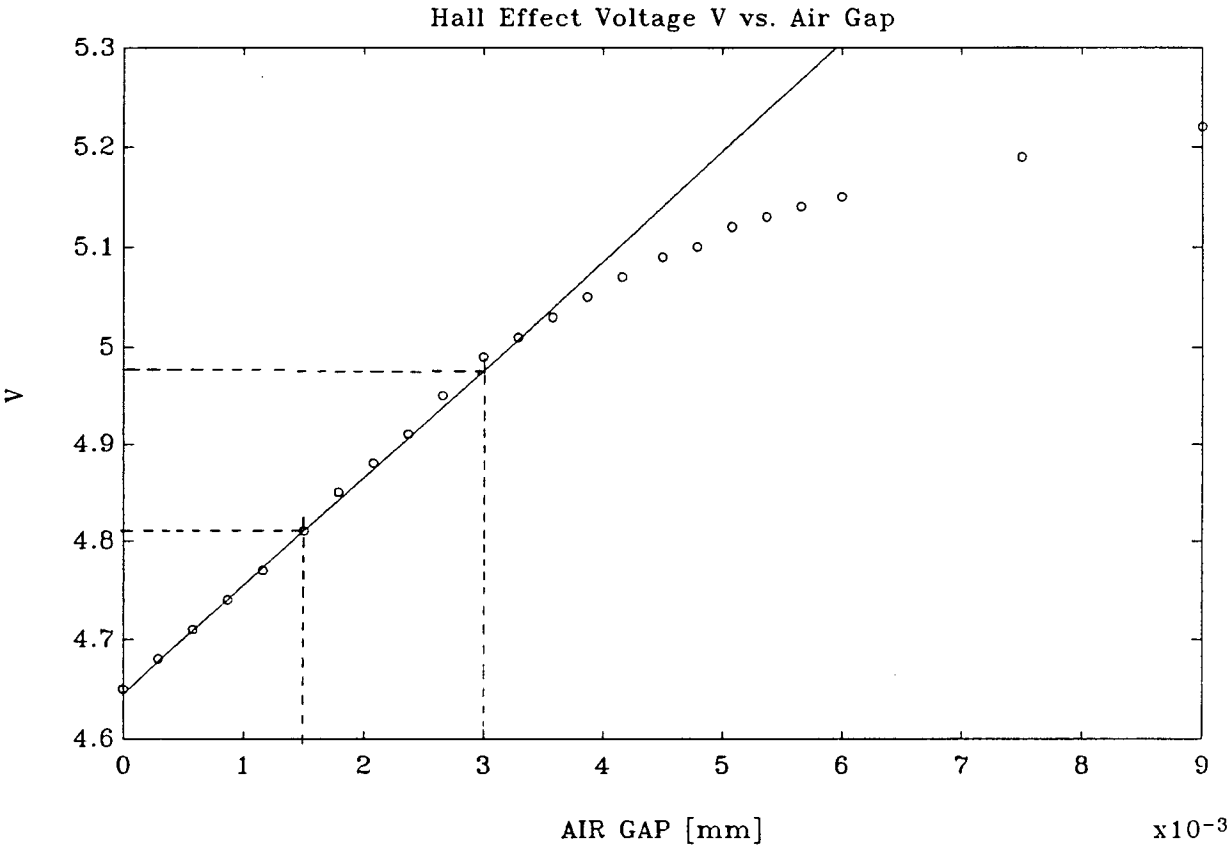
τ ... electric time constant of the electromagnet (15.6 ms for 1.5 mm air gap)

m ... mass of the shaft (0.683 kg)

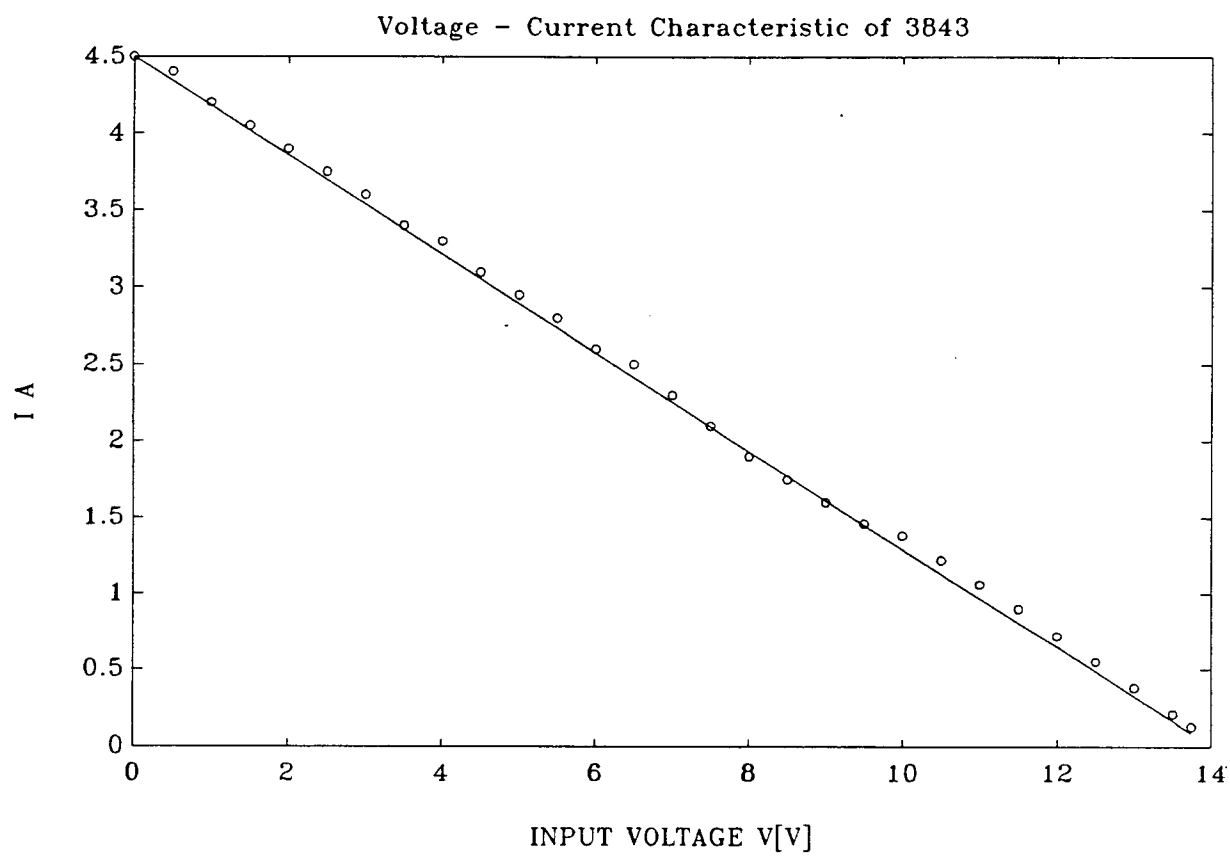
g ... gravity constant (9.81 m/s²)

F_{ext} ... force representing a disturbance

Output Voltage of the Hall Effect Sensor vs. Air Gap

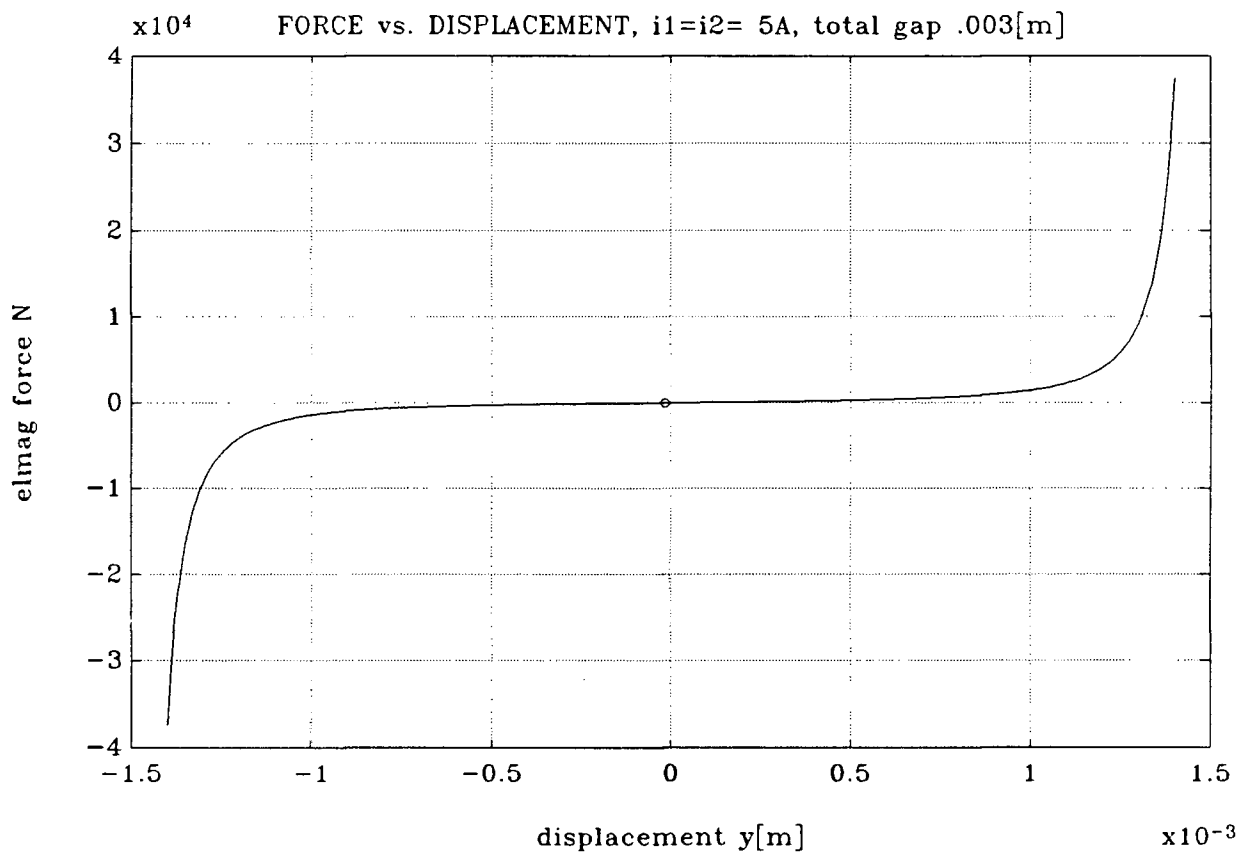


Output Current vs. Input Voltage of the Current Driver
using 3843 Integrated Circuit



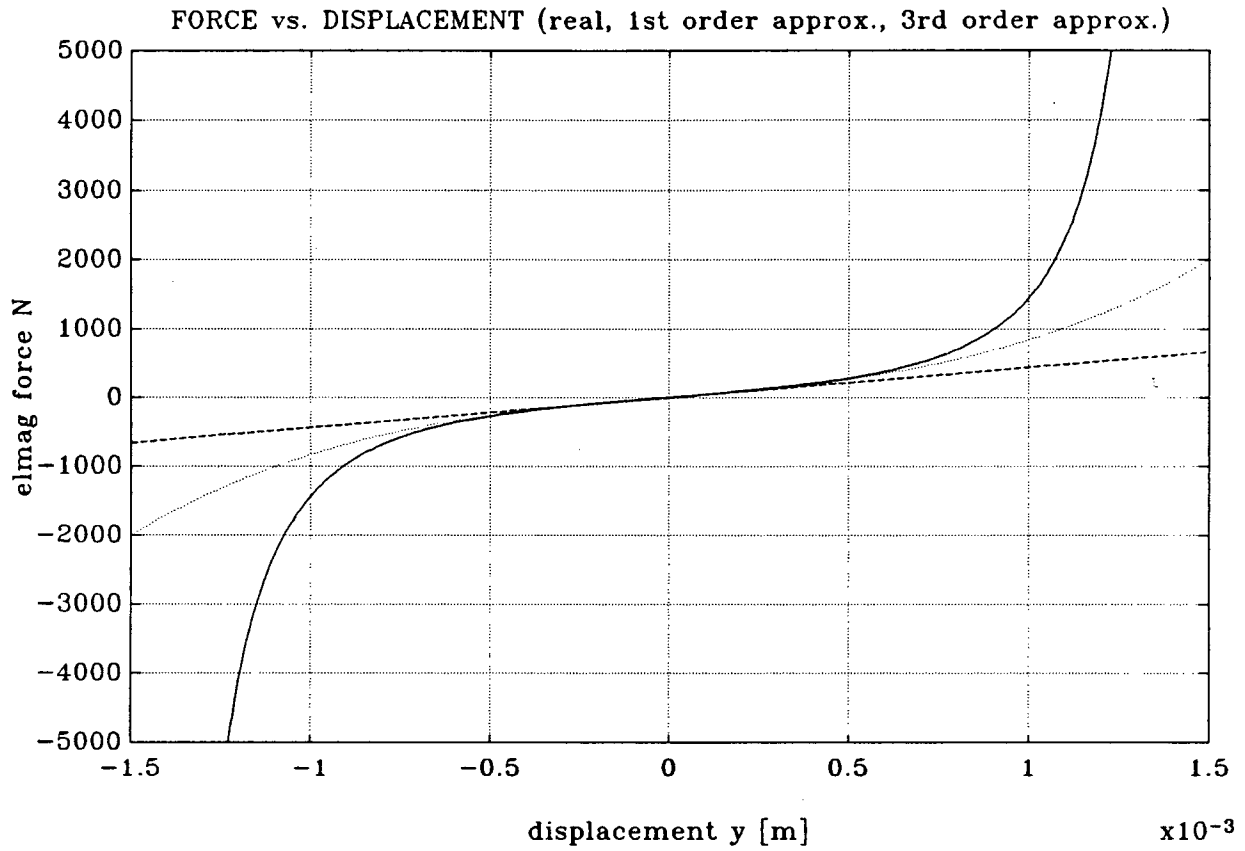
Force of the Electromagnet acting on the Shaft vs. Displacement

($i_1 = i_2 = 5 \text{ A const.}$)



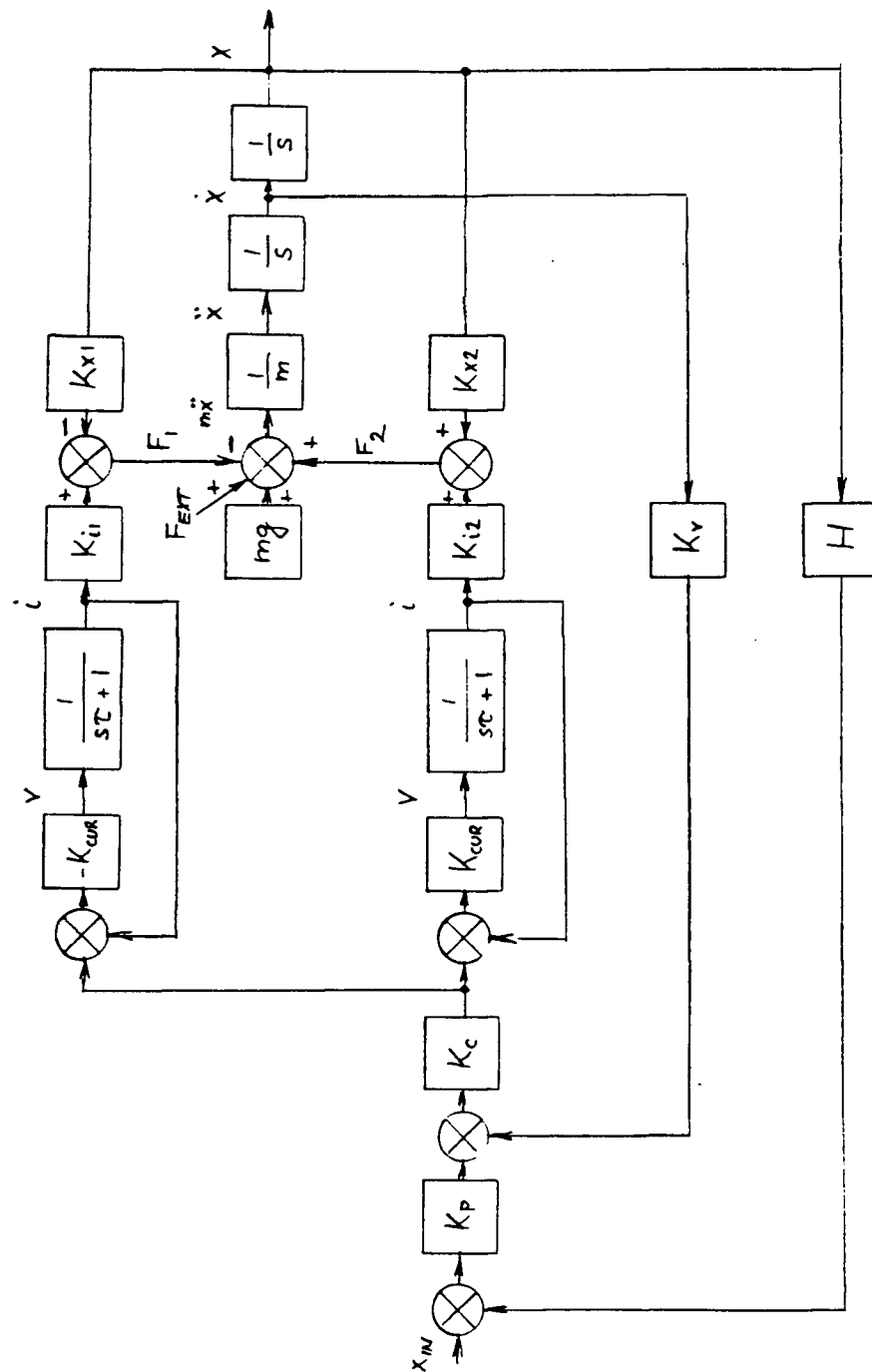
Force vs. Displacement

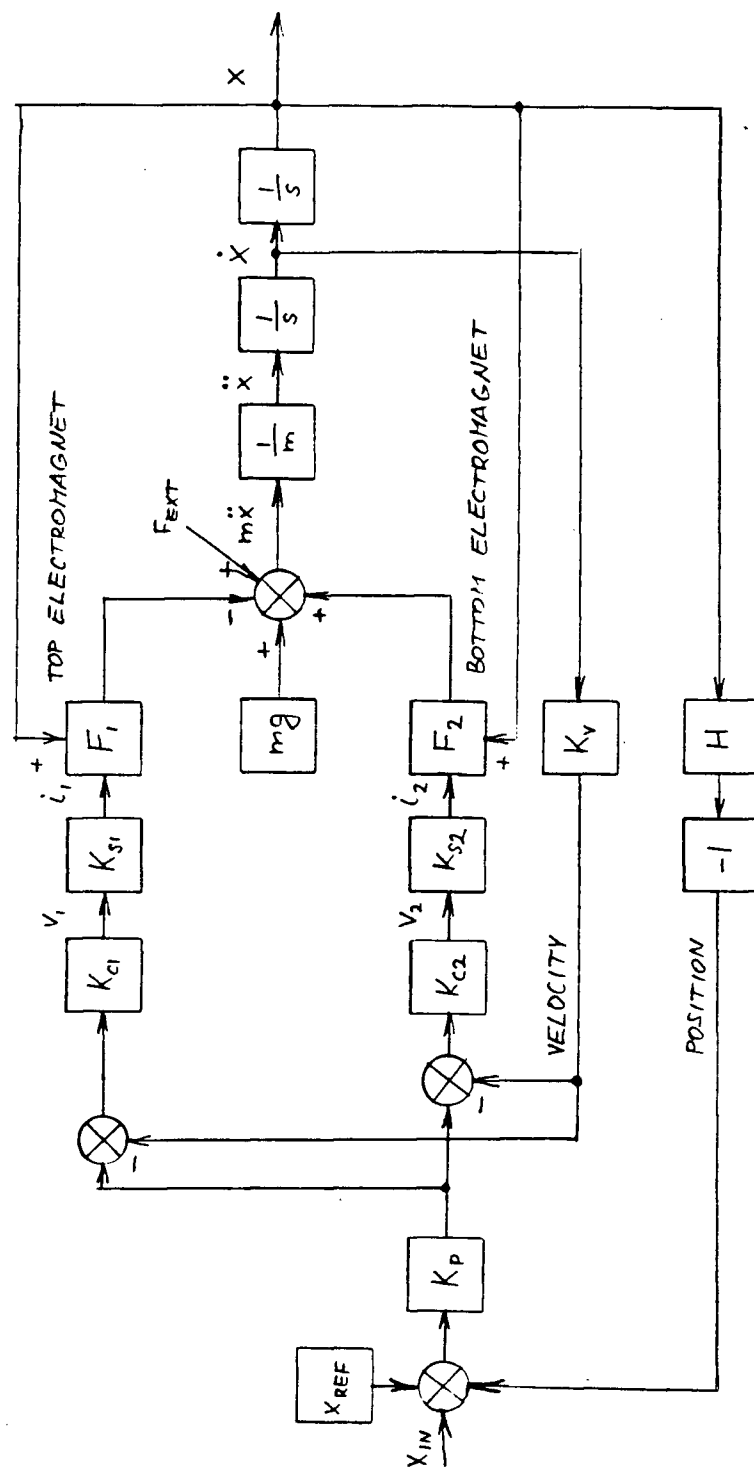
(calculated, 1st order approximation and 3rd order approximation)



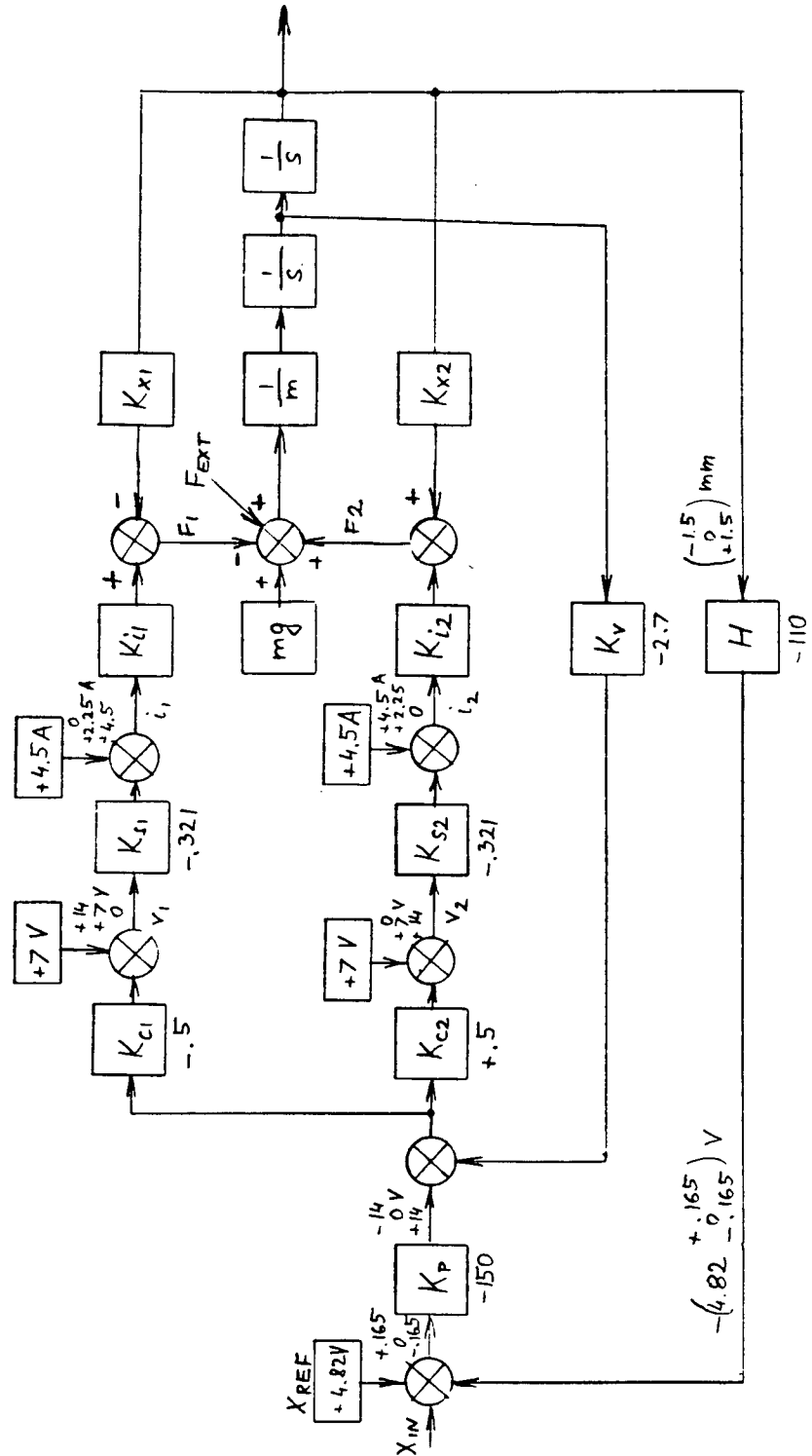
Block Diagram for Small Signal with Linearized Force

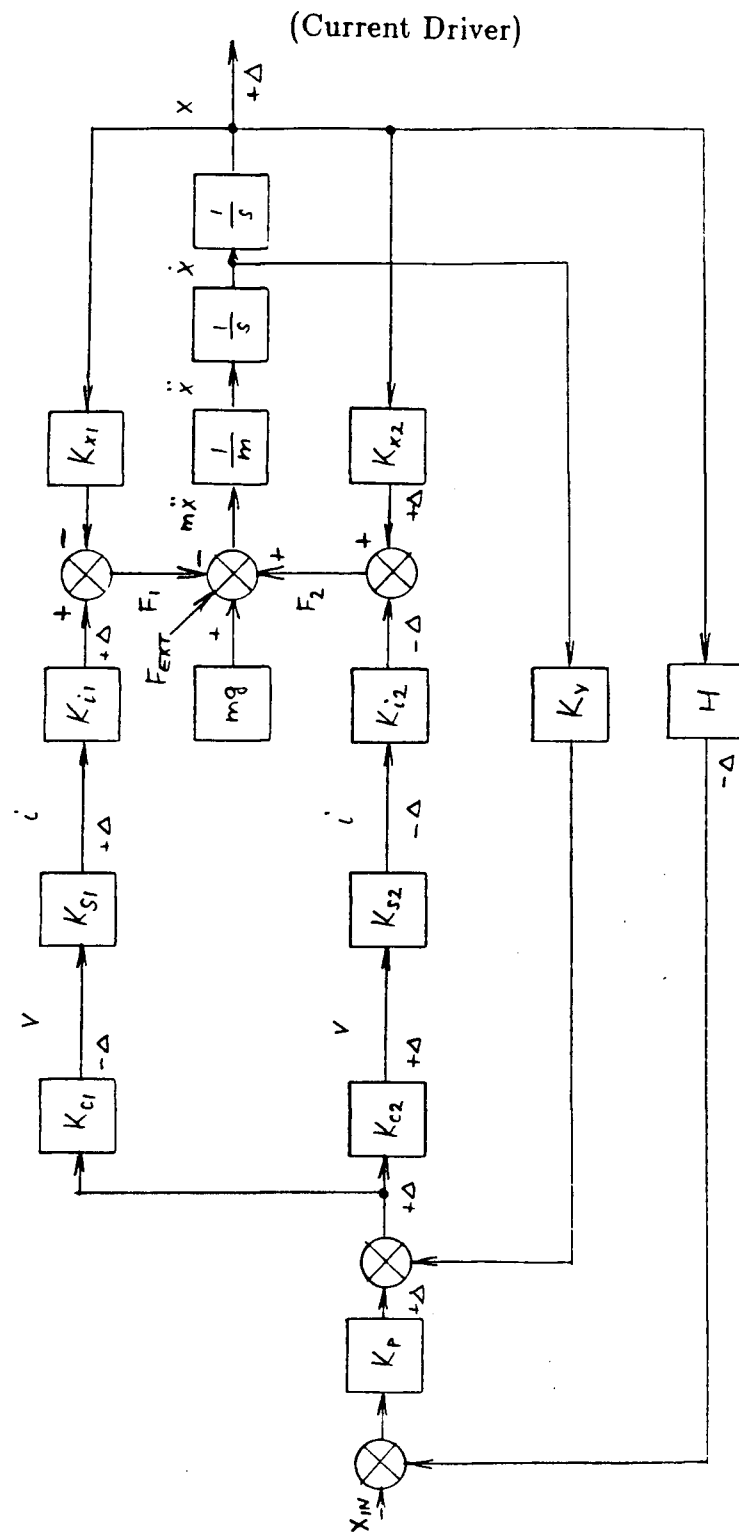
(Current Feedback)

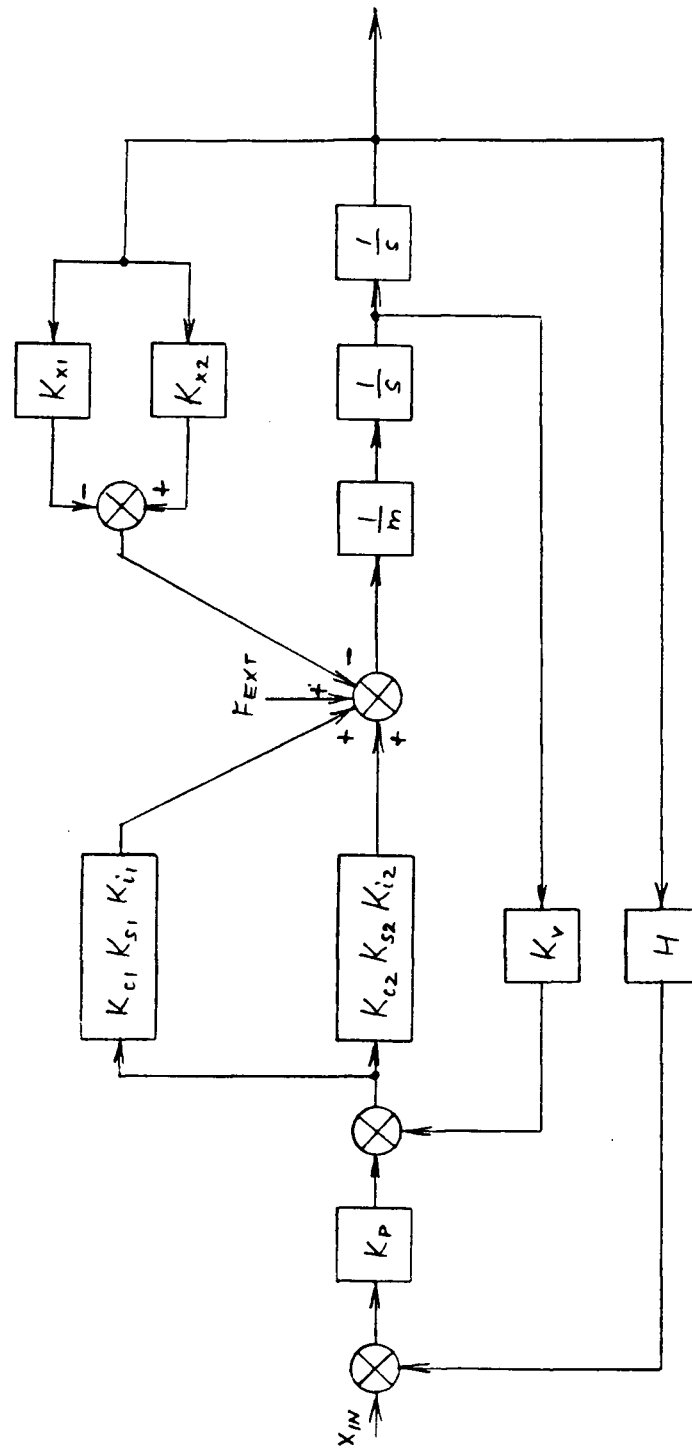




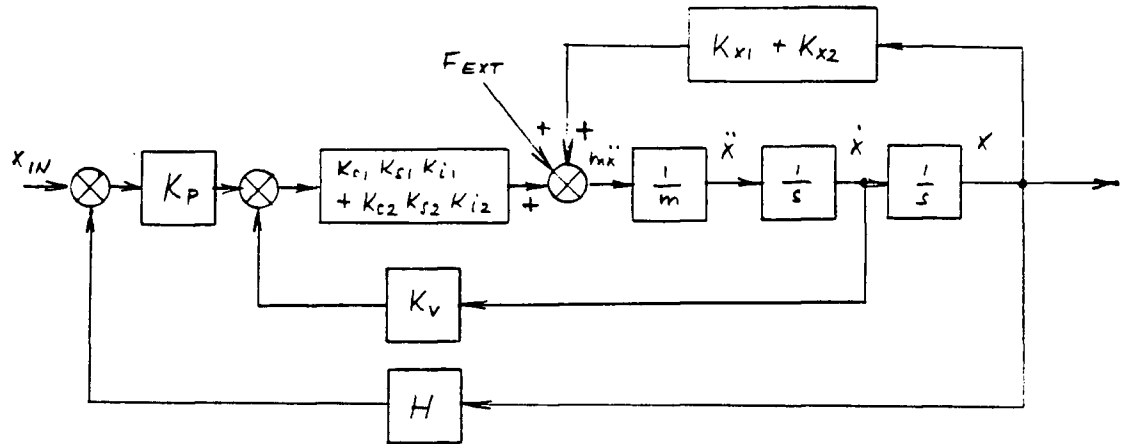
Block Diagram with Linearized Force (Current Driver)







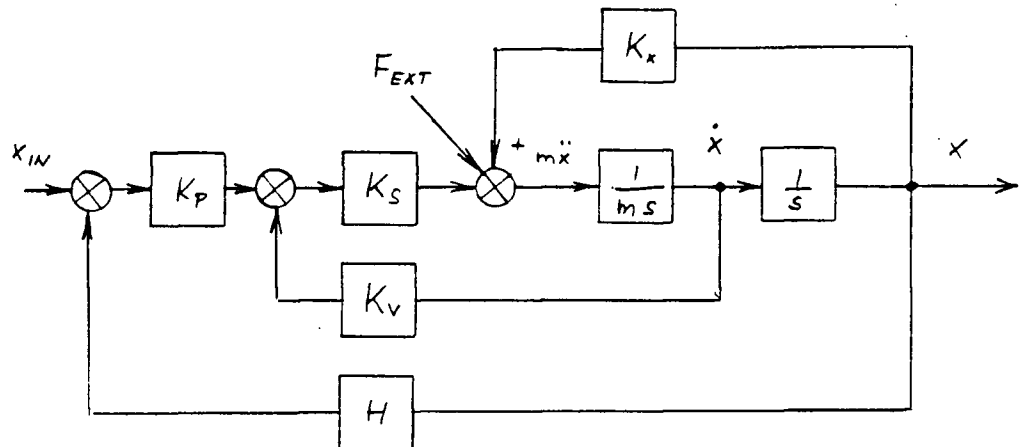
Simplification 2 (Current driver)



$$K_S = K_{c1} K_{s1} K_{i1} + K_{c2} K_{s2} K_{i2}$$

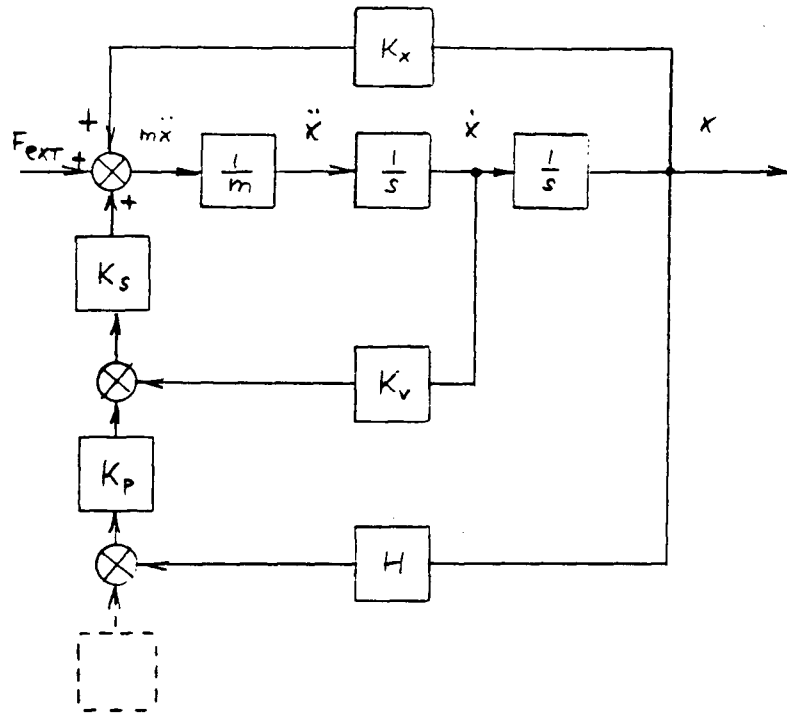
$$K_X = K_{x1} + K_{x2}$$

Simplification 3 (Current Driver)



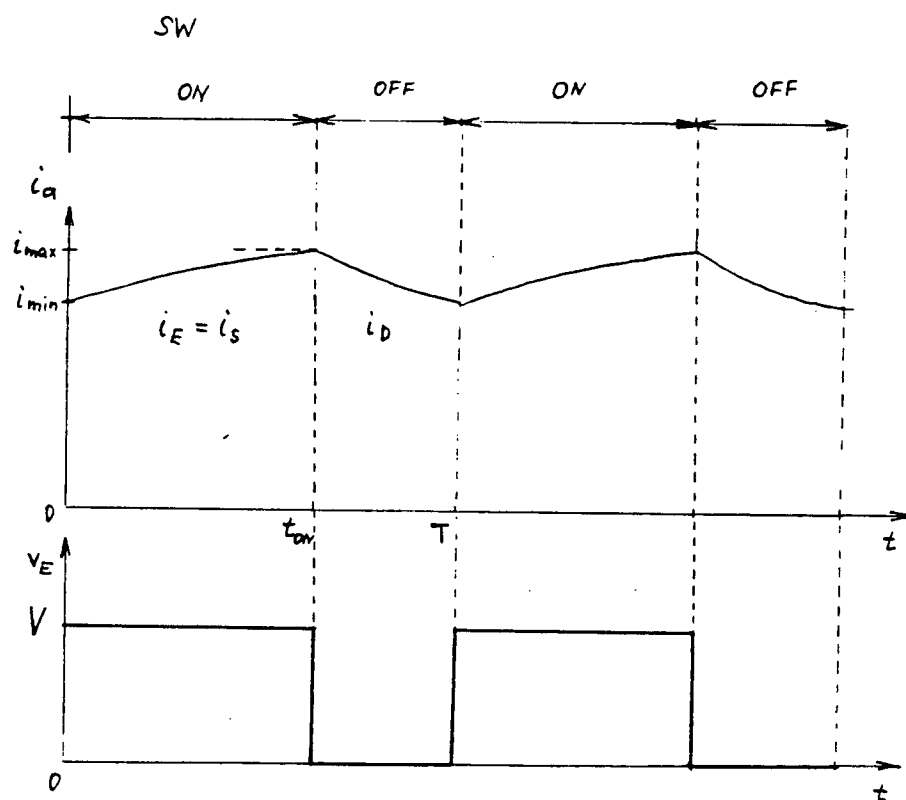
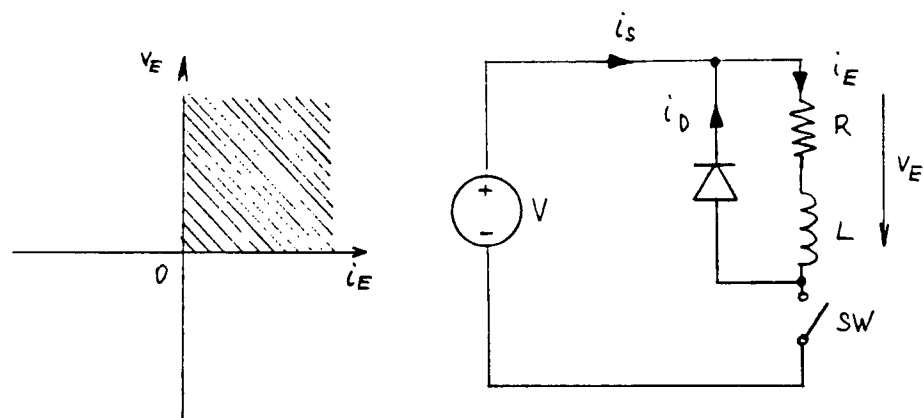
$$\frac{x}{x_{IN}} = \frac{\frac{1}{ms^2} K_P K_S}{1 - K_X \frac{1}{ms^2} + K_S K_V \frac{1}{ms} + K_P K_S H \frac{1}{ms^2}} \approx \frac{K_P K_S}{s^2 m + s K_S K_V + K_P K_S H - K_X}$$

Simplification 4 (Current Driver)

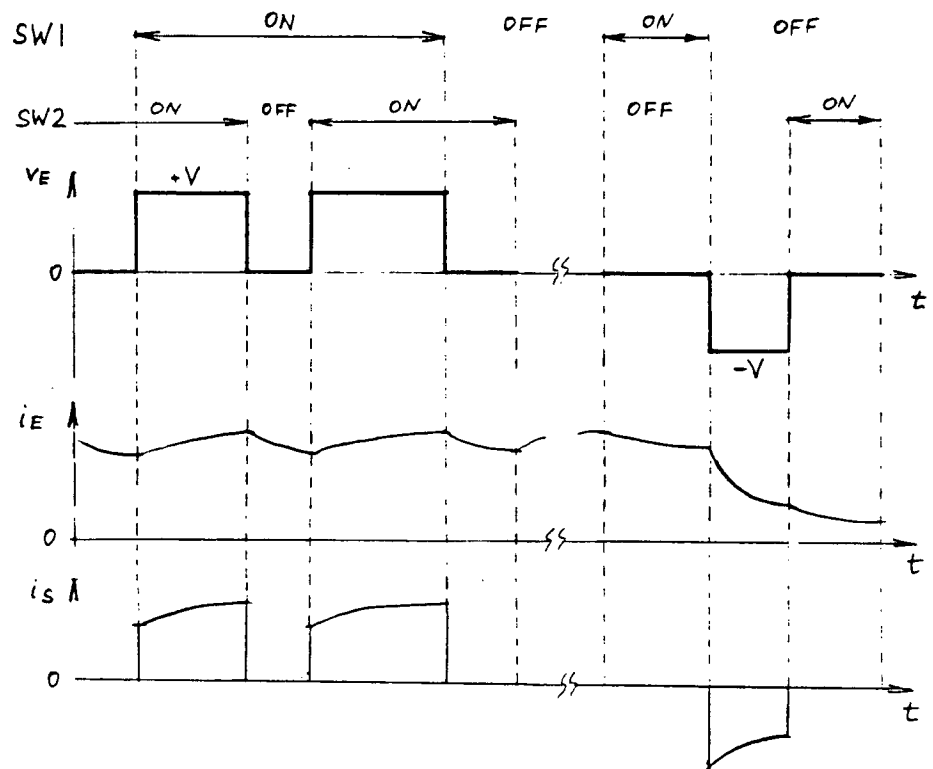
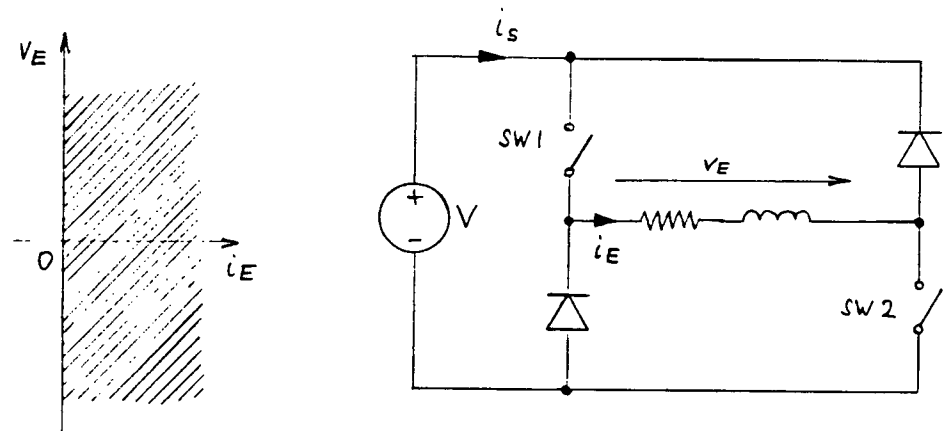


$$\frac{x}{F_{EXT}} = \frac{\frac{1}{ms^2}}{1 - \frac{1}{ms^2}K_X + \frac{1}{ms}K_VK_S + \frac{1}{ms^2}HK_PK_S} = \frac{1}{s^2m + sK_VK_S + HK_PK_S - K_X}$$

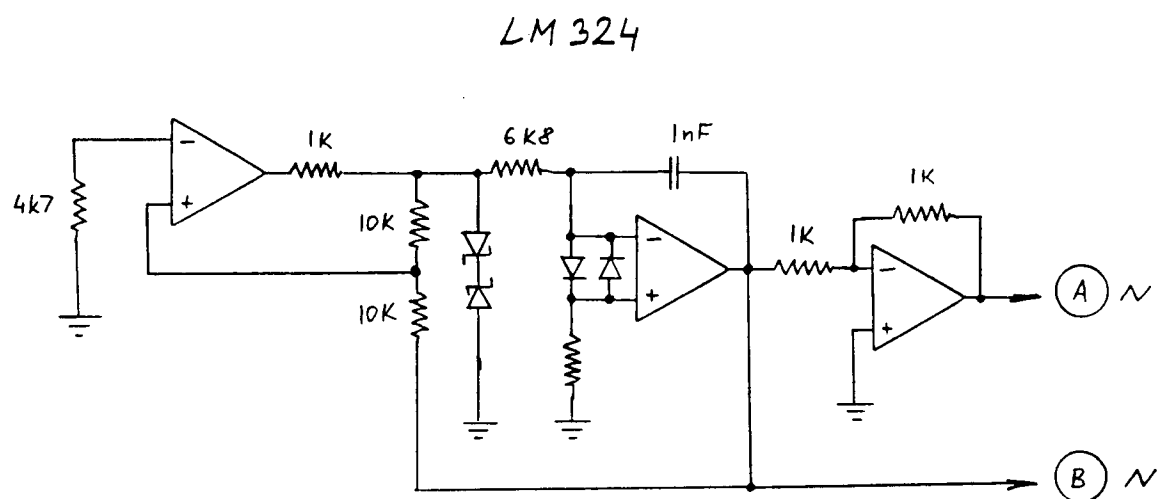
Class A Chopper (one quadrant switching amplifier) [9]



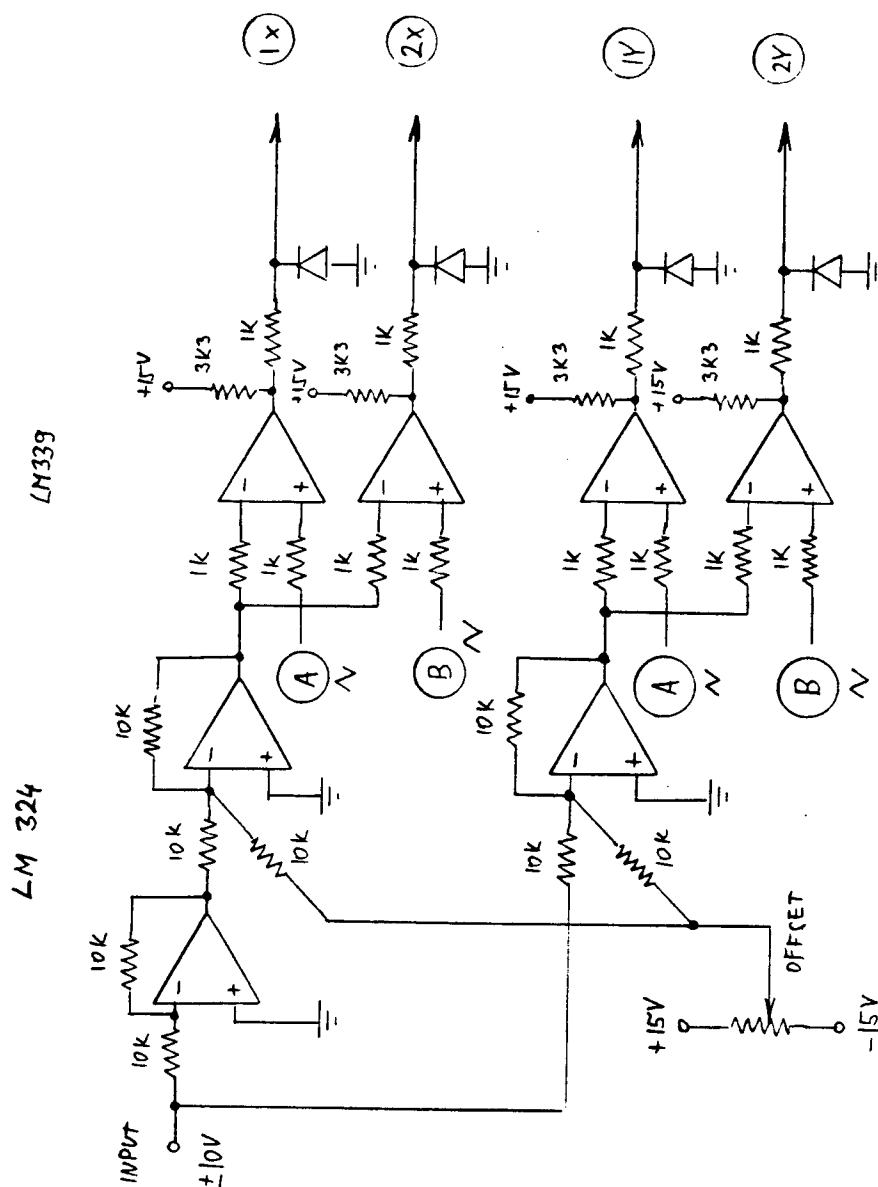
Class D Chopper (two quadrant switching amplifier) [9]



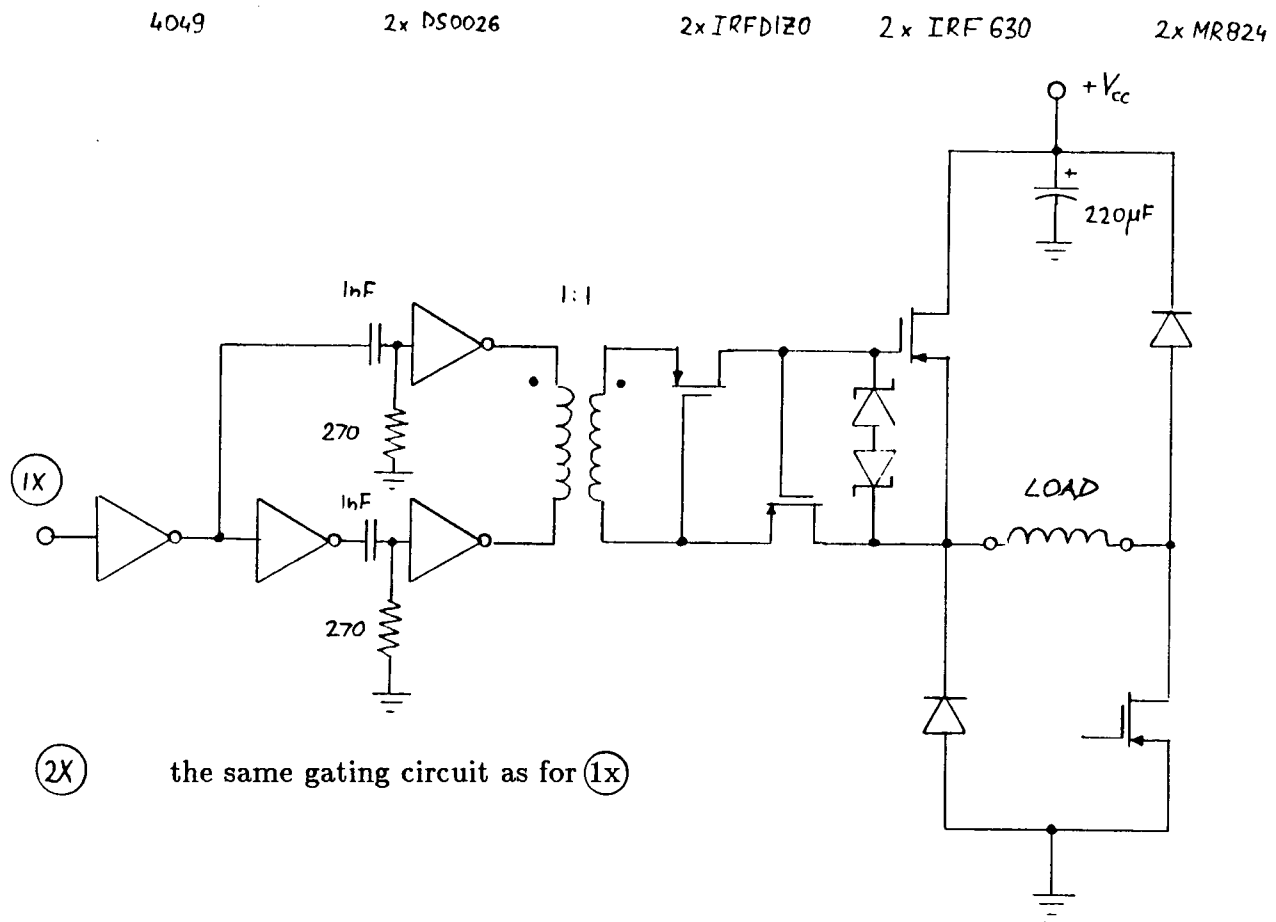
A Saw Wave Generator for the Comparator Circuit (A16)



for the D-Class Chopper (A17)

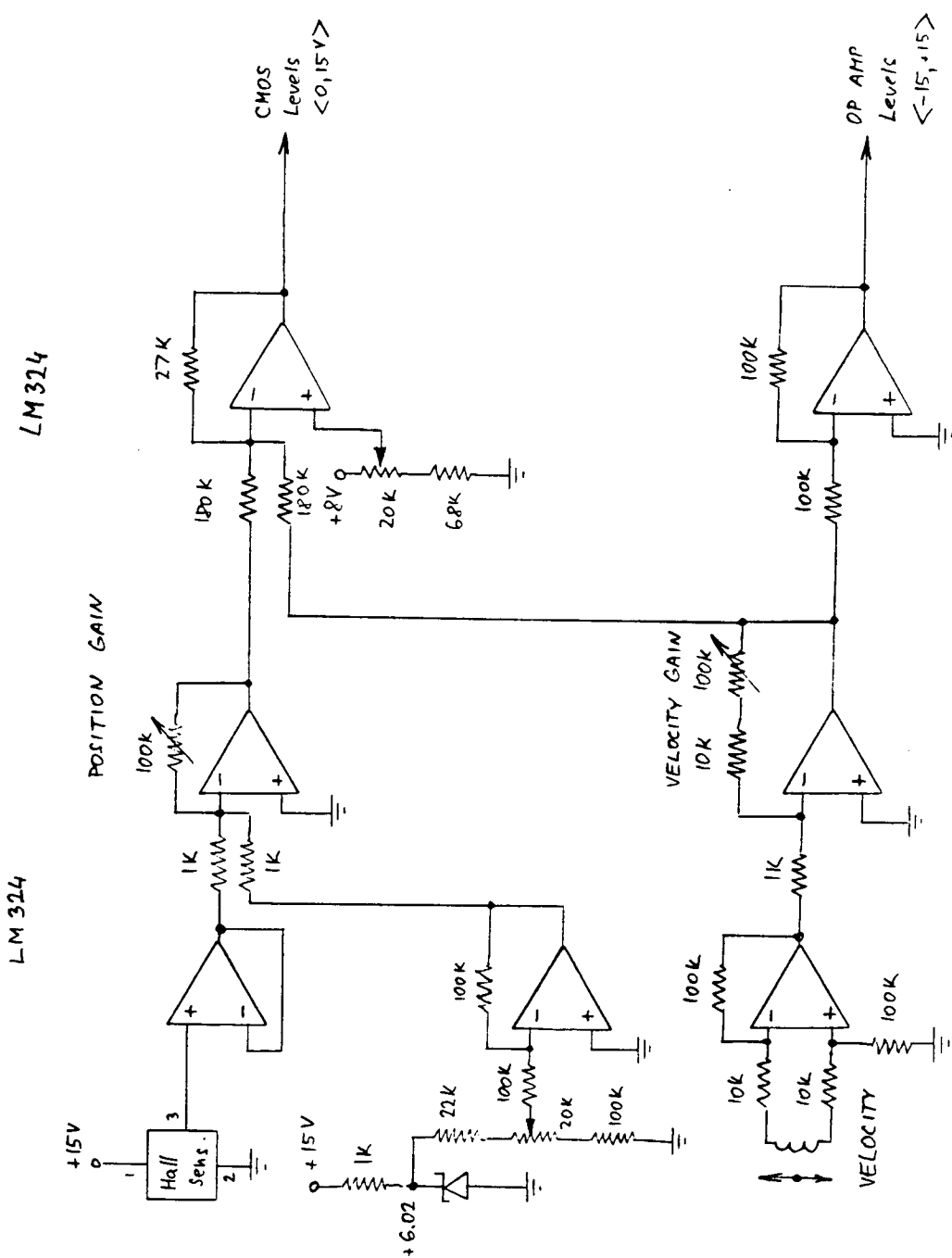


D-Class Chopper (two quadrant switching amplifier)

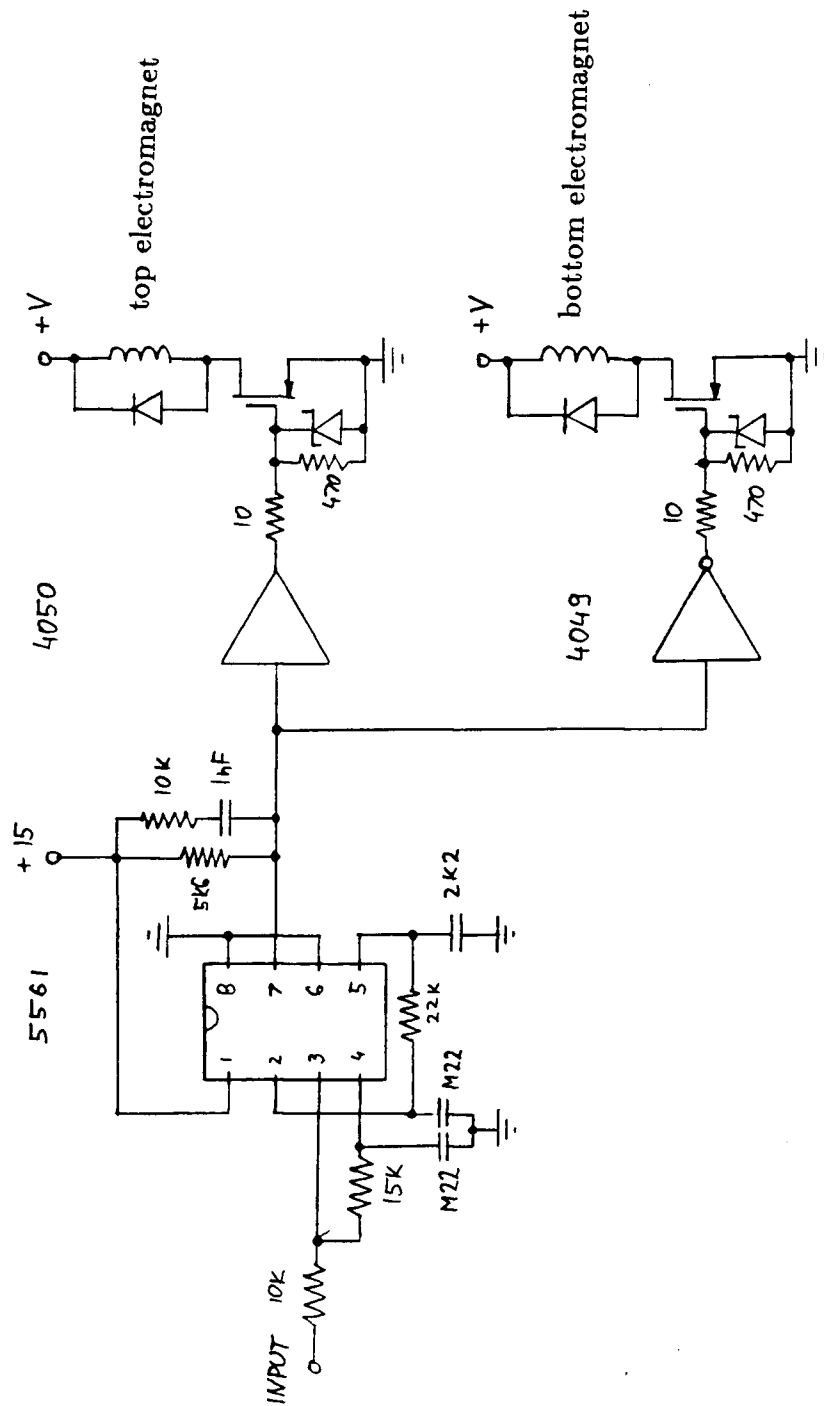


Analog Part of the Control Circuit for the Magnetic Bearing

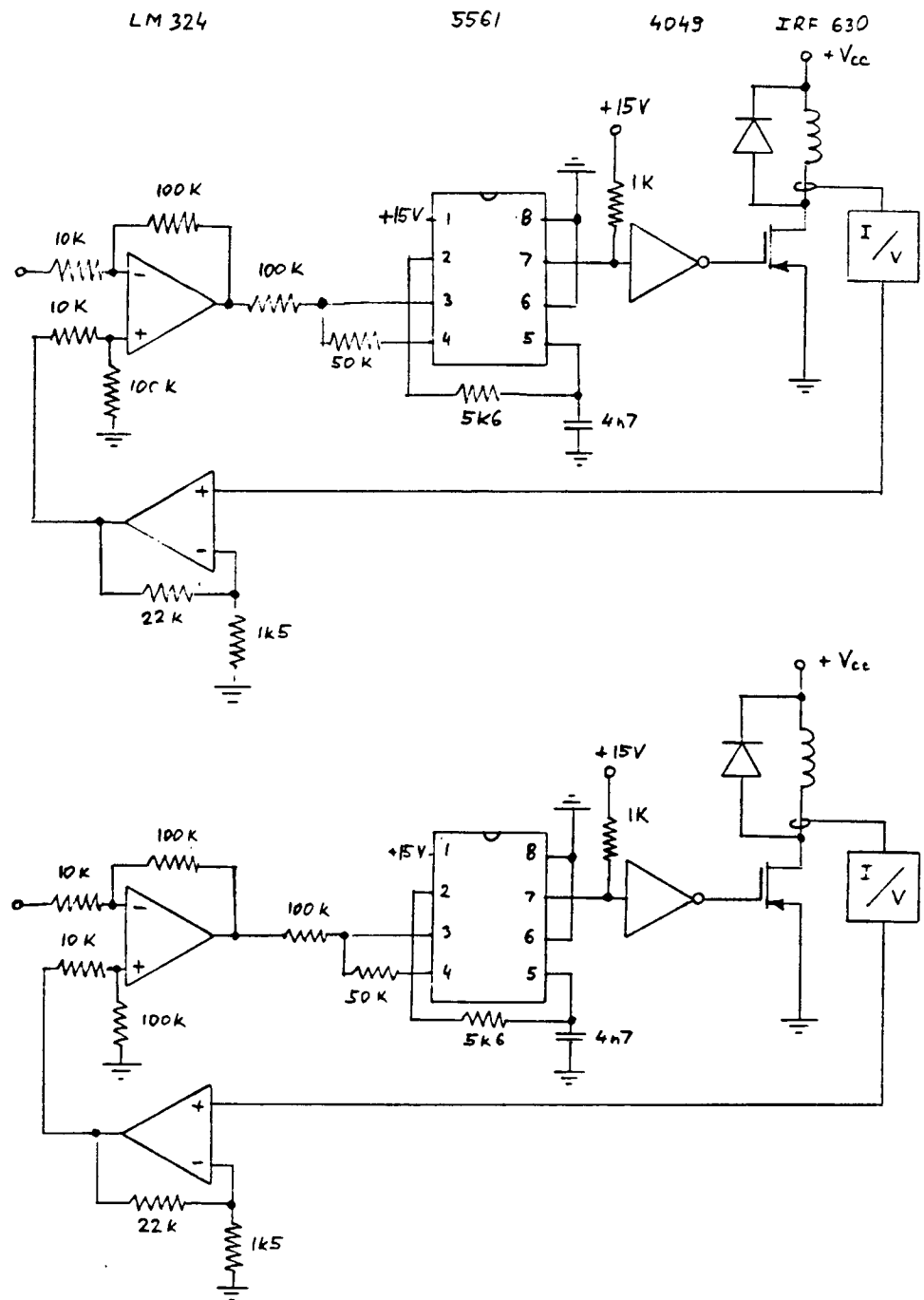
(position and velocity signals)



Simple A Class Chopper (Voltage Driver)

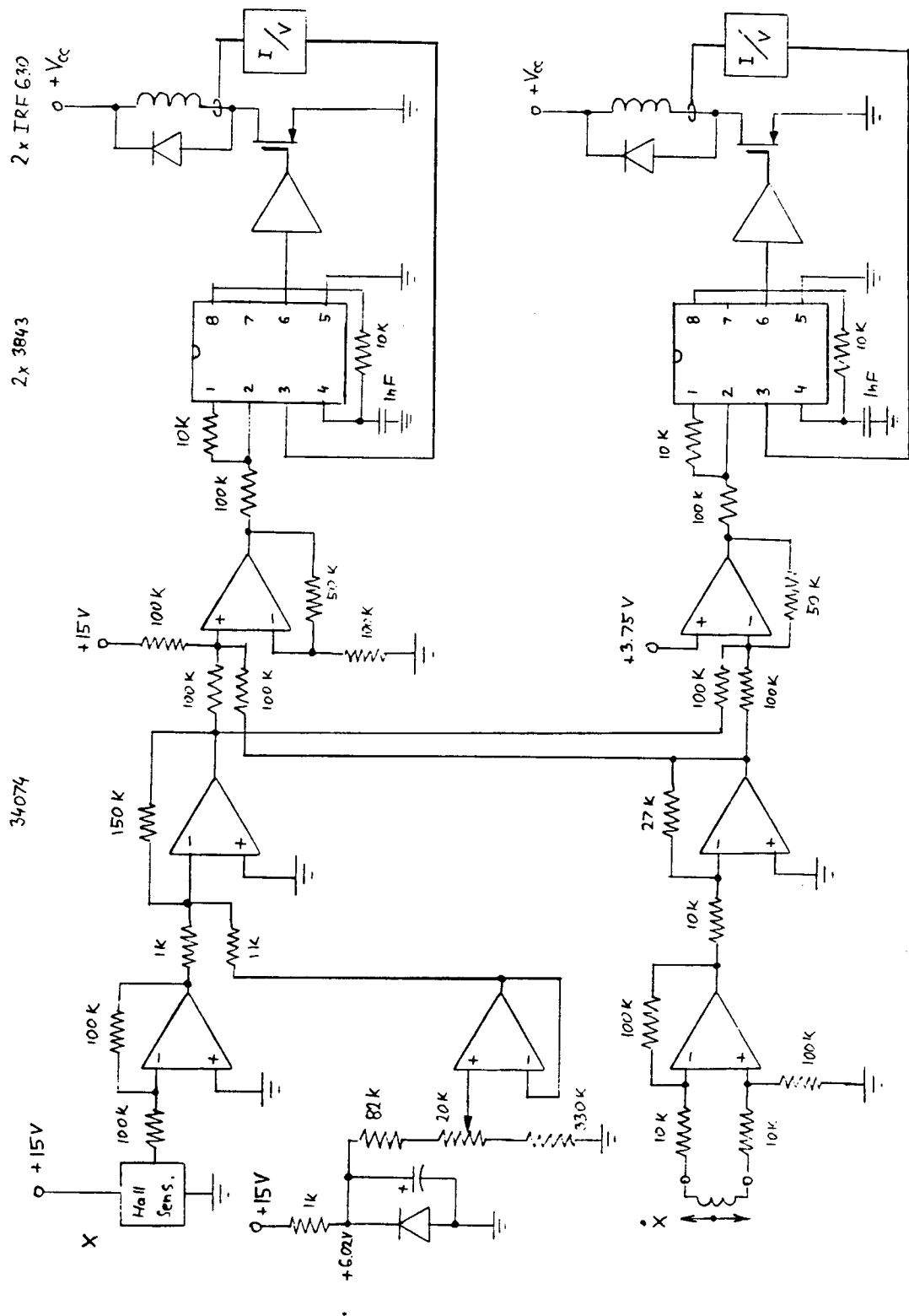


A Class Chopper (Current Feedback)

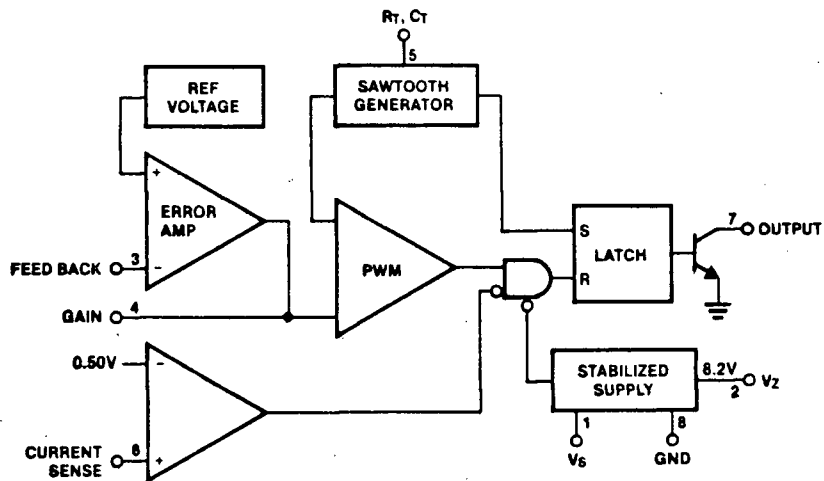


The Complete Control Circuit (Current Driver)

75



NE/SE5561 [14]



UC3842 [15]

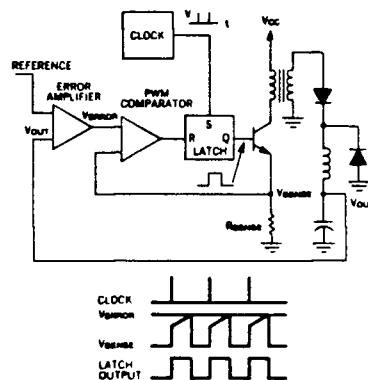
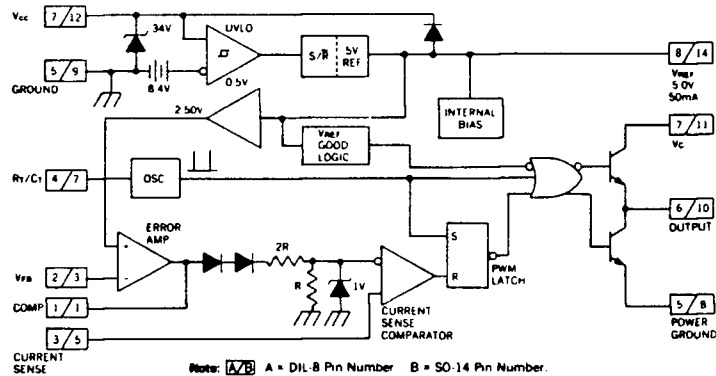
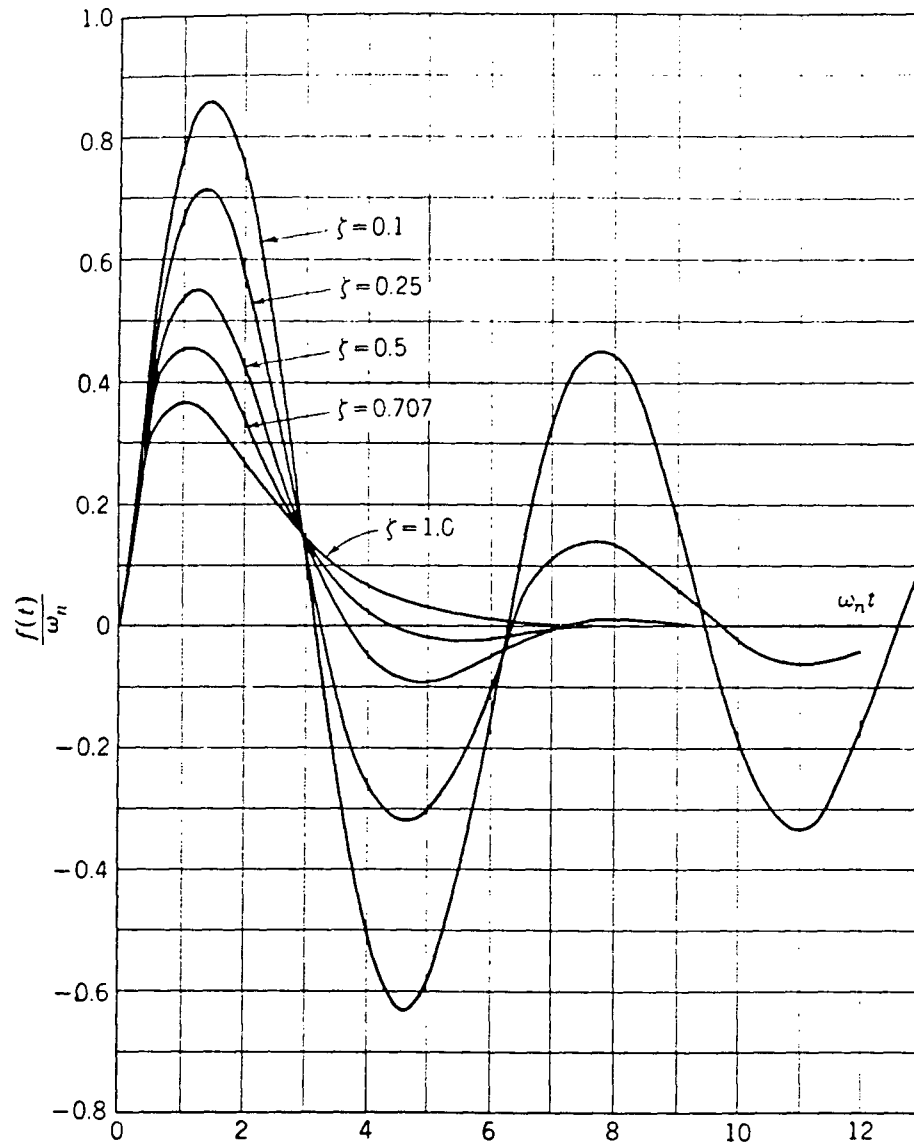
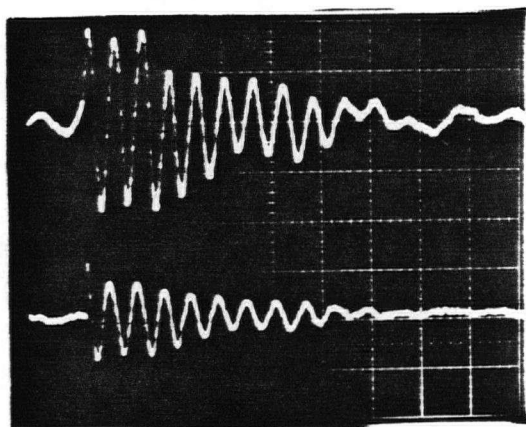
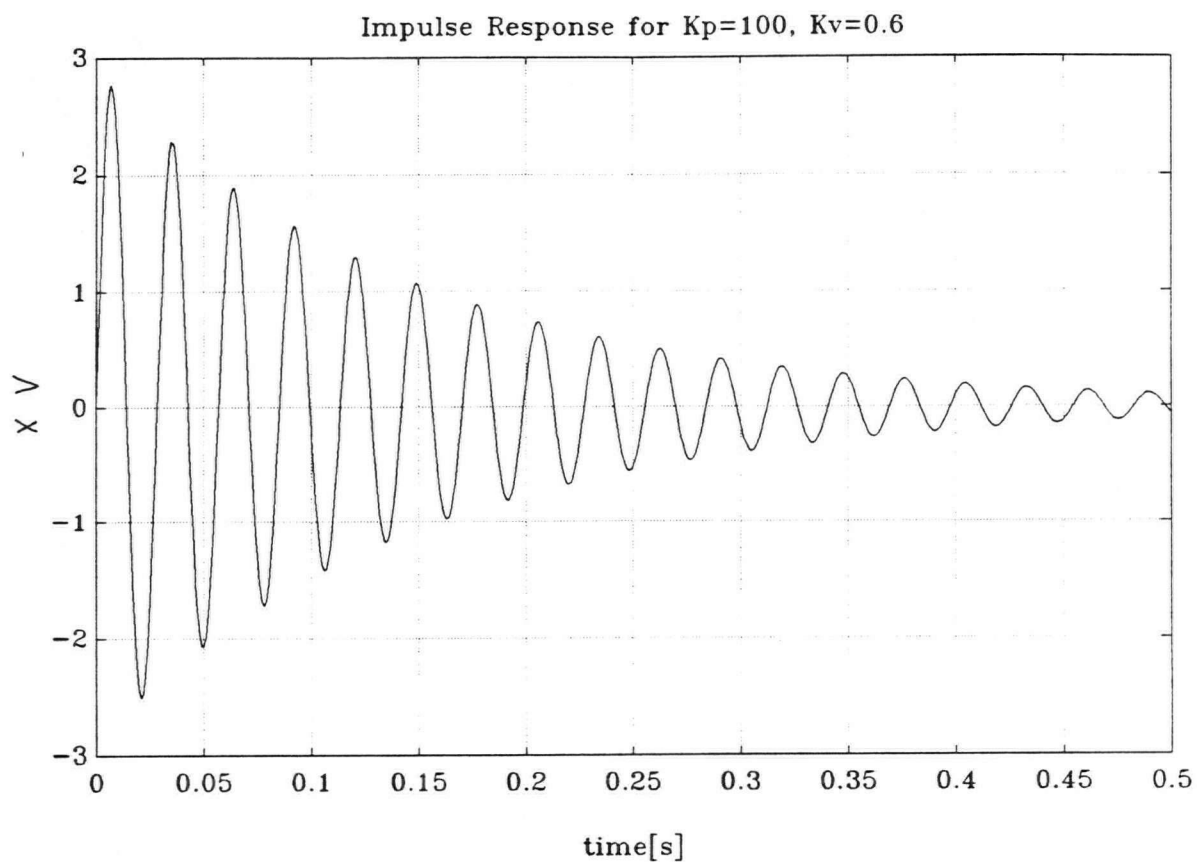


FIGURE 1. TWO-LOOP CURRENT-MODE CONTROL SYSTEM.

Impulse Response for $F(s) = \frac{\omega_n^2}{s^2 + 2\zeta\omega_n s + \omega_n^2}$ [11]

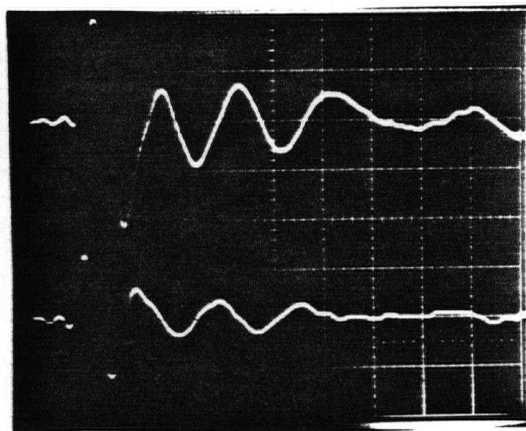
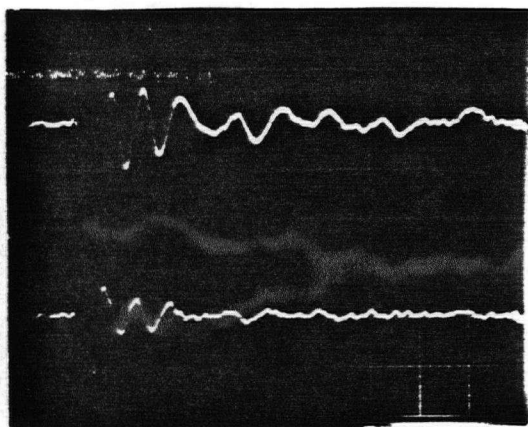
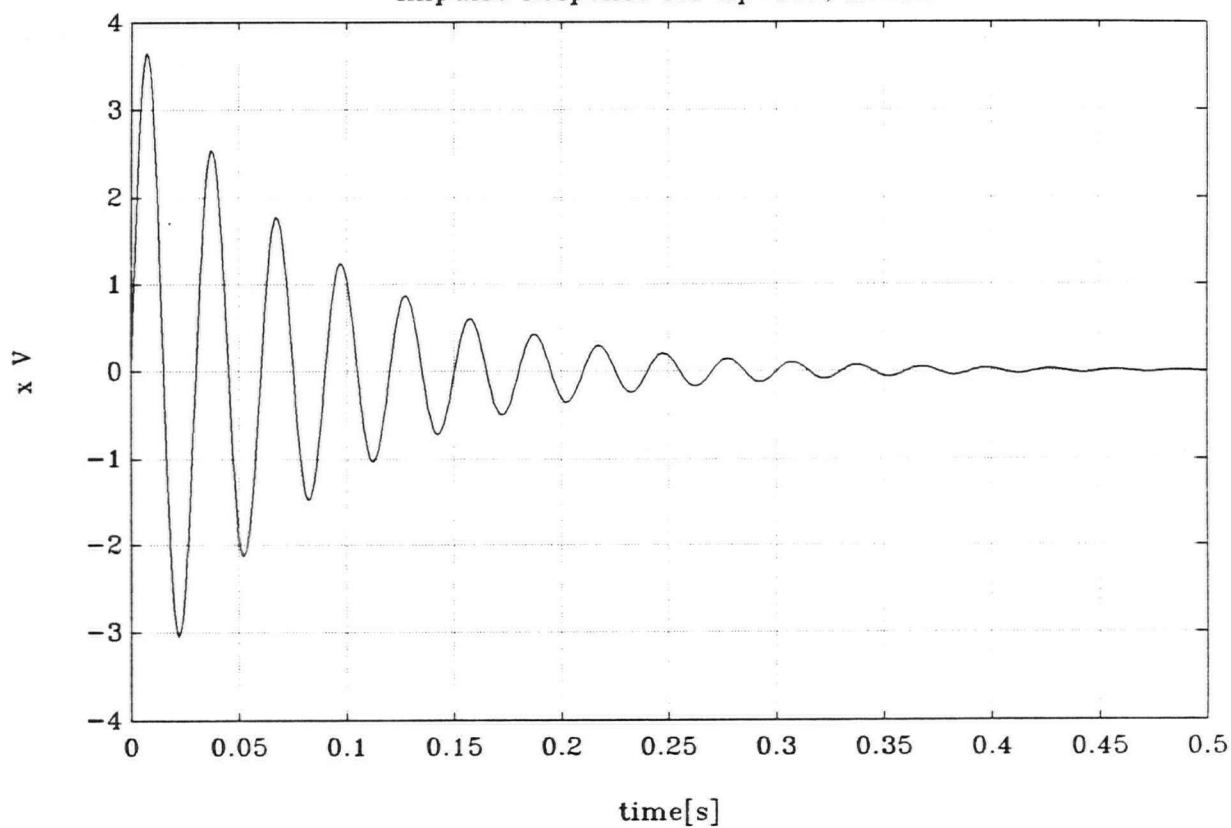




POS. : $K_P = 100$ 2V/div

VEL. : $K_V = 0.6$ 5V/div

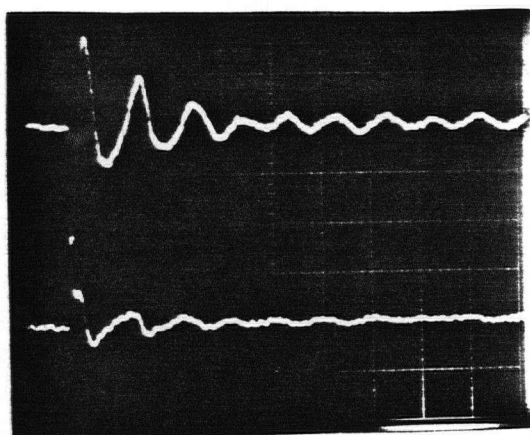
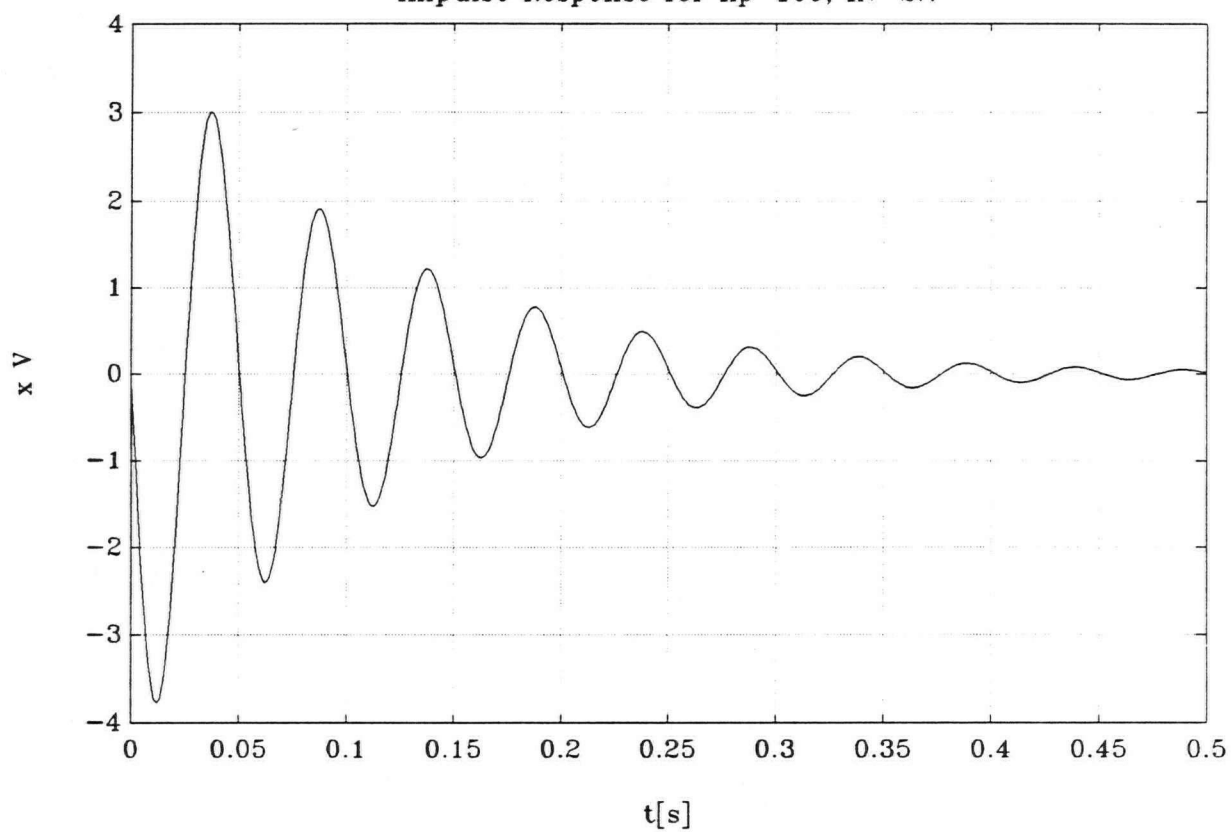
TIME : 50ms/div

Impulse Response for $K_p=100$, $K_v=0.7$ 

POS. : $K_p = 100$ 2V/div

VEL. : $K_v = 0.7$ 5V/div

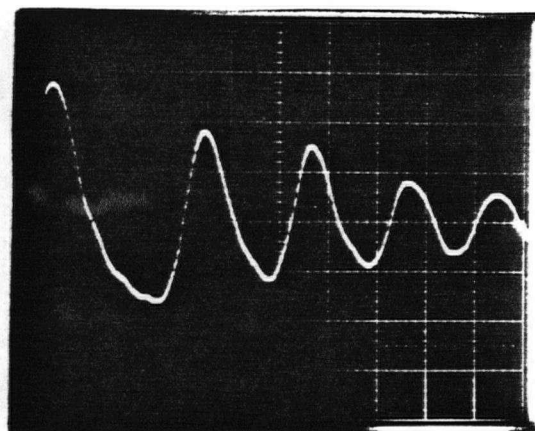
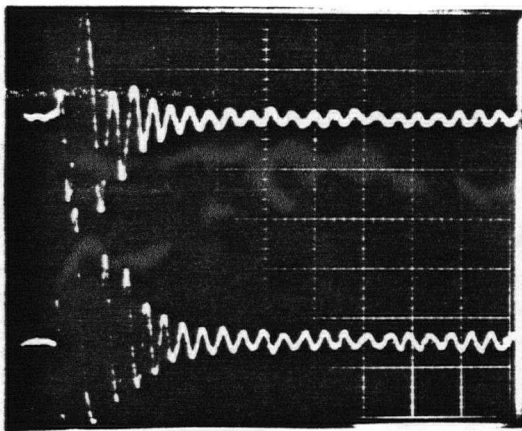
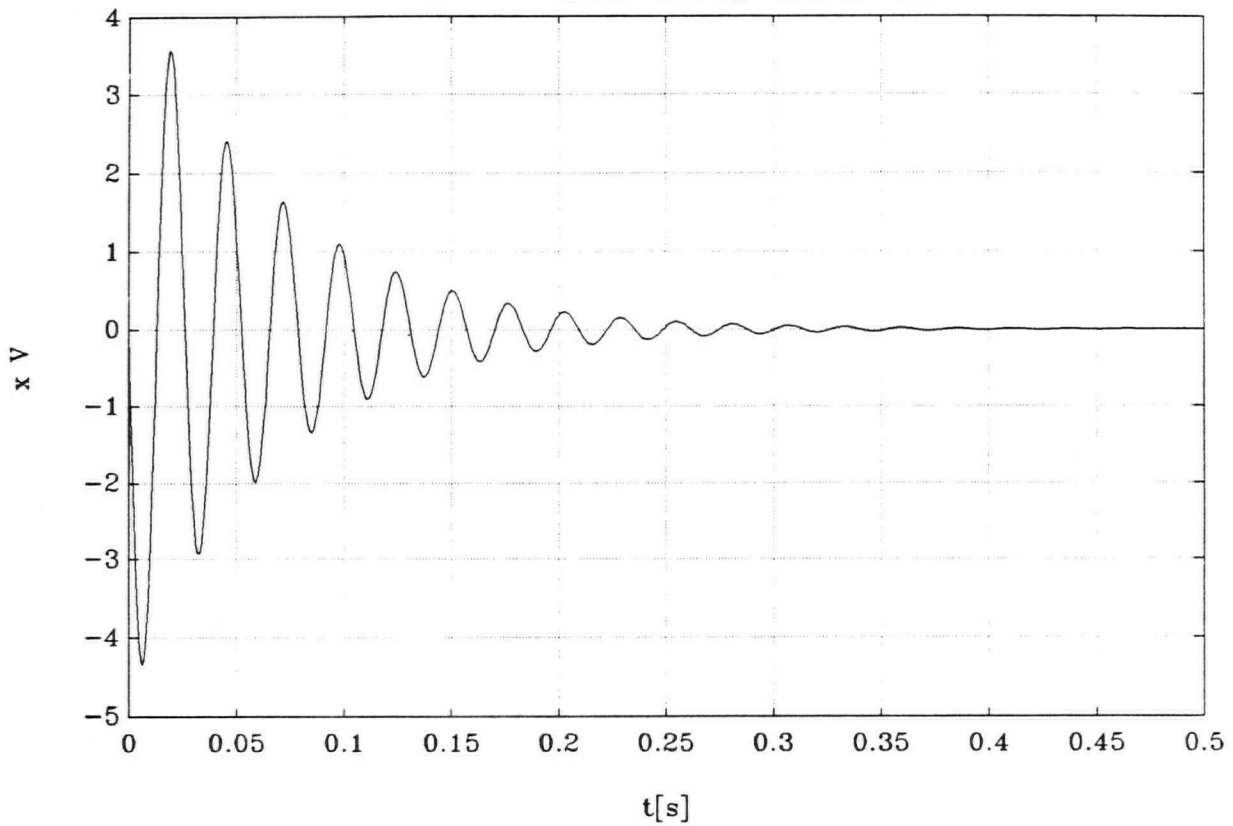
TIME : 50ms/div, 20ms/div

Impulse Response for $K_p=100$, $K_v=2.7$ 

POS. : $K_P = 100$ 2V/div

VEL. : $K_V = 2.7$ 5V/div

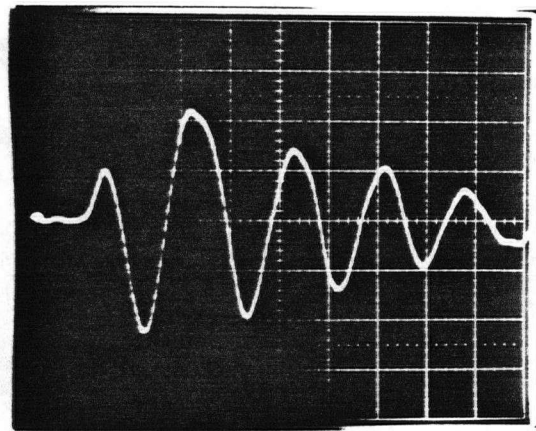
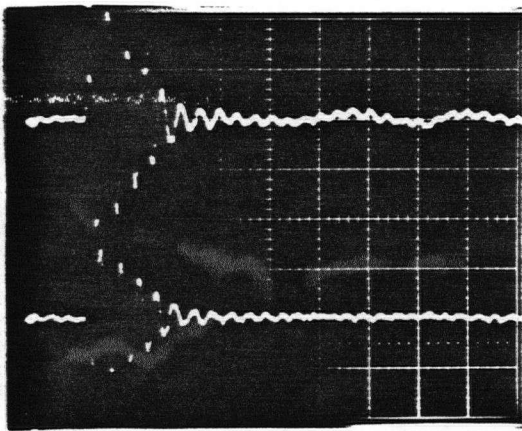
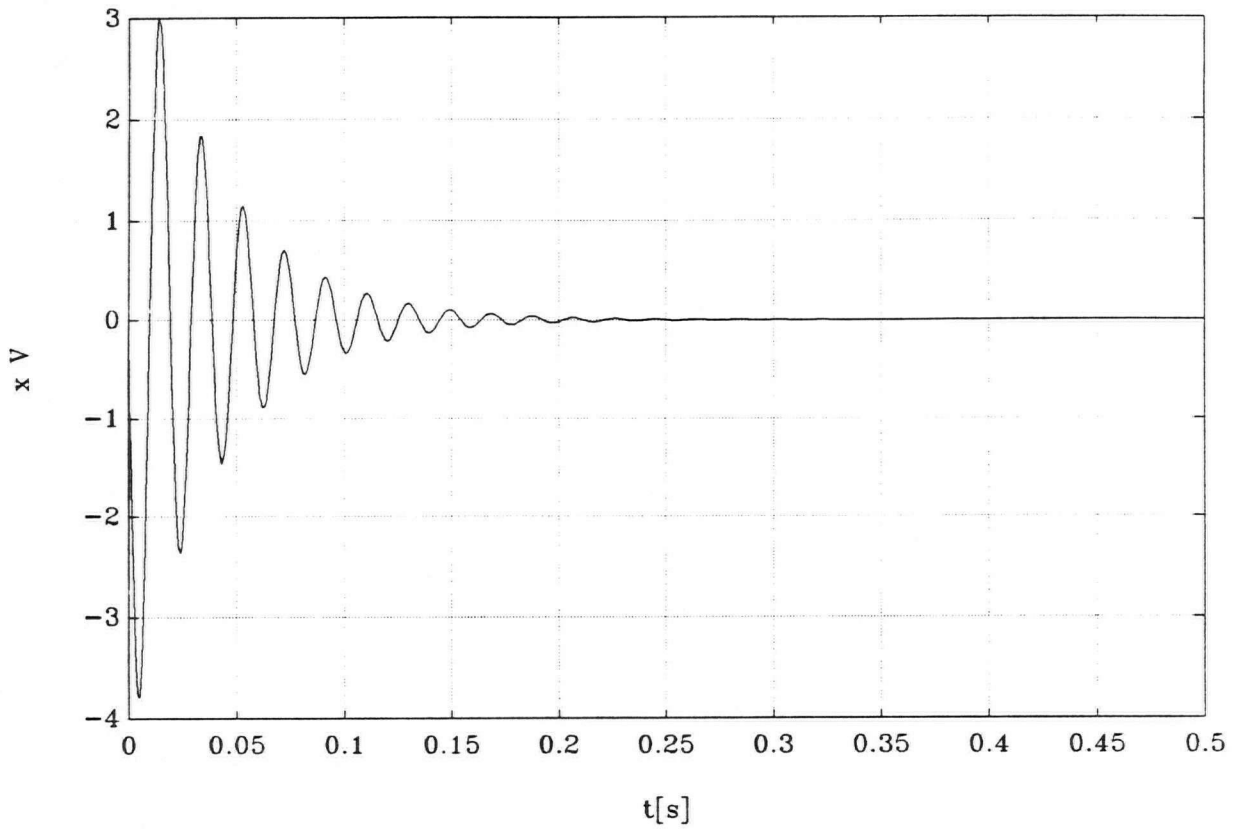
TIME : 50ms/div

Impulse Response for $K_P=150$, $K_V=0.9$ 

POS. : $K_P = 150$ 2V/div

VEL. : $K_V = 0.9$ 5V/div

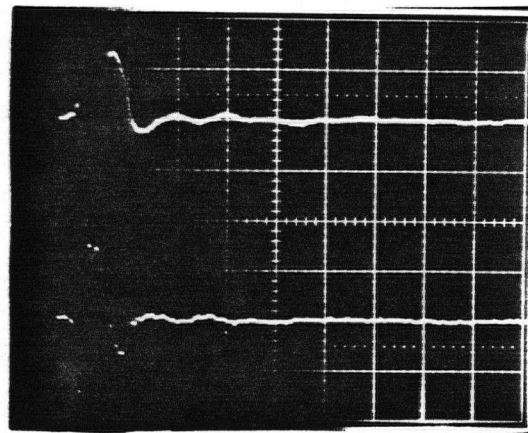
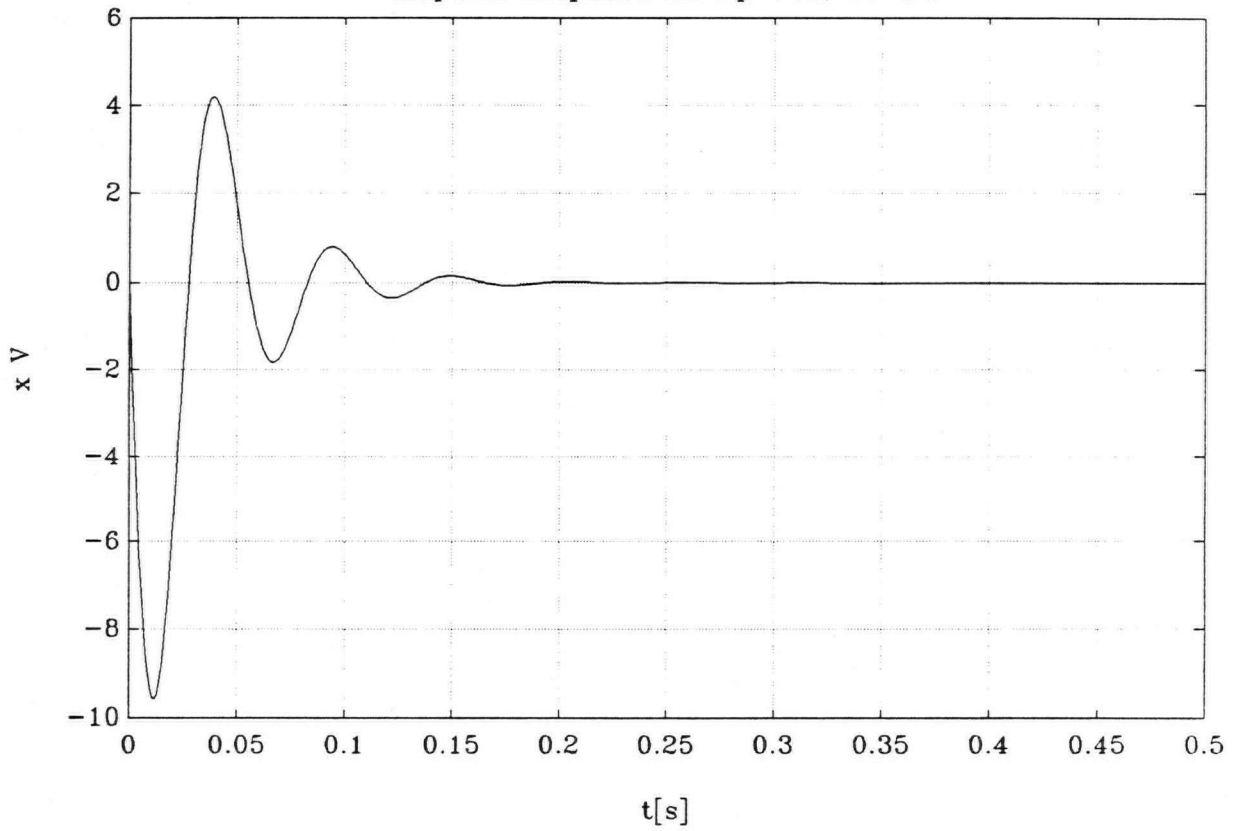
TIME : 50ms/div, 10ms/div

Impulse Response for $K_p=150$, $K_v=1.5$ 

POS. : $K_p = 150$ 2V/div

VEL. : $K_v = 1.5$ 5V/div

TIME : 50ms/div, 10ms/div

Impulse Response for $K_P=150$, $K_V=2.7$ 

POS. : $K_P = 150$ 2V/div

VEL. : $K_V = 2.7$ 5V/div

TIME : 50ms/div

Measured Stiffnesses of the Compensated Magnetic Bearing

In the compensated magnetic suspension system with closed loop the equation is derived from the block diagram in the Appendix on p.58. The simplification process is shown on pp.58 - 65. The result is the following expression:

$$s^2 + s \frac{K_s K_v}{m} + \frac{K_p K_s H - K_x}{m}$$

and compared to

$$s^2 + 2s\xi\omega_n + \omega_n^2$$

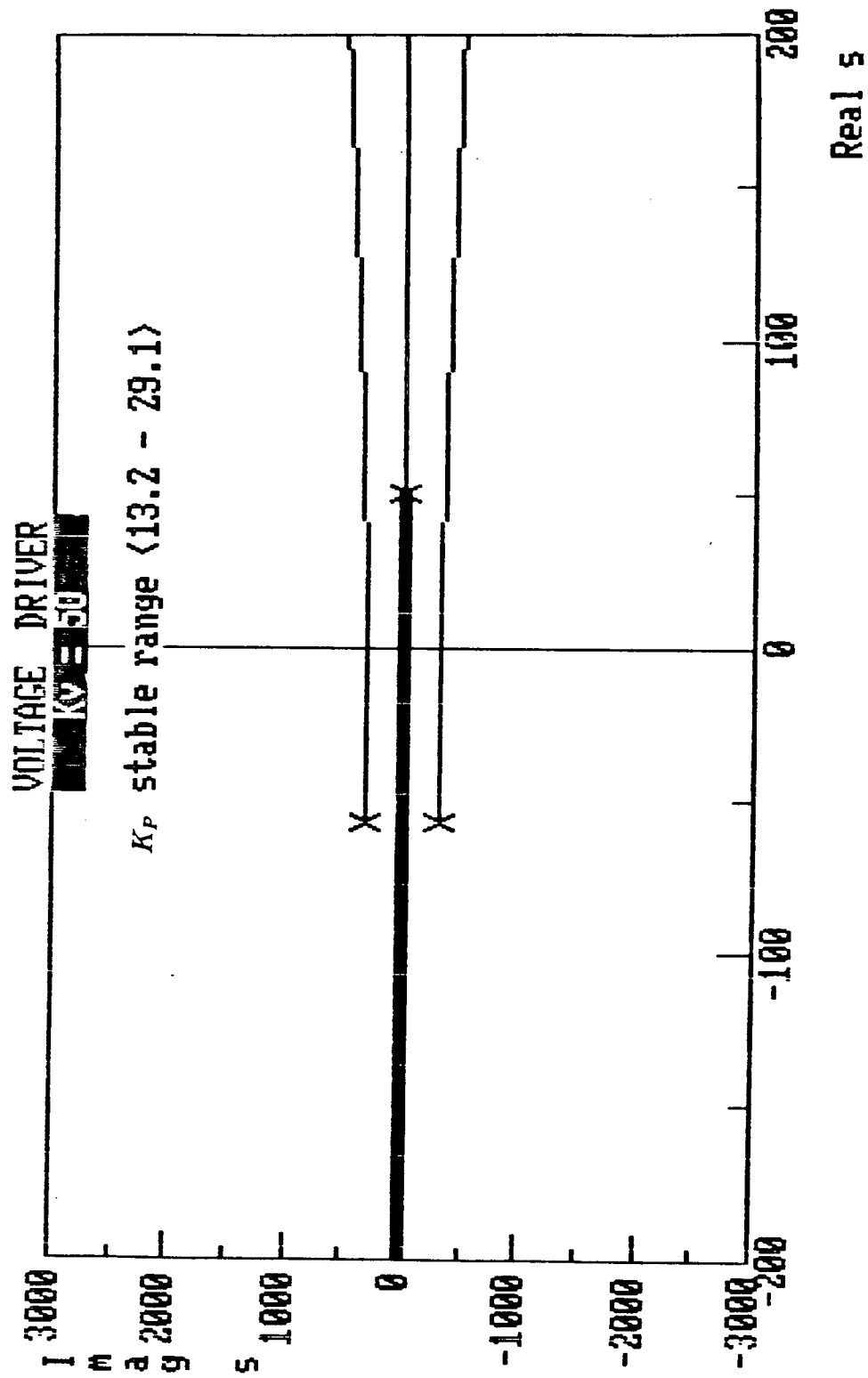
it gives

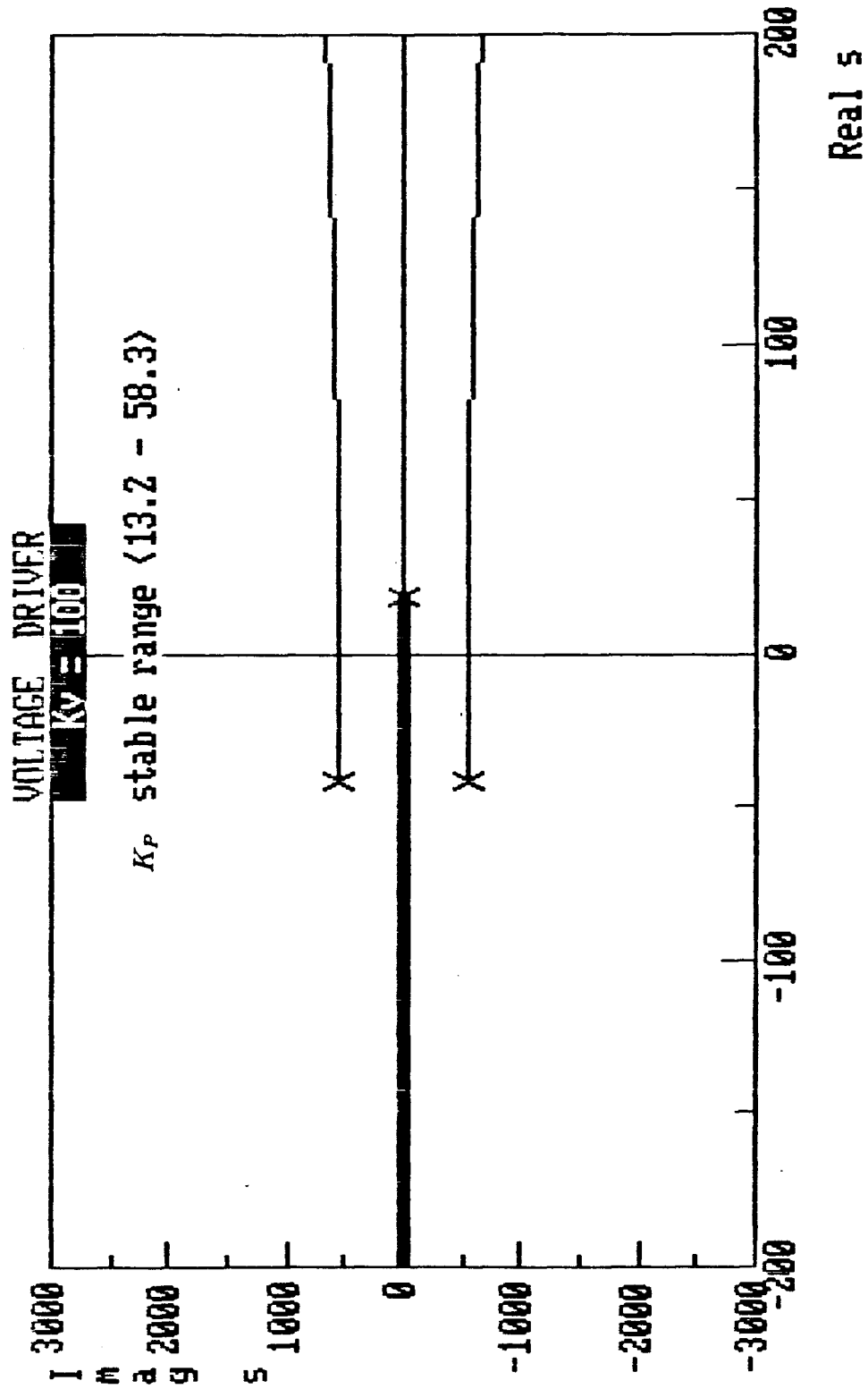
$$2\xi\omega_n = \frac{K_s K_v}{m}$$

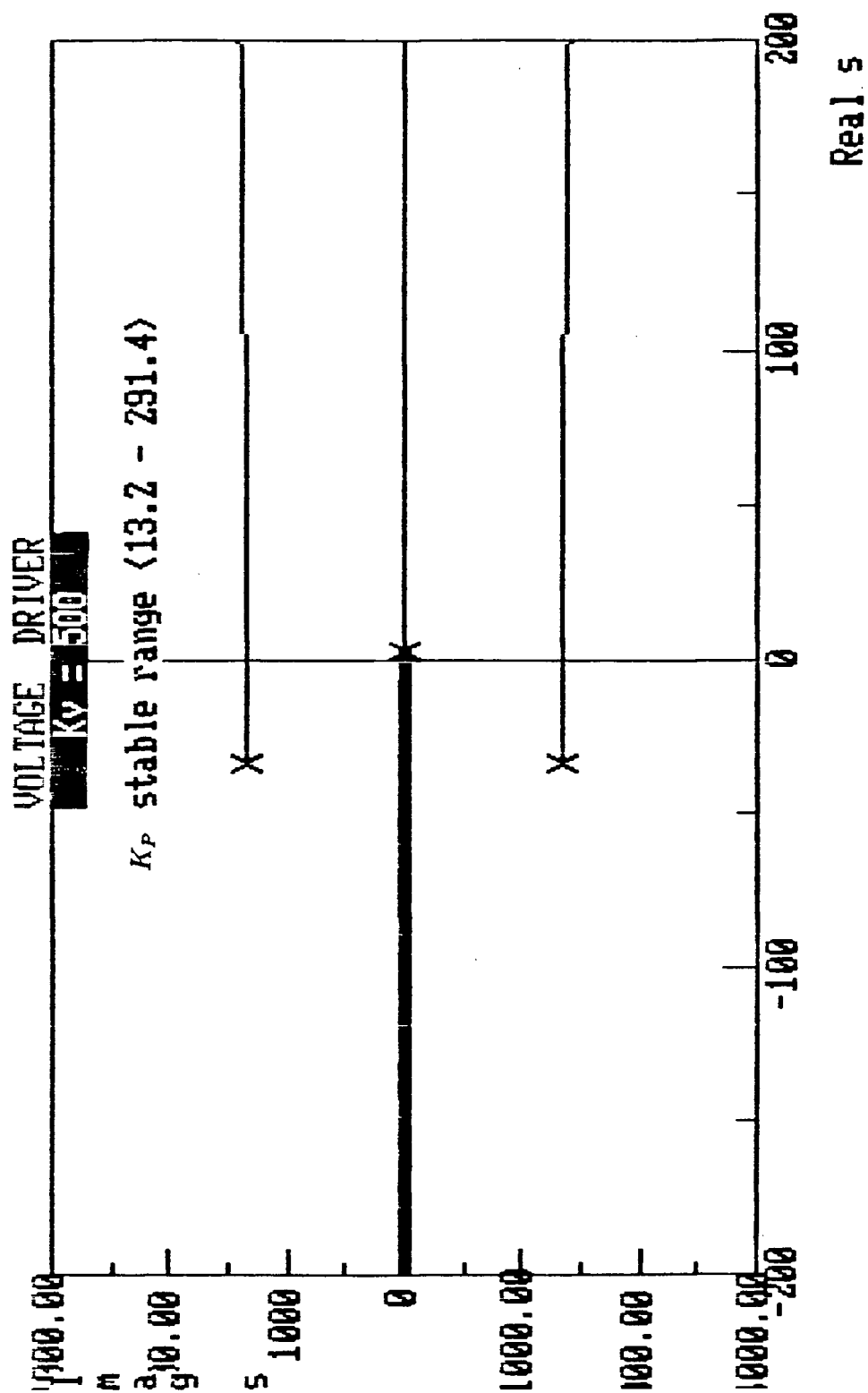
$$\omega_n^2 = \frac{K_p K_s H - K_x}{m} = \frac{K}{m}$$

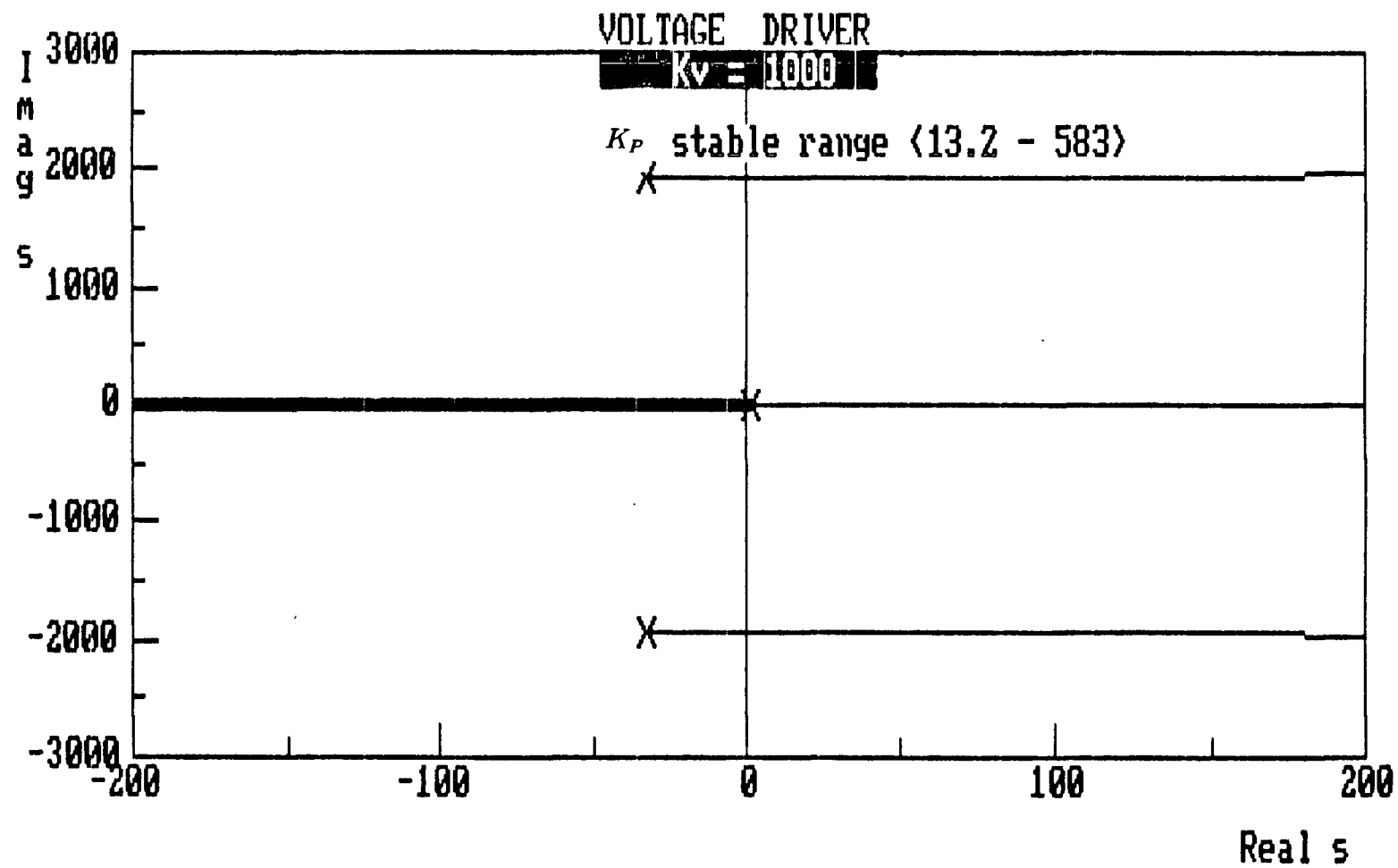
The following values were calculated:

Parameters		Calculated	Measured	Difference
K_p	K_v	K	K	%
100	0.6	10870	12900	18.7
100	0.7	10870	12900	18.7
100	2.7	10870	12900	18.7
150	0.9	42110	48600	15.4
150	1.5	42110	48600	15.4
150	2.7	42110	48600	15.4
150	5.0	42110	48600	15.4

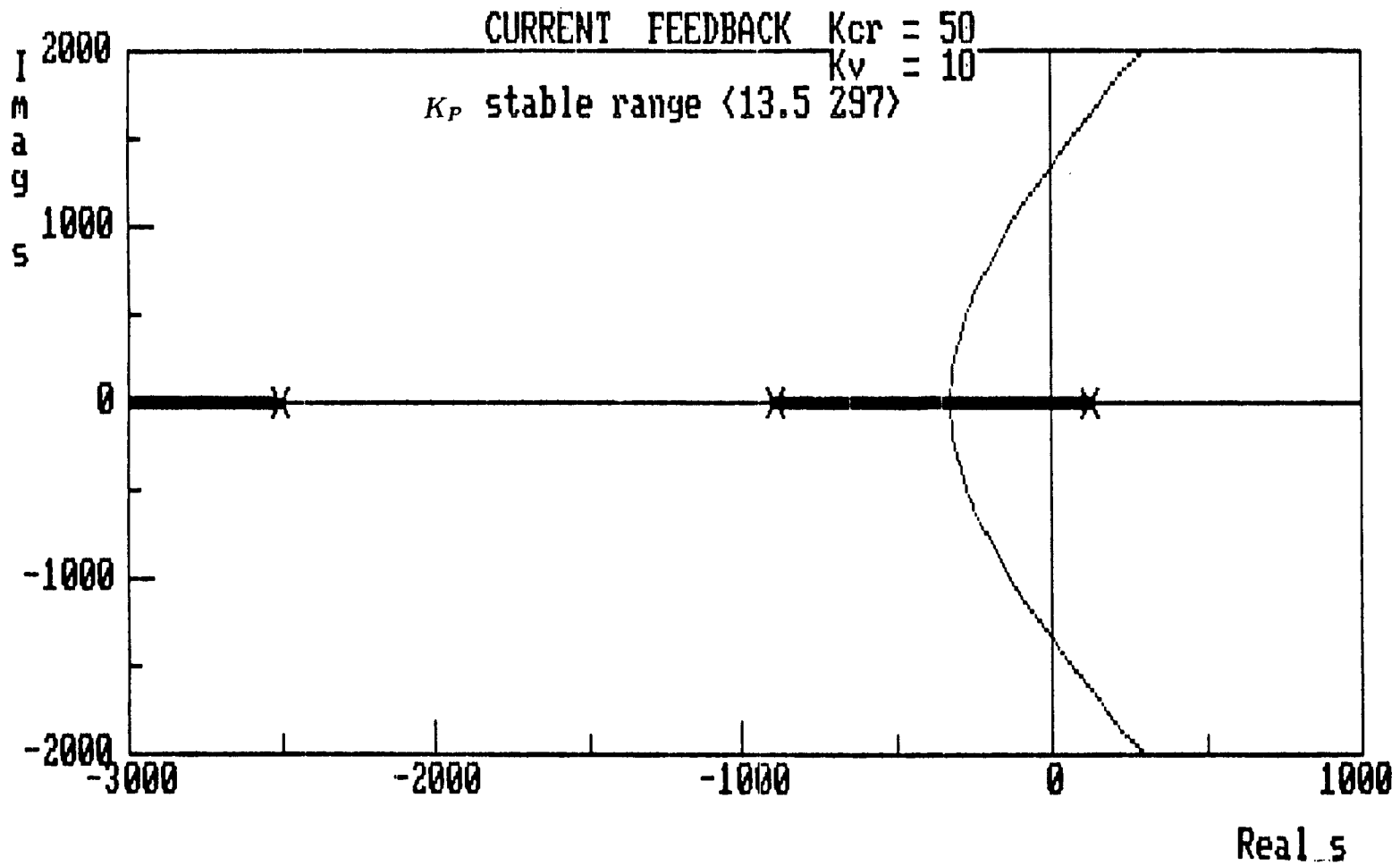


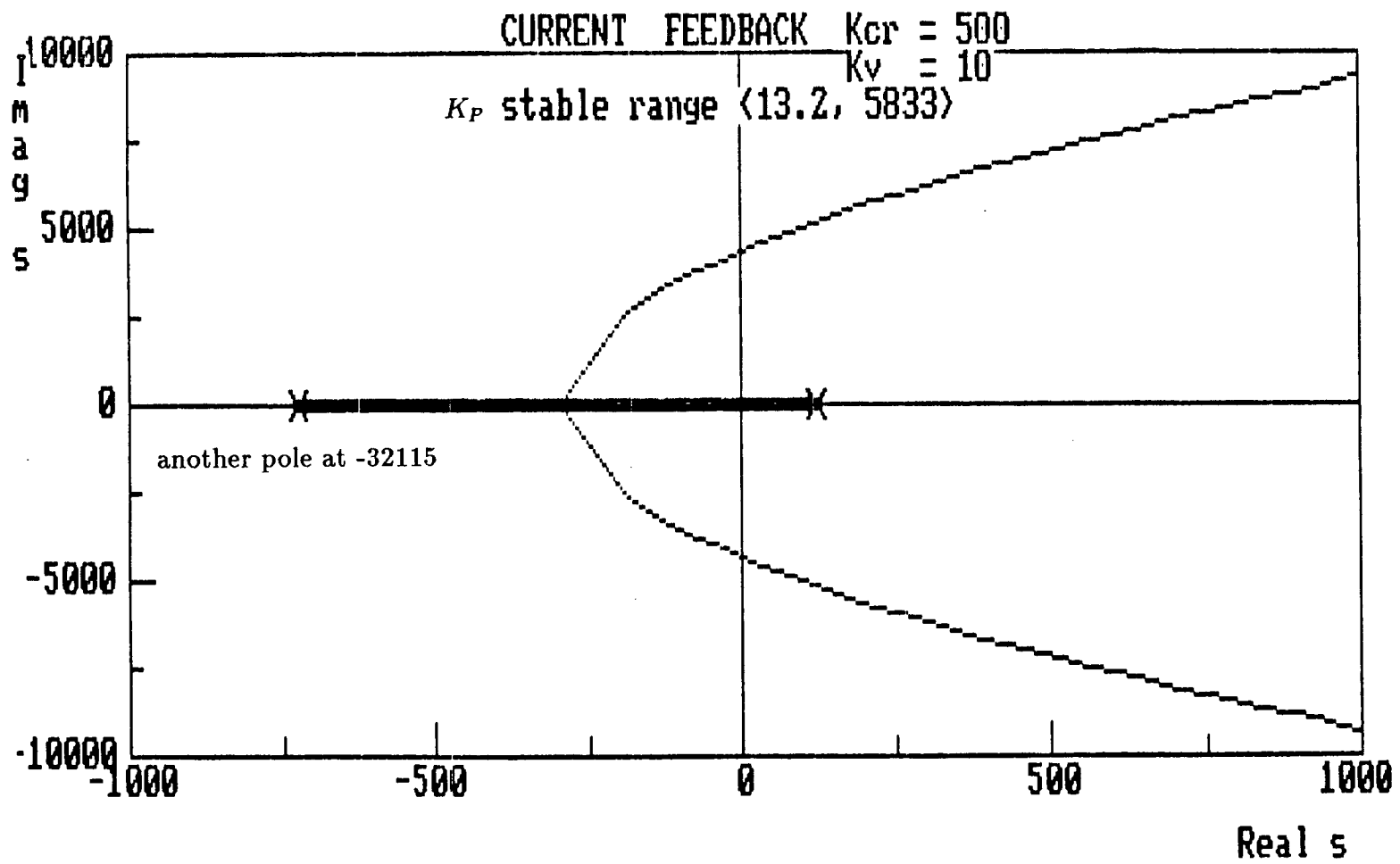


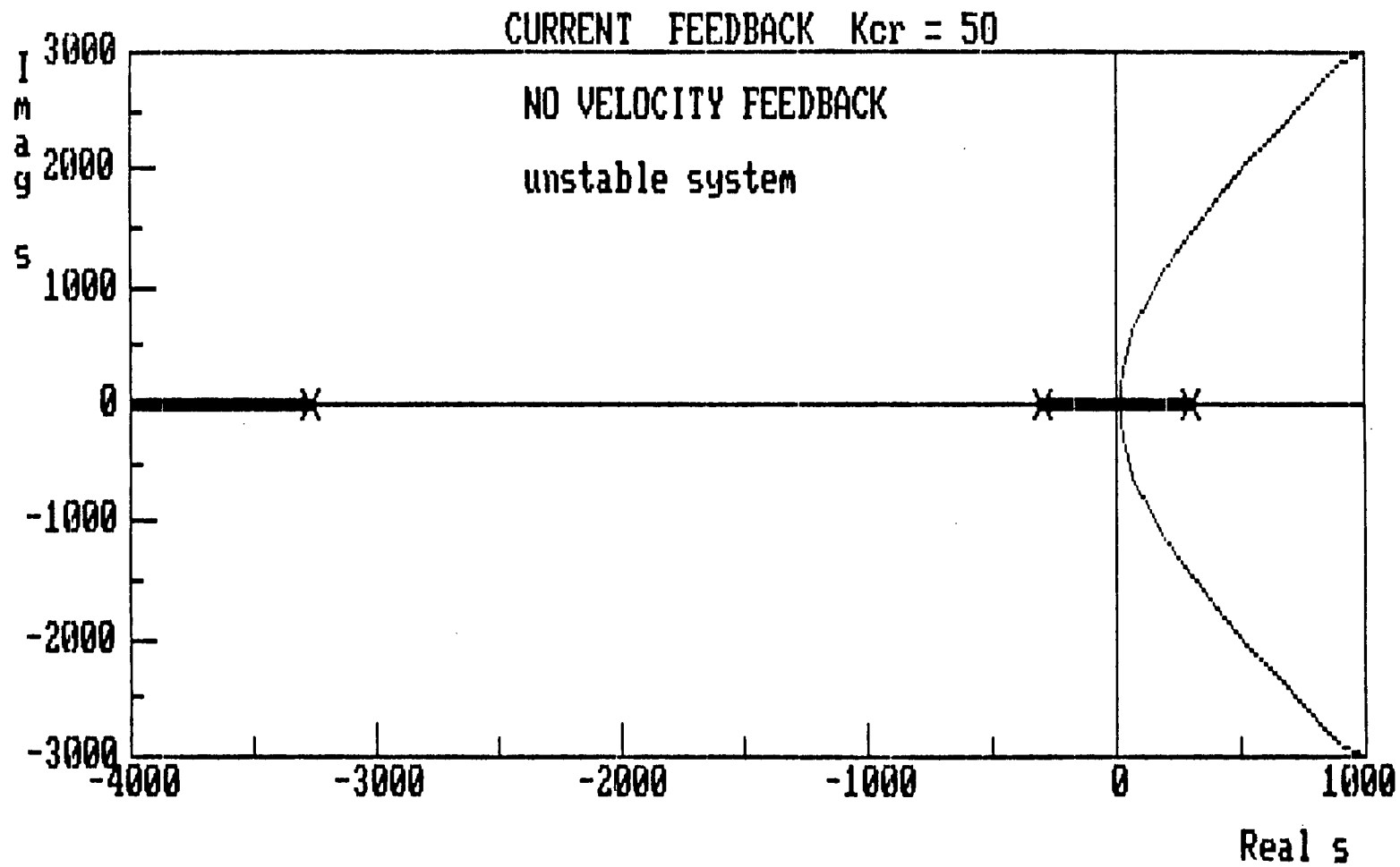




Root Locus of the Stabilized System using a Voltage Driver

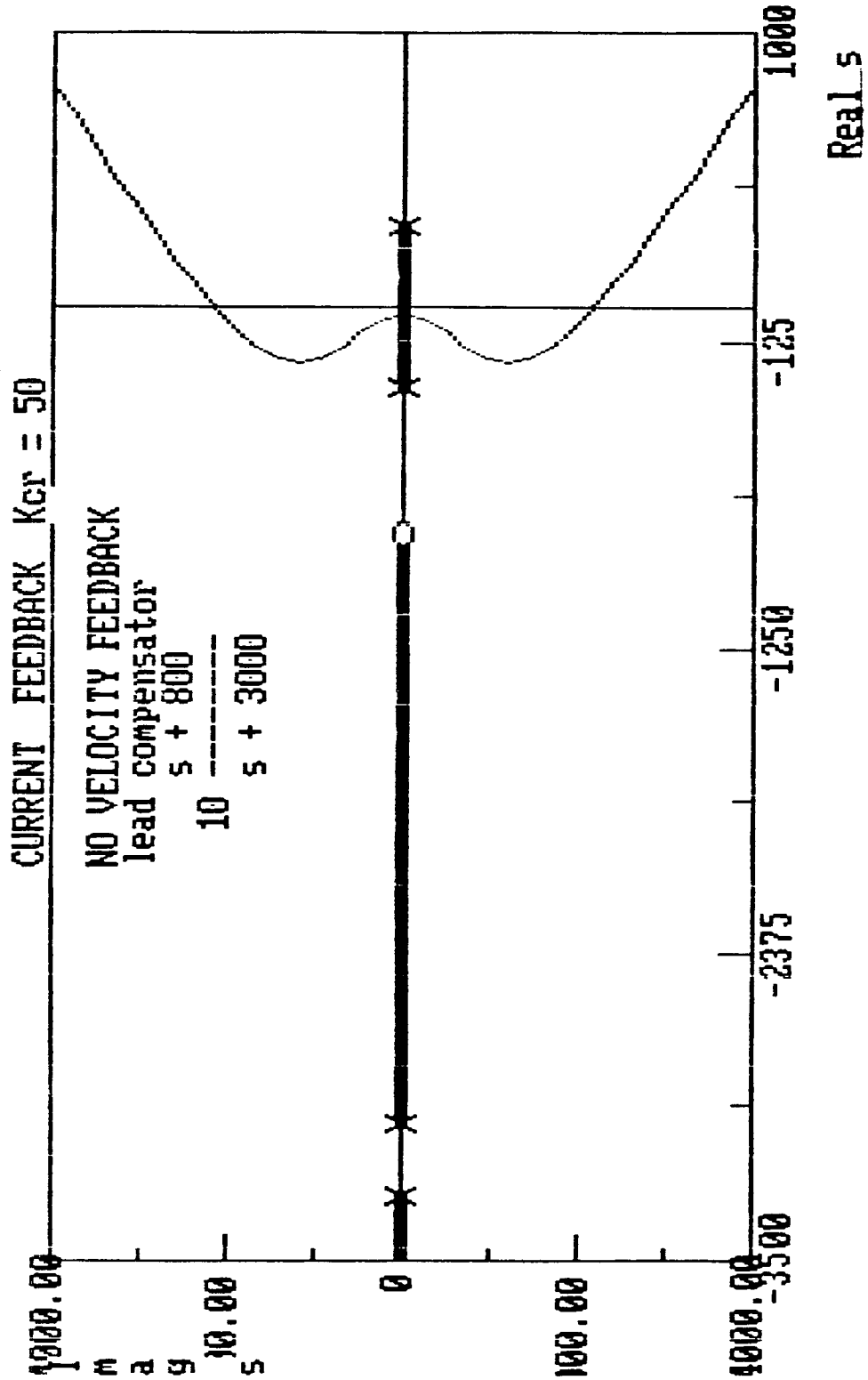






Root Locus of the Unstable System (no velocity feedback)

Root Locus of the System (without the velocity feedback)
using a Lead Cascade Compensator



2.7 RC Network Synthesis for Feedback Amplifier

RC networks can be used for synthesis of various feedback amplifier functions, using the transmittance function. Appendix A44 - A49 contains a table of the most common RC configurations ¹.

We assume the following for the operational amplifier:

$A_0 = \infty$ open-loop gain

$BW = \infty$ bandwidth

$I_B = 0$ bias current

$R_{IN} = \infty$ input impedance

$R_0 = 0$ output impedance

The transimpedance $Z_T = \frac{v_i}{i_o}$ of a circuit is defined as the input voltage divided by the output current when the output is shorted. This is the type of transfer function which is needed since the currents are summed at the op-amp input node (in the inverting arrangement of an op-amp the + input is grounded).

As an example a lead type of network is design here to represent a transfer function:

$$Z_T = 10 \frac{s + 800}{s + 3000}$$

Various combinations could be chosen for Z_{T1} , Z_{T2} , but let's choose

$$Z_{T1} = 10(s + 800)$$

and

$$Z_{T2} = s + 3000$$

¹Reproduced from F.R.Bradley and R.McCoy, "Driftless DC Amplifier", *Electronics*, April 1952. This table was developed by S.Godet of the Reeves Instrument Corporation, New York.

Referring to the table in A44, equation (J1-3), the procedure is following:

$$Z_{T1} = 10(s + 800) = 10 * 800(0.00125s + 1)$$

so that $A = 8000$ and $T = 0.00125$ [s].

Let $C_1 = 1 \mu\text{F}$ (a practical value picked) then

$$R_1 = \frac{2T}{C_1} = 2500 [\Omega]$$

And similarly

$$Z_{T2} = s + 3000 = 3000(0.00033s + 1)$$

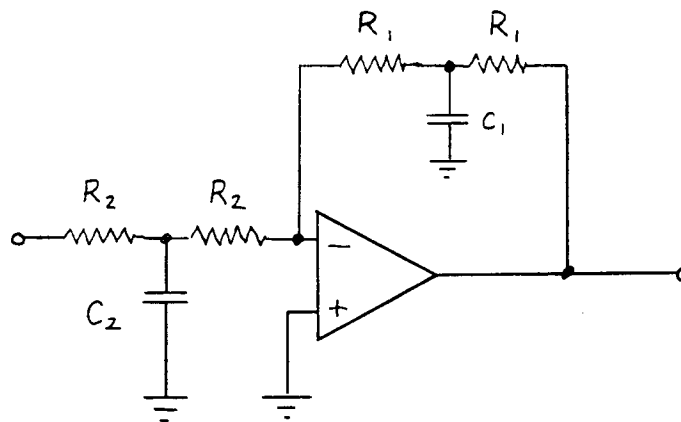
so that $A = 3000$ and $T = 0.00033$ [s].

Again, let pick a value of $C_2 = 10 \text{ nF}$ then

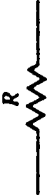
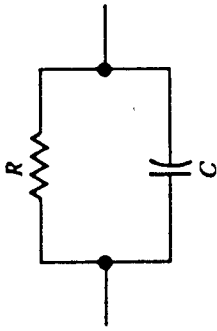
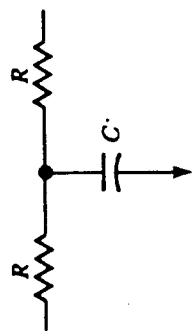
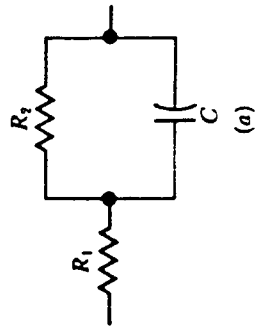
$$R_2 = \frac{2T}{C_2} = 66700 [\Omega]$$

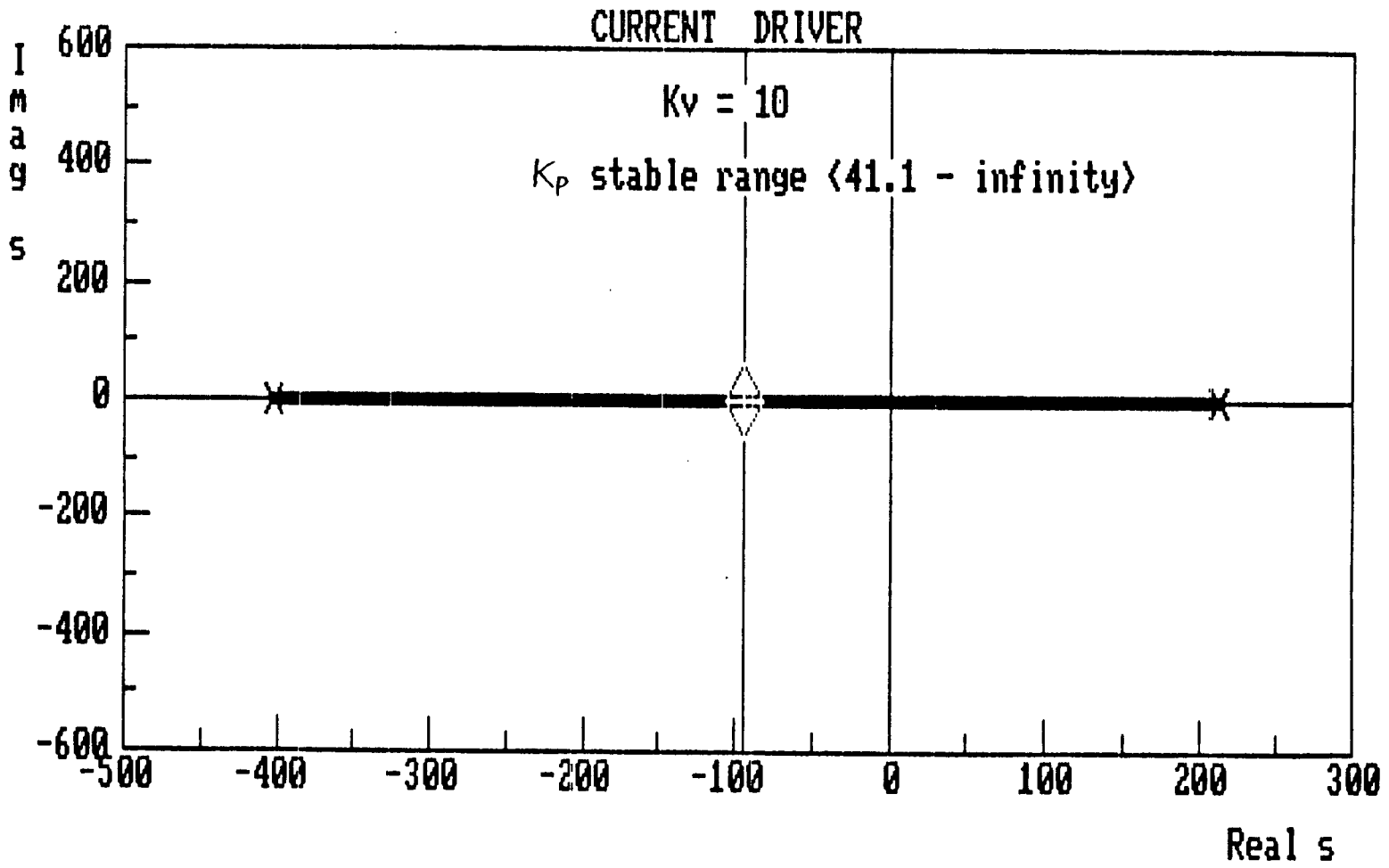
If the calculated value is not available, the procedure can be repeated for a different value of C . At DC (i.e. $s = 0$), the gain is:

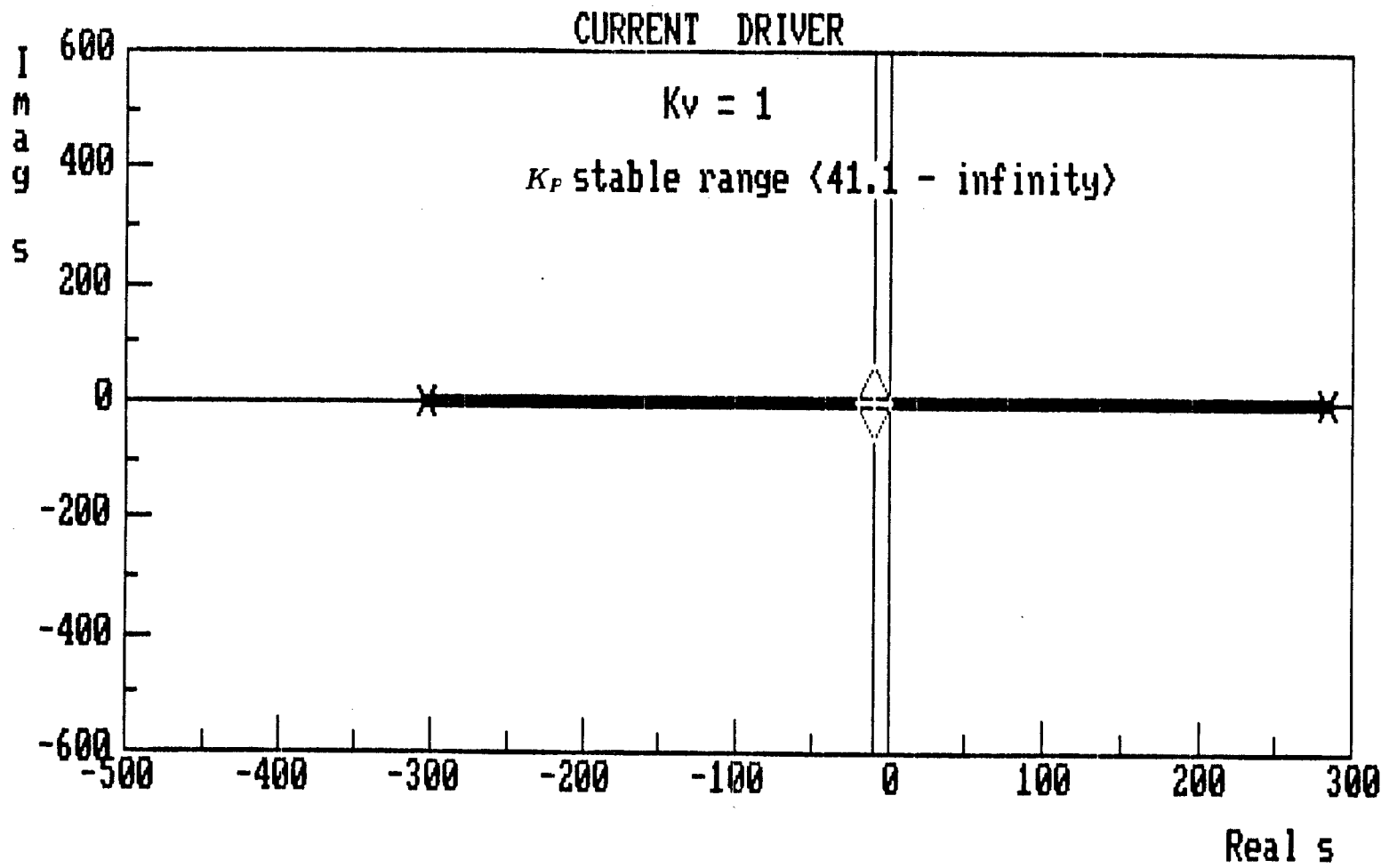
$$A_v = \frac{10 * 800}{3000} = 2.667$$



RC Network Synthesis for a Feedback Amplifier

Transfer Impedance Function (v_o/i_i)	Network	Relations	Inverse Relations
A (I1-1)		$A = R$	$R = A$
$\frac{A}{1+sT}$ (I1-2)		$A = R$ $T = RC$	$R = \frac{A}{T}$ $C = \frac{T}{A}$
$A(1+sT)$ (I1-3)		$A = 2R$ $T = \frac{RC}{2}$	$R = \frac{A}{2}$ $C = \frac{4T}{A}$
$A\left(\frac{1+s\theta T}{1+sT}\right)$ $\theta < 1$ (I1-4)		$A = R_1 + R_2$ $T = R_2 C$ $\theta = \frac{R_1}{R_1 + R_2}$	$R_1 = A\theta$ $R_2 = \frac{A(1-\theta)}{T}$ $C = \frac{T}{A(1-\theta)}$





Root Locus of the Stabilized System using a Current Driver

$d/2$ [mm]	Weight[N]	I [A]	i [A]	$F1$ [N]
0.25	6.70	0.20	0.20	6.73E+00
0.50	6.70	0.40	0.40	6.73E+00
0.75	6.70	0.59	0.59	6.73E+00
1.00	6.70	0.79	0.79	6.73E+00
1.25	6.70	0.99	0.99	6.73E+00
1.50	6.70	1.19	1.19	6.73E+00
1.75	6.70	1.39	1.39	6.73E+00
2.00	6.70	1.59	1.59	6.73E+00
2.25	6.70	1.78	1.78	6.73E+00
2.50	6.70	1.98	1.98	6.73E+00
2.75	6.70	2.18	2.18	6.73E+00
3.00	6.70	2.38	2.38	6.73E+00

$d/2$ [mm]	$d/2$ [mm]	i [A]	Kx [N/m]	Kx/m	Ki [N/A]	Ki/m
1.50	1.50	0.5	1.94E+02	2.84E+02	1.16E+00	1.70E+00
1.50	1.50	1.0	7.75E+02	1.14E+03	2.33E+00	3.41E+00
1.50	1.50	1.5	1.74E+03	2.55E+03	3.49E+00	5.11E+00
1.50	1.50	2.0	3.10E+03	4.54E+03	4.65E+00	6.81E+00
1.50	1.50	2.5	4.85E+03	7.10E+03	5.82E+00	8.52E+00
1.50	1.50	3.0	6.98E+03	1.02E+04	6.98E+00	1.02E+01
1.50	1.50	3.5	9.50E+03	1.39E+04	8.14E+00	1.19E+01
1.50	1.50	4.0	1.24E+04	1.82E+04	9.31E+00	1.36E+01
1.50	1.50	4.5	1.57E+04	2.30E+04	1.05E+01	1.53E+01
1.50	1.50	5.0	1.94E+04	2.84E+04	1.16E+01	1.70E+01
1.50	1.50	5.5	2.35E+04	3.43E+04	1.28E+01	1.87E+01
1.50	1.50	6.0	2.79E+04	4.09E+04	1.40E+01	2.04E+01
1.50	1.50	6.5	3.28E+04	4.80E+04	1.51E+01	2.21E+01
1.50	1.50	7.0	3.80E+04	5.56E+04	1.63E+01	2.38E+01
1.50	1.50	7.5	4.36E+04	6.39E+04	1.74E+01	2.55E+01
1.50	1.50	8.0	4.96E+04	7.27E+04	1.86E+01	2.72E+01
1.50	1.50	8.5	5.60E+04	8.20E+04	1.98E+01	2.90E+01
1.50	1.50	9.0	6.28E+04	9.20E+04	2.09E+01	3.07E+01
1.50	1.50	9.5	7.00E+04	1.02E+05	2.21E+01	3.24E+01
1.50	1.50	10.0	7.75E+04	1.14E+05	2.33E+01	3.41E+01

$d/2$ [mm]	$d/2$ [mm]	$i1$ [A]	$i2$ [A]	$F1$ [N]	$F2$ [N]	Kx [N/m]	Kx/m
1.50	1.50	2.33	2.00	2.53E+01	1.86E+01	5.85E+04	8.56E+04
1.50	1.50	1.00	1.00	4.65E+00	4.65E+00	1.24E+04	1.82E+04
1.50	1.50	1.50	1.50	1.05E+01	1.05E+01	2.79E+04	4.09E+04
1.50	1.50	2.00	2.00	1.86E+01	1.86E+01	4.96E+04	7.27E+04
1.50	1.50	2.50	2.50	2.91E+01	2.91E+01	7.75E+04	1.14E+05
1.50	1.50	3.00	3.00	4.19E+01	4.19E+01	1.12E+05	1.63E+05
1.50	1.50	3.50	3.50	5.70E+01	5.70E+01	1.52E+05	2.23E+05
1.50	1.50	4.00	4.00	7.44E+01	7.44E+01	1.99E+05	2.91E+05
1.50	1.50	4.50	4.50	9.42E+01	9.42E+01	2.51E+05	3.68E+05
1.50	1.50	5.00	5.00	1.16E+02	1.16E+02	3.10E+05	4.54E+05
1.50	1.50	5.50	5.50	1.41E+02	1.41E+02	3.75E+05	5.50E+05
1.50	1.50	6.00	6.00	1.68E+02	1.68E+02	4.47E+05	6.54E+05
1.50	1.50	6.50	6.50	1.97E+02	1.97E+02	5.24E+05	7.68E+05
1.50	1.50	7.00	7.00	2.28E+02	2.28E+02	6.08E+05	8.90E+05
1.50	1.50	7.50	7.50	2.62E+02	2.62E+02	6.98E+05	1.02E+06
1.50	1.50	8.00	8.00	2.98E+02	2.98E+02	7.94E+05	1.16E+06
1.50	1.50	8.50	8.50	3.36E+02	3.36E+02	8.96E+05	1.31E+06
1.50	1.50	9.00	9.00	3.77E+02	3.77E+02	1.01E+06	1.47E+06
1.50	1.50	9.50	9.50	4.20E+02	4.20E+02	1.12E+06	1.64E+06
1.50	1.50	10.00	10.00	4.65E+02	4.65E+02	1.24E+06	1.82E+06

$d/2$ [mm]	$d/2$ [mm]	$i1$ [A]	$i2$ [A]	$F1$ [N]	$F2$ [N]	Ki [N/A]	Ki/m
1.50	1.50	2.33	2.00	2.53E+01	1.86E+01	4.03E+01	5.90E+01
1.50	1.50	1.00	1.00	4.65E+00	4.65E+00	1.86E+01	2.72E+01
1.50	1.50	1.50	1.50	1.05E+01	1.05E+01	2.79E+01	4.09E+01
1.50	1.50	2.00	2.00	1.86E+01	1.86E+01	3.72E+01	5.45E+01
1.50	1.50	2.50	2.50	2.91E+01	2.91E+01	4.65E+01	6.81E+01
1.50	1.50	3.00	3.00	4.19E+01	4.19E+01	5.58E+01	8.17E+01
1.50	1.50	3.50	3.50	5.70E+01	5.70E+01	6.51E+01	9.54E+01
1.50	1.50	4.00	4.00	7.44E+01	7.44E+01	7.44E+01	1.09E+02
1.50	1.50	4.50	4.50	9.42E+01	9.42E+01	8.38E+01	1.23E+02
1.50	1.50	5.00	5.00	1.16E+02	1.16E+02	9.31E+01	1.36E+02
1.50	1.50	5.50	5.50	1.41E+02	1.41E+02	1.02E+02	1.50E+02
1.50	1.50	6.00	6.00	1.68E+02	1.68E+02	1.12E+02	1.63E+02
1.50	1.50	6.50	6.50	1.97E+02	1.97E+02	1.21E+02	1.77E+02
1.50	1.50	7.00	7.00	2.28E+02	2.28E+02	1.30E+02	1.91E+02
1.50	1.50	7.50	7.50	2.62E+02	2.62E+02	1.40E+02	2.04E+02
1.50	1.50	8.00	8.00	2.98E+02	2.98E+02	1.49E+02	2.18E+02
1.50	1.50	8.50	8.50	3.36E+02	3.36E+02	1.58E+02	2.32E+02
1.50	1.50	9.00	9.00	3.77E+02	3.77E+02	1.68E+02	2.45E+02
1.50	1.50	9.50	9.50	4.20E+02	4.20E+02	1.77E+02	2.59E+02
1.50	1.50	10.00	10.00	4.65E+02	4.65E+02	1.86E+02	2.72E+02